Manual quantification for right and left ventricular function using Cardiac Magnetic Resonance Imaging

ETOVS NR 56/08

BY

NANETTE WILLEMSE

This work is submitted in fulfilment of the requirements for the M.Med.Sc (Medical Physics) degree in the Faculty Health Sciences, Medical Physics Department, at the University of the Free State.

July 2012

Supervisor: Prof. W.I.D. Rae

Co-supervisor: Prof. C.P. Herbst

TABLE OF CONTENTS

1 RIGHT VENTRICULAR FUNCTION: CLINICAL IMPORTANCE AND ANATOMICAL CONNOTATION

1.1 INTRODUCTION

Up to now, imaging and quantification of the left ventricle (LV) and its functions have enjoyed a lot of attention. The cylindrical shape of the left ventricle makes it easy to locate and identify, as well as to approximate the surface with mathematical shapes for contouring of the structure (Lalande et al. 1999). Clinical non-invasive investigation of the left ventricle is done routinely using echocardiography, Computed Tomography (CT), nuclear medicine techniques and Magnetic Resonance Imaging (MRI).

However, right ventricular (RV) function has also been recognised as an important prognostic factor for many heart diseases of which a few are congenital heart disease, cardiomyopathy, and pulmonary hypertension (Marcu et al. 2006). It is also valuable to determine left and right ventricular function simultaneously, as a normal right ventricular function with abnormal left ventricular function is evidence of coronary artery disease (Dilsizian et al. 1990).

Therefore it has become important to evaluate right ventricular functionality quantitatively, as is done routinely for the left ventricle through the use of non-invasive imaging techniques (Selton-Suty & Juillière 2009).

Unfortunately, the shape of the right ventricle makes it very hard to fit the same type of mathematical shape or use the same geometric assumptions, as for the left ventricle. Also, its location in the chest cavity produces difficulties for imaging, for example its overlap with the right atrium on first pass radionuclide angiography, which introduces a big limitation to this imaging technique (Drake et al. 2007).

At Universitas Hospital in Bloemfontein, there is no accepted measure of right ventricular function. Therefore, the need has arisen to develop a method of assessing right ventricular functionality in Universitas Hospital.

1.2 PROGNOSTIC IMPORTANCE OF RIGHT VENTRICULAR FUNCTION

Although left ventricular ejection fraction (LVEF) is a dominant predictor of mortality following a myocardial infarction, in some clinical conditions right ventricular ejection fraction (RVEF) may also supply even further prognostic information. The assessment of right ventricular systolic and diastolic function provides complementary information in the prognosis of patients with heart failure due to ischemic or idiopathic dilated cardiomyopathy. The combination of right ventricular systolic and diastolic dysfunction is indicative of a very poor prognosis (Meluzin et al. 2005).

Patients, who underwent the Mustard repair for transposition of the great arteries as children, may experience an inability of the right ventricle to sustain the systemic circulation later in their lives. According to Roos-Hesselink et al. (2004, p. 1268), the most frequent cause of late mortality after the Mustard repair in the literature is sudden death, presumably arrhythmic. However, in their study, the major cause of death in the first 14 years after surgery was also sudden or arrhythmic, but changed to progressive heart failure in the period from 14 to 25 years after surgery. The study of Roos-Hesselink et al. further shows some late attrition, substantial long-term morbidity, and most importantly a clear deterioration in systemic right ventricular function and clinical condition after the Mustard operation.

Arrythmogenic right ventricular cardiomyopathy (ARVC) is a cause of sudden cardiac death in an otherwise healthy younger population. Many patients may be asymptomatic, and diagnosed by familial screening. The disease is characterised by progressive replacement of normal myocardium in the right ventricle by fibrofatty tissue, and may be detected by imaging (Murphy et al. 2010).

In a study by van Wolferen et al. (2007) cardiac MRI was used to investigate whether parameters of RV structure and function have prognostic significance in patients with idiopathic pulmonary arterial hypertension (IPAH). It was demonstrated that a large RV end-diastolic volume (RV EDV), low LV end-diastolic volume (LV EDV) and a low stroke volume (SV) were associated with a poor prognosis, and a further RV dilatation and a decrease in SV and LV EDV were strong predictors of treatment failure and death at follow-up.

Patients with right ventricular dysfunction complicating acute myocardial infarction have a more than 4-fold increased risk for in–hospital mortality compared with those without RV dysfunction (Bueno et al. 1997). However, in a study by Larose et al. (2007, p. 861) RV function assessed late after clinical myocardial infarction (MI) is also an important predictor of post-MI mortality, independent of patient age, LV infarct size or LV EF. Evaluation of RV function may improve the risk stratification of patients with MI beyond current practice and refine their medical management. Antoni et al. (2010, p. 269) confirmed these findings in patients with acute myocardial infarction

treated with primary percutaneous coronary intervention (PCI), as well as that RV strain is an independent predictor of all-cause mortality, re-infarction, and hospitalization for heart failure.

Haddad et al. (2008, pp.1717-1728) discuss several clinical important factors of RV function, under which heart failure, RV myocardial infarction, and IPAH are listed again. They also mention that RV dysfunction can be seen in both left-sided and right-sided valvular heart disease. Mitral stenosis often leads to pulmonary hypertension and RV dysfunction. RV failure, "which occurs more commonly in patients with severe mitral stenosis and significant pulmonary hypertension", may be the cause of mortality in 60% to 70% of untreated patients. (Lewis et al. 1952, cited in Haddad et al. 2008)

On the other hand, it has also been shown in a study by Testani et al. (2010, p.514) that there is a strong association between RV dysfunction and changes in renal function during the treatment of acute de-compensated heart failure. RV dysfunction was a strong predictor of a substantially lower incidence of worsening renal function and a higher occurrence of improved renal function in these patients, an effect likely intervened by relief of venous congestion. This is most likely explained by the ability of venous congestion to adversely affect renal function.

With all of the abovementioned information considered, it is obvious that the right ventricle has to be examined and its functionality determined to evaluate the true prognosis of patients in order to treat them appropriately.

1.3 HISTORY OF CARDIAC EXAMINATION

Scientists and medical practitioners have been intrigued by the functioning of the heart for centuries. Measurements on the heart have been an interesting and evolving subject and practice since the 1700's. Individuals such as Jean Baptiste de Sénac, Leopold Auenbrugger and Willem Einthoven have tried numerous ways to examine the heart, measure and describe its anatomy and function. (Medical and clinical engineering n.d.). In 1836, there were already different opinions on the capacity relation between the left and right ventricles, but all justified with their own techniques (Quain 1836).

More recently, Sandler and Dodge (1968, pp. 325-334) proposed a method for calculating LV volume from radiography film or screening images taken in a single A-P plane. This was a great improvement on the method by Robertson and Duff in 1922, where the capacity of the left ventricle was measured by filling it with water, post-mortem. At approximately the same time, Weissler, Harris and Schoenfeld (1969) suggested the use of pre-ejection period and LV ejection time measurements as a bedside evaluation of cardiac performance.

As technology improved, personal computers were also implemented in medicine to acquire cardiovascular data (Herbst et al. 1991). However, still more investigative techniques were developed which led to imaging of the heart in-vivo, as well as non-invasively; and knowledge on the anatomy and physiology of the heart advanced.

1.4   CARDIOLOGICAL PHYSIOLOGY AND ANATOMY

1.4.1   CLINICAL AND PHYSIOLOGICAL FUNCTION AND EVALUATION OF THE HEART

With the description of the influences RV functionality has on the prognosis of patients, it is clear that the physiology of the right ventricle has an important role in the heart.

With every rhythmic contraction of the heart, blood is pumped into the aorta and pulmonary arteries, ensuring a continued circulation of blood through the body and the lungs. Blood is distributed by smaller arteries throughout the body, and returns via veins which join to form the superior and inferior vena cava and four pulmonary veins that return the blood to the heart (Meyer et al. 2002).

During each heart cycle an electrical signal triggers myocardium contraction, generating pressure and volume changes. This causes mechanical opening and closure of the valves and blood flow, followed by relaxation of the cardiac muscle (diastole) (Meyer et al. 2002).

In the ventricles, the atrioventricular valves are closed, with the pressure increasing in the ventricles. When it exceeds the pressure in the pulmonary artery and aorta, ejection of blood starts when the pulmonary and aortic valves are forced open, and the ventricles contract to further eject blood into the arteries. The volume of blood ejected is the stroke volume (SV). At the end of the ejection phase, the ventricles relax and the pulmonary and aortic valves close again. The atrioventricular (mitral and tricuspid) valves will open due to the fall in pressure in the ventricles, and blood will flow into the ventricles from the atria (Rogers 1999, p. 2).

The volume of the ventricle at the end of relaxation (diastole) is the end-diastolic volume (EDV) and that at the end of contraction (systole) is the end-systolic volume (ESV). The stroke volume (SV) is also equal to the difference between the EDV and ESV, or can be expressed as an ejection fraction (EF), where the SV is expressed as a fraction of the EDV.

The SV is determined by three major factors, namely, preload, afterload and contractility. Preload is the pressure within the ventricle at end-diastole, and is also represented by the load present before contraction. RV afterload is the load that the RV has to surmount when ejecting blood, and is influenced by pulmonary vascular resistance (Haddad et al. 2008). Contractility is the ability of the myocardium to contract (Rogers 1999, p. 3).

These factors influence the right ventricular functionality. It has been shown that the RV stroke volume decreases when there is an increase in pulmonary arterial pressure, thus with an increase in afterload (Haddad et al. 2009).

In a normal functioning heart, the stroke volumes of the left and right ventricles are equal because the RV is connected in series to the LV. As the RV EDV is greater than the LV EDV, the RV EF will be lower than the LV EF (Haddad et al. 2009). This then shows again that the left ventricle "works harder" than right, which is due to the higher arterial pressure in the systemic than in the pulmonary circulation (Moore & Dalley 1999, p. 131).

Thus, the factors EDV, ESV, SV and EF give a good overview on the global functioning of the left and right ventricles, and will be of interest to evaluate.

To implement a non-invasive means, such as imaging, to evaluate the right ventricular clinical and physiological functionality, more information on the anatomy of the right ventricle is necessary.

1.4.2   ANATOMY OF THE HEART

The heart is a complex structure consisting of different chambers (right atrium, right ventricle, left atrium and left ventricle), valves, tissues and functions. The heart is a muscular pump which distributes blood to all parts of the body. The right side of the heart receives oxygen-poor blood from the body, and pumps it to the lungs for oxygenation. The left side of the heart receives the oxygen-rich blood back from the lungs, and pumps it into the body. The atria are the chambers that receive blood from either the body or lung circulation, and the ventricles are the distribution chambers pumping blood to either the lungs or body (Moore & Dalley 1999, p. 120).

The wall of each heart chamber is made up of three layers: the thin internal endocardial membrane, the thick middle myocardium (muscle) and the thin external epicardium (Moore & Dalley 1999, p. 120). The right ventricle is separated from the left ventricle by the interventricular septum, which also forms part of the walls of both ventricles.

In figure 1.4.1 (Gray 1918) is an illustration of the heart in a long axis view where the interventricular septum between the left and right ventricles can be seen, as well as atrioventricular valves and papillary muscles, which are discussed below in the following paragraphs.
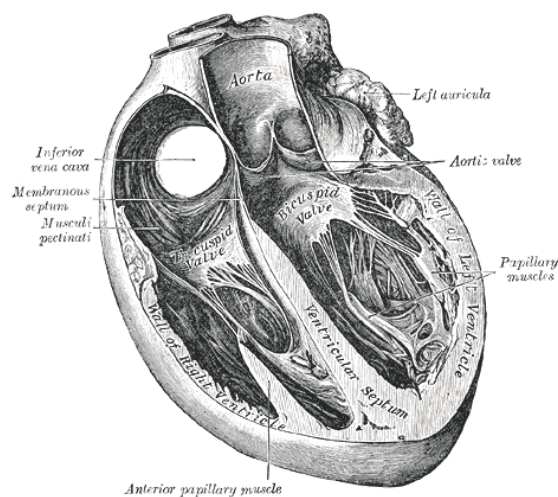
Figure 1.4.1: Image of a section of the heart showing the interventricular septum, right ventricle and left ventricle (Gray 1918, fig. 498).

1.4.2.1   Left ventricular anatomy

The left ventricle has a conical shape, and its wall is twice as thick as that of the right ventricle. Blood enters the left ventricle from the left atrium. The mitral valve lies between the left atrium and left ventricle, preventing blood flowing back into the atrium when the valve is closed. The mitral valve has two cusps that are connected to the papillary muscles through the cordae tendineae. The outflow part of the left ventricle leads to the aortic orifice where the aortic valve is attached. Blood leaves the left ventricle as it is pumped into the ascending aorta (Moore & Dalley 1999, p. 131).

1.4.2.2 Right ventricular anatomy

The right ventricle is the most anterior chamber of the normal heart and lies directly behind the sternum. It is quite triangular in shape, but when studied from a short-axis view, it is curving around the left ventricle in a crescent shape (Ho & Nihoyannopoulos 2006). Its free wall is much thinner than that of the left, is thickest at the base of the heart and thins off towards the apex. The right ventricle can be divided into three parts, the inlet (right atrioventricular orifice), the apical component (cavity) and the outlet (conus arteriosus) (Gray 1918).

The inflow part of the ventricle is situated at the base of the ventricle, and receives blood through the right atrioventricular orifice and the right atrium, which is guarded by the tricuspid valve. The tricuspid valve with its three cusps prevents the backward flow of blood into the right atrium when the ventricle contracts, with the help of the papillary muscles. The cusps are attached to the fibrous ring around the orifice, and to the chordae tendineae which is in turn attached to the papillary muscles. The contraction of the papillary muscles tightens the cordae tendineae which draw the cusps together and thus the valves closed, preventing regurgitation of blood (Moore & Dalley 1999, p. 127).

On the inside surface of the ventricle irregular muscular elevations, the trabeculae carneae, are found. The cavity capacity size of the right ventricle is slightly larger than the left (Haddad et al. 2009).

The upper and left angle of the ventricle forms a conical compartment, the conus arteriosus or outflow part. The circular opening of the pulmonary artery is here at the top of the outflow region, and is guarded by the pulmonary semiluminar valves (Gray 1918). Blood leaves the right ventricle as it is pumped into the pulmonary artery, and henceforth the pulmonary circulation.

The right ventricle has a truly complex structure, and therefore this complicates its accurate imaging.

1.4.2.3 Difficulties due to anatomy in imaging and segmentation of RV

Due to the position of the right ventricle in the chest cavity, imaging of the right ventricle with traditional imaging methods such as echocardiography, nuclear medicine techniques and planar radiography is very difficult (Frist et al. 1995). Lying directly behind the sternum, the right ventricle is obscured by bone, and in planar blood-pool studies, the right atrium overlaps with the right ventricle (Bartlett et al. 1996).

The complex shape and orientation of the right ventricle further complicate its imaging. With echocardiography, the right ventricle cannot be viewed in its entirety in a single view, but has to be imaged from different windows to acquire several planes (Ho & Nihoyannopoulos 2006).

In most segmentation methods and analyses of the left ventricle, algorithms based on a model of the ellipsoidal shape of the left ventricle are employed with geometrical assumptions to contour the ventricle automatically. However, the complexity of the shape of the right ventricle, does not lend itself to geometrical assumptions.

The papillary muscles that stretch through the ventricle form part of the muscle mass of the ventricle, but not the volume as such, as the volume is related to the amount of blood in the ventricle (Drake et al. 2007). The papillary muscles contribute to the complexity of the internal shape of the right ventricle, further disqualifying the fitting of geometric profiles to the right ventricle.

The relatively thin wall of the right ventricle in relation to that of the left (Moore & Dalley 1999, p. 131), requires imaging that produces high resolution images to be able to identify and segment the right ventricular endocardium.

With all of these complexities taken into account, it is clear that an evaluation of the right ventricular functionality with accurate results needs an imaging method that can overcome the difficulties at hand.

However, MRI has been shown to prevail over many of the anatomic difficulties of the right ventricle. The endocardium and epicardium of the relatively thin wall of the right ventricle can be delineated on MR images, as well as the trabeculations in its interior and the tricuspid valve (Markiewicz et al. 1987) due to the higher spatial resolution of cardiac MRI.

Furthermore, cardiac MRI is a gated imaging method, and can provide images of the heart throughout the cardiac cycle, resulting in the possibility of measurements at end-diastole and end-systole.

Thus cardiac MRI can potentially be used to accurately quantify the functionality of the right ventricle, and will be discussed as well as examined in this study. A comparison with other imaging modalities will follow in chapter 2.

1.5   RIGHT VENTRICULAR FUNCTION MEASUREMENT IN SOUTH AFRICA

Not much data on the RV based on MRI measurements in South Africa were available when the investigation was started, thus the study would contribute to the development of the method in South Africa. Some data are available in literature from studies in other countries with which to compare the proposed study data.

1.6   OVERVIEW OF THESIS STRUCTURE

With the above description of the importance of right ventricle function and the associated difficulties in its determination in mind, the aim of the proposed study will be lain down, followed by a discussion of different available modalities for the measurement of right ventricle function wherein cardiac MRI will be identified as the preferred method to investigate.

A summary of cardiac MRI principles will follow, where after the methods employed in the proposed study will be discussed in full. Results pertaining to reliability, validity, subgroup data and comparisons to literature data will be illustrated and discussed, and lastly conclusions drawn on the investigations.

1.7   AIM

The aim of this study was to evaluate the feasibility of a method where MRI was used for the determination of RV function in the Bloemfontein Academic Complex. This was achieved by a detailed study of the anatomy of the RV followed by MR imaging of normal volunteers comparing the measured RV functional parameters with parameters predicted by the LV function.

2 METHODS OF RV VOLUME AND FUNCTION DETERMINATION

Various techniques have been tried to determine accurate RV volumes and function (Frist et al. 1995). Some of these include right heart catheterization, echocardiography and radionuclide imaging. In the next few paragraphs, non-invasive imaging techniques of the right ventricle will be discussed according to method, benefits and drawbacks.

2.1 ECHOCARDIOGRAPHY

The non-invasive method used most widely to investigate the right ventricle is echocardiography, which can investigate structure, blood flow and functionality in a single examination (Selton-Suty & Juillière 2009). As the right ventricle lies in more than one plane, different echocardiographic imaging views are necessary to image the entire ventricle. The echocardiographer can then investigate if the right ventricle is dilated and quantify the degree of dilation qualitatively, as compared to the left ventricle (Selton-Suty & Juillière 2009).

RV EF can be determined by contouring the endocardial border in echocardiographs of the ventricle at end-systole and end-diastole, but it is difficult due to the RV shape, and geometric assumptions as used for the LV are less accurate for RV (Mitoff et al. 2012).

Spatial resolution of new echocardiography systems approaches that of MRI, and temporal resolution is better than MRI (Holinski et al. 2011).

2.1.1 BENEFITS AND DRAWBACKS OF ECHOCARDIOGRAPHY

Two-dimensional echocardiography is probably nowadays the first choice to determine left ventricular volume and function. The imaging modality is fast (typically 15 minutes on average), well established, available in most hospitals and clinics, well tolerated and relatively low-cost in comparison to other imaging modalities (Mitoff et al. 2012). The technique also holds no radiation risk.

Although echocardiography is brilliant in the evaluation of left ventricular volume, function and morphology, it has a limited ability in assessment of these factors for the right ventricle. A large part of the RV free wall lies directly behind the sternum and ribs, and cannot be seen with echocardiography (Murphy et al. 2010). Thus the anterior location and complex shape of the right ventricle limits the assessment of its morphology by echocardiography.

Three-dimensional echocardiography has been employed in recent years, and the first studies concluded that shape could be reconstructed and volume and function quantified by this imaging technique without geometrical assumptions (Jiang et al. 1994). In studies where RV volumes and ejection fractions measured with three-dimensional echocardiography were compared to that measured with MRI or radionuclide studies, the echocardiography data showed a good correlation with the other techniques. However, the three-dimensional echocardiography still often underestimates right ventricular volumes in adults (Kjaergaard et al. in 2006). Some scientists even went so far as to state that the determination of right ventricular volume is "not a matter for echocardiography" (Marabotti, Bedini & L'Abbate 2008), based on the complex three-dimensional geometry of the right ventricle that prevents echocardiographic estimation of the volumes by mathematics as in the case of the left ventricle.

2.1.2 CONCLUSION FOR ECHOCARDIOGRAPHY

Although echocardiography is the first choice in LV function assessment and excellent in determining LV function, the complex shape of the RV precludes the use of echocardiography for accurate RV functional analysis.

2.2 NUCLEAR MEDICINE TECHNIQUES

Nuclear medicine imaging techniques to determine right ventricular function may include first-pass radionuclide angiography, planar gated blood-pool studies or tomographic gated blood-pool studies (Mitoff et al. 2012).

First-pass imaging is obtained by injection of a bolus dose of ^{99m}Tc-pertechnetate and then acquiring a sequence of images in a right-anterior-oblique position as the bolus travels through the heart. A region of interest over the RV and measurement of the tricuspid valve plane provide computation of RV ejection fraction (Selton-Suty & Juillière 2009).

Planar gated blood-pool studies obtain images in the left-anterior-oblique orientation (Chin et al. 1997) to prevent overlap between the two ventricles. These studies can give information on myocardial wall motion and ventricular function expressed as ejection fraction. In gated blood-pool studies, it is assumed that the concentration of radionuclide tracer is constant and therefore the change in measured blood-pool counts over the cardiac cycle is used to determine the ejection fraction (Bartlett et al. 1996).

Tomographic gated blood-pool studies provide three-dimensional information of the cardiac chambers (Bartlett et al. 1996). Volumes can be calculated on these images by drawing regions of interest on transaxial images and determining the pixel count of each region. The pixel count is summed over all the image slices for both end-diastole and end-systole to offer the corresponding relative volumes. The ejection fraction can then be derived from these volumes (Chin et al. 1997).

A nuclear medicine cardiac scan can be acquired in 15 – 30 minutes, depending on the type of procedure.

2.2.1 BENEFITS AND DRAWBACKS OF NUCLEAR MEDICINE TECHNIQUES

Factors like attenuation, background counts and angle of view all contribute to the difficulty of assessing right ventricular function with nuclear medicine techniques (Bartlett et al. 1996). Patient background activity and an increase in scatter may incorrectly increase the counts in the ventricular area, resulting in inaccurate measurements (Chin et al. 1997).

If the bolus in first-pass studies is not injected correctly, the counts in the RV region will be reduced and the ejection measurement will be erroneous (Selton-Suty & Juillière 2009).

The overlap of the right atrium and right ventricle leads to great errors and differences in RV ejection fraction measurements (Bartlett et al. 1996) and stroke count ratio measurements (Dilsizian et al. 1990) in planar gated blood-pool studies. On the other hand, SPECT, or tomographic imaging, has the advantage of providing three-dimensional images (Bartlett et al. 1996) which allows better division between the RV and adjacent structures (Mitoff et al. 2012), most likely improving assessment.

Overall difficulties in the assessment of RV ejection fraction consist of imaging the RV without overlap of the other cardiac chambers, the accuracy of distinguishing between RV and the pulmonary artery or other cardiac chambers, and the determination of the end-diastolic and end-systolic frames (Mitoff et al. 2012). Spatial and temporal resolution of MRI is however also superior to that of nuclear medicine studies.

2.2.2 CONCLUSION FOR NUCLEAR MEDICINE TECHNIQUES

First-pass radionuclide studies can be used to measure RV ejection fraction, as well as gated blood-pool studies, but not without relatively large uncertainties and error. Detailed anatomic information is not possible, and there is a radiation risk associated with these studies.

2.3 COMPUTED TOMOGRAPHY

Multi-detector computed tomography (MDCT) is not a first-line choice for assessment of the right ventricle, but is still used widely. Retrospective ECG gating is employed in the imaging to determine dynamic information and RV function (Dupont, Drăgean & Coche 2011). The use of contrast injection leads to a better distinction between the layers in the cardiac wall and thus optimizes RV function determination (Kerl et al. 2008).

RV ejection fraction measurements can be done on short-axis or axial reconstructed images (Alfakih et al. 2003), where endocardial borders are drawn on end-diastolic and end-systolic images on all slices through the ventricle. As MDCT is a cross-sectional imaging technique, it does not depend on geometric assumptions and therefore increases its accuracy of RV volume assessment (Plumhans et al. 2008).

2.3.1 BENEFITS AND DRAWBACKS OF CT

MDCT imaging has already improved right ventricular function assessment in comparison to nuclear medicine techniques and echocardiography, in terms of image quality, the visibility of surrounding structures, spatial and temporal resolution and the absence of geometric assumptions. MDCT acquisition is a fast imaging method, where an entire data set can be imaged in a single breath-hold (Mitoff et al. 2012). An entire examination may be finished within 10-15 minutes, with an excellent spatial resolution (< 0.75 mm) and temporal resolution (80-200 ms) (Mahesh & Cody 2007).

However, RV data cannot be acquired simultaneously with LV data, and examination of the RV would lead to additional radiation dose when both ventricles are examined (Selton-Suty & Juillière 2009). As it has been shown in a study by Einstein, Henzlova and Rajagopalan (2010, p. 319) that MDCT angiography is correlated to a

"nonnegligible lifetime attributable risk" of cancer, and for combined cardiac and aortic scans, the radiation dose from cardiac MDCT is a disadvantage and cannot be ignored.

The necessity of iodinated contrast injections for cardiac MDCT is also contributing to the drawbacks of CT imaging (Dupont, Drăgean & Coche 2011).

2.3.2 CONCLUSION FOR CT

Thus the radiation delivered together with the iodinated contrast medium limits CT as a technique of choice for RV function assessment.

2.4 MAGNETIC RESONANCE IMAGING

Cardiac Magnetic Resonance Imaging (MRI) is a non-invasive technique for the evaluation of right and left ventricular function and cardiac masses. The tomographic feature of MRI has the ability to prevail over most of the limitations discussed in the other imaging techniques above (Frist et al. 1995). Currently, cardiac MR imaging is done on 1.5T or 3T scanners, using cardiac phased-array coils. The cardiac imaging is ECG gated, and breath-hold techniques with fast imaging pulse sequences are used (Selton-Suty & Juillière 2009). Both the left and right ventricle can be imaged in the same imaging series. By drawing contours on the MR images representing the endocardial borders of the ventricles, the corresponding ventricular volumes and ejection fractions can be calculated from the contour areas.

Some MRI studies do however require the use of gadolinium contrast medium, but it has been proved to be safer than iodinated contrast agents (Grobner 2006). Scans are typically acquired with a spatial resolution of 1-3 mm and temporal resolution of 20-90 ms (Miller et al. 2002).

2.4.1 BENEFITS AND DRAWBACKS OF MRI

Magnetic Resonance Imaging (MRI) has been described as the "technique of choice" (Selton-Suty & Juillière 2009) and the "gold standard" (Mitoff et al. 2012) for cardiac imaging by more than one author. No geometrical assumptions influence the data and accurate RV mass, volume and function can be assessed (Mitoff et al. 2012). RV function assessment with cardiac MRI has good inter-study reproducibility (Grothues et al. 2004) and high inter- and intra-observer reproducibility (Mooij et al. 2008). MRI also gives true information on morphology of the heart, muscle perfusion and blood flow (Petitjean & Dacher 2011) and can image any orientation of the heart (Marcu et al. 2006). MRI does not make use of ionising radiation.

Unfortunately, with MRI there are also difficulties to be taken into account. Patients with metal implants, implanted pacemakers, defibrillators and resynchronisation devices cannot be imaged due to safety reasons (Pitcher et al. 2011), and neither can patients with severe claustrophobia. Long examination times in a supine position and repeated breath-hold periods might limit the use of MRI and are stressful and tiresome for patients with symptomatic heart failure (Mitoff et al. 2012) and high-grade dyspnea, and can also lead to degradation of image quality.

These abovementioned limitations are quite important, as many of the patients in need of this cardiac imaging have intracardiac devices (Selton-Suty & Juillière 2009), suffer from congestive heart failure already, or have advanced cardiac disease for whom new treatments are most likely to be beneficial (Pitcher et al. 2011). Furthermore, MRI is not readily available in clinical practices everywhere, especially in South African government hospitals, which might make further studies difficult.

2.4.2 CONCLUSION FOR MRI

From the discussions on the anatomy, physiology and imaging of the right ventricle, a strong indication for the use of MRI as a non-invasive technique for the evaluation of right ventricular function has come forth. MRI can be used as an imaging modality of the right ventricle, as it allows any orientation to be imaged, gives detailed information of the anatomy, and has progressed significantly, allowing good quality gating and imaging of the heart. In addition to volumetric and functionality investigations of the ventricle, MRI can also be applied in the assessment of valve function, vascular anatomy and function, myocardial scar determination, myocardial perfusion and myocardial tissue characteristics (Pitcher et al. 2011).

There is no radiation risk associated with MRI, the technique is safe and can be repeated if necessary. Volumetric scans can be acquired without the use of contrast medium. MRI does not rely on geometrical assumptions, and the volumes and ventricular function derived are accurate and representative of the true ventricle.

2.5   CONCLUSION

From the discussions above, cardiac MRI seemed to prevail over the other imaging modalities, especially in the application of an investigative study where volunteers are employed. As MRI was the favourable option, and was available in Universitas Hospital through collaboration with the Radiology department, the quantification method studied was based on imaging with cardiac MRI.

3 PRINCIPLES OF CARDIAC MAGNETIC RESONANCE IMAGING AND SEGMENTATION

The combination of complex anatomy, cardiac activity and respiratory motion makes the heart a challenging organ to image. Fortunately, MRI can image any orientation of the body, and has made significant contributions to cardiac imaging. Cardiac Magnetic Resonance Imaging (MRI) offers the largest comprehensive evaluation of cardiac function and anatomical structure (Dahya & Spottiswoode 2010).

This chapter will provide an overview on the principles of cardiac MRI as applied routinely in Universitas Hospital, and the resultant segmentation of the ventricles.

3.1 CARDIAC MAGNETIC RESONANCE IMAGING

Magnetic Resonance Imaging (MRI) applies the magnetic properties of the nucleus of the atom, resonance in the form of energy coupling and external magnetic field gradients to localize the nuclear magnetic resonance signal and to reflect clinically relevant information as images displaying the magnetic properties of the proton (Bushberg et al. 2002).

MRI does not make use of ionising radiation and is considered to be a non-invasive diagnostic technique. Unlike radiography or echocardiography, MR images can be obtained in any anatomic plane, thus delivering three-dimensional reconstructions of the anatomy. This fact is a big advantage and an indication for using MRI as a non-invasive study technique of the right ventricle (Al-Shafei et al. 2001).

Cardiac MRI is a tomographic technique that can be applied to image practically any cardiac plane and allows true quantification and function analysis of cardiac ventricular volumes, and ventricular tissue characterization (Marcu et al. 2006). It can also be used in angiography, imaging of blood velocity and flow and contrast-enhanced lung perfusion.

Cardiac MRI does not rely on geometric assumptions (Geva et al. 1998; Shors et al. 2004), provides a method of accurately visualising the complex internal architecture of the right ventricular cavity (Markiewicz et al. 1987) and offers improved reproducibility over other imaging modalities (Williams and Frenneaux 2008).

The quality of the images strongly depends on the pulse sequences and image acquisition protocol used. The standard imaging procedure to determine ventricular function will be discussed below, as prescribed in the "Signa® LX Release 9.0: learning and reference guide" provided by GE Healthcare (General Electric Company 2001a).

3.1.1 CARDIAC MRI ACQUISITION

The acquisition protocol used at Universitas is a good representation of protocols followed all over the world. All MR examinations in the Radiology Department are done on a 1.5T MRI scanner (Signa® twinspeed, GE Healthcare, Milwaukee, WI, USA). For cardiac scans, a phased array cardiac coil is used.

The imaging is assisted by cardiac gating and triggering, accomplished by the use of electrocardiogram (ECG) monitoring. Gating and triggering are discussed in full in Appendix B.

The image acquisition procedure consists of two main sections, namely initial imaging to determine the general position of the heart, and then volumetric imaging. This standard cardiac imaging procedure consists of four imaging views of the heart: one for axial localisation, and three for volumetric calculations. All of these images are acquired with no spacing between adjacent slices.

3.1.1.1 Imaging to determine general positioning

From the coronal localizer, the area over which the axial scan for positioning is to be acquired is defined, and details can be found in Appendix B. The axial scan is acquired as T1 Fast-Spin Echo (T1 FSE) weighted images. These axial images are further used to plan the position of the volumetric scans.

3.1.1.2 Volumetric imaging

All volumetric imaging is done using cardiac gating and triggering, and also using the breath-hold technique. The volumetric scans are acquired with a 2D FIESTA pulse sequence. This is a vendor-specific balanced steady state free precession (SSFP) pulse sequence, and is discussed in full in Appendix B. The slice thickness is 9mm for all slices.

The standard cardiac imaging procedure involves three views of the heart being acquired. These imaging views are as follows:

1. 2-Chamber view
2. 4-Chamber view
3. Short-Axis view

Each imaging view is planned on the previously acquired view, thus the three views are linked to a single coordinate system. The entire dataset thus comprises multiple gated slices of 9 mm thick, acquired for 20 time intervals or phases per heart cycle for each slice through the heart, for all 3 orientations.

The duration of the imaging of each slice varies from 7 to 11 seconds. A full description of the imaging parameters follow under heading 3.1.2.

Every orientation imaged, provides a basis from which to plan the next view to be imaged, and the planning process applied can be found in Appendix B. Examples and descriptions of the three imaging views are shown below.

3.1.1.2.1 2-Chamber View

Two examples of 2CV images can be seen in figure 3.1.1. The 2CV scans provide slices through the heart where the left ventricle and left atrium (2 heart chambers) can be seen together on an image, and the right ventricle and right atrium together on other images. The left ventricle and atrium can be seen in the image on the left, and the right ventricle and atrium of the right. On average, 6 slices were imaged through the cardiac area to encompass the 2 ventricles.
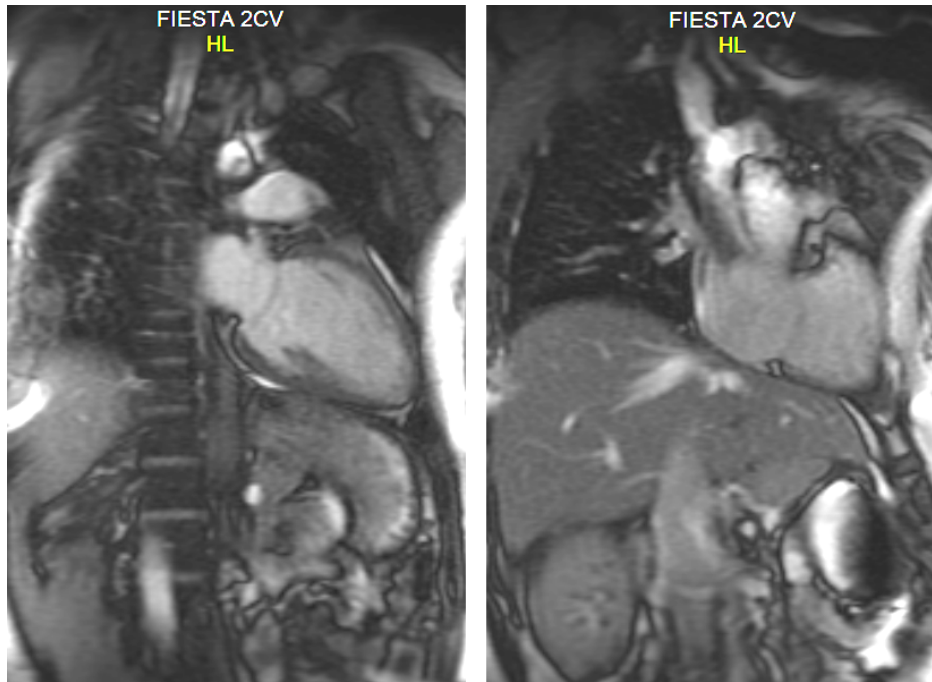
Figure 3.1.1: Examples of 2CV images where the left ventricle and left atrium (left image) and the right ventricle and atrium (right image) can be seen.

3.1.1.2.2 4-Chamber View

Figure 3.1.2 shows an example of the heart on a 4CV image. The 4CV scans provide slices through the cardiac area where both the left and right ventricles and atria are visible in the same plane or image. This imaging view is also known as a long axis imaging view. 8 slices were imaged through the heart on average to include both ventricles.
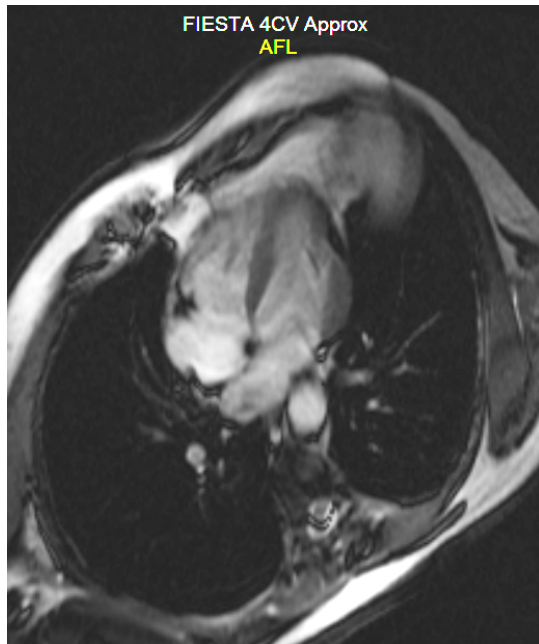
Figure 3.1.2: Example of a 4CV image where all four the cardiac chambers can be seen

3.1.1.2.3 Short-Axis View

Figure 3.1.3 shows an example of the heart on a SA image. The SA scans provide slices through the cardiac area where the left and right ventricles are visible in the same plane or image. Short axis imaging is quite well established and mostly used in cardiac volumetric imaging. It covers the ventricles from apex to base in 10 image slices on average.
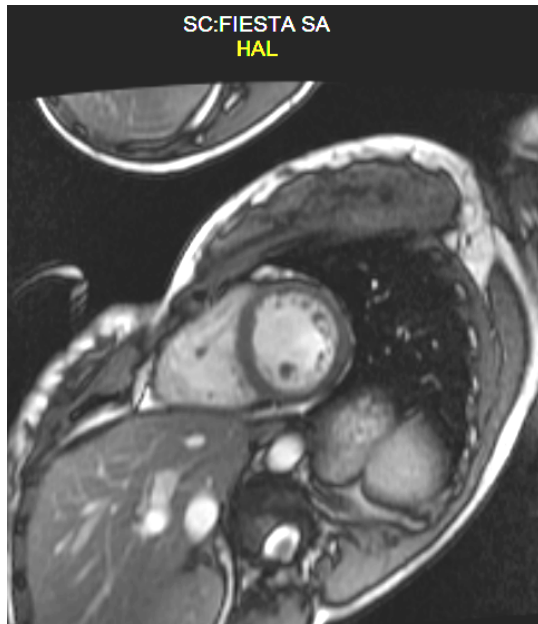
Figure 3.1.3: Example of a SA image where the left and right ventricles can be seen, and a large wrap around artefact is noted from the bottom of the image onto the top of the image.

3.1.2 IMAGING PARAMETERS

Balanced SSFP such as FIESTA is a pulse sequence in which a train of RF excitation pulses with an alternating large flip angle is used. All three gradient axes are fully balanced to produce steady-state magnetization. The signal intensity in balanced SSFP sequences depends on the T2/T1 ratio, which is high for blood and low for myocardium, resulting in greater contrast between blood and myocardium. A full description of the 2D FIESTA pulse sequence is given in Appendix B.

For the axial images, the effective echo-time (TE) is ~41ms and the repeat time (TR) for each slice ~1500ms. A flip angle of 90 degrees is used.

In the volumetric imaging with the 2D FIESTA pulse sequence, the effective echo-time (TE) is ~1.6ms and the repeat time (TR) ~ 3.8ms. A flip angle of 40° is used, a field of view of 350mm and an acquisition matrix of 256x256. The 2D FIESTA pulse sequence produces adequate contrast between the myocardium and blood, and imaging can be done without the use of contrast medium. One slice of 9mm thickness is imaged at a time. The cardiac gated imaging provides 20 phases (images) per RR-interval on each slice, acquired prospectively. (Details in appendix B)

The Society of Cardiovascular Magnetic Resonance has a number of resources describing current imaging standards and protocols. Different techniques are described for different specific diseases, and are standardised accordingly (Kramer et al. 2008). With the standard imaging procedure in place, attention should also be paid to exceptions and routine problems that may interfere with smooth-running quality imaging and resulting segmentation.

3.2 IMPLICATIONS FOR SEGMENTATION AND VOLUME DETERMINATION

As seen from the discussions on the prognostic value of right ventricular function, the evaluation of right ventricular function is important in the diagnosis and management of many cardiac disorders. Imaging of the right ventricle has always been deemed rather challenging, primarily because of its complex anatomy and biomechanics. Therefore it follows that the contouring and segmentation of the right ventricle is especially difficult due to its variable shape and poorly defined edges.

3.2.1 ANTICIPATED PROBLEMS IN IMAGING AND SEGMENTATION

Difficulties in the imaging process may very well lead to resultant problems in segmentation; therefore it is important to pay attention to all steps in the method.

Gating problems are commonly experienced. Even with optimal lead placement, magneto-hydrodynamic effects from flowing ions in the magnetic field and gradient switching noise may distort the signal from the ECG after the patient is placed within the magnet (Saremi et al. 2008). Also, when a patient's heart rate is very unstable, imaging with prospective gating will fail.

When patient movement occurs during or even between imaging series, it contributes to problems. Movement during imaging will result in motion artefacts that may influence the volume measurements. Movement between different views or slices will misrepresent the volume of the heart, and disrupt the continuous coordinate system, and the three imaging views will not be linked anymore. Movement in the form of blood flow also contributes to the formation of artefacts.

Automatic edge detection software for the right ventricle is not very effective. Because the shape of the right ventricle is not cylindrical like the left ventricle, or any other shape that can be easily modelled, segmentation becomes a problem. The segmentation technique is also complex and without substantial training and experience, accurate measurements may not be easily achieved (Pitcher et al. 2011). The complex geometry of the right ventricle anatomy and its physiology as described in chapter 2, definitely contributes to the segmentation difficulties. Papillary muscles in the ventricles make the contouring even more complex, and may contribute significantly to inaccuracies if included in the blood volume.

Petitjean and Dacher (2011, p. 170, 171) state that segmentation difficulties occur mostly due to grey level inhomogeneities in the blood flow and wall irregularities (trabeculations) inside the heart chamber, which disables the clear delineation of the endocardium. They further say that the grade of difficulty of segmentation also depends on the slice level of the image on the apex-base axis. In a short-axis view series, segmentation of the ventricles is easier on a "mid-ventricular image" than on apical and basal slices.

Partial volume artefacts arise from the finite size of the voxel over which the signal is averaged (Bushberg et al. 2002). This results in a loss of detail and spatial resolution. The relatively large slice thickness of 9mm contributes to the occurrence of partial volume effects.

These abovementioned difficulties may seem to critically influence the proposed study and method, but for many of these problems solutions have been proposed, and with a thorough knowledge of the expected difficulties, most can be overcome.

3.2.2   OPTIMIZATION OF CARDIAC MRI AND SEGMENTATION

Through experience and the development of imaging methods, solutions have been proposed to optimize cardiac MRI and ventricular segmentation.

Balanced steady-state free precession (SSFP) sequences provide a better signal to noise ratio in images, increased contrast between myocardium and blood, and therefore greatly improved image quality in comparison with those obtainable with spoiled GRE sequences (Carr et al. 2001). The SSPF sequence implemented in the standard cardiac MRI, 2D FIESTA, is therefore part of the optimization. FIESTA cine sequences of the heart produces "bright blood" images. Typical images with contours can be seen in figure 3.2.1, where images 1a to 1d represent end-diastole on four separate slices through the heart, and images 2a to 2d end-systole on the corresponding slices. Right ventricular contours are in green and left ventricular contours in red.
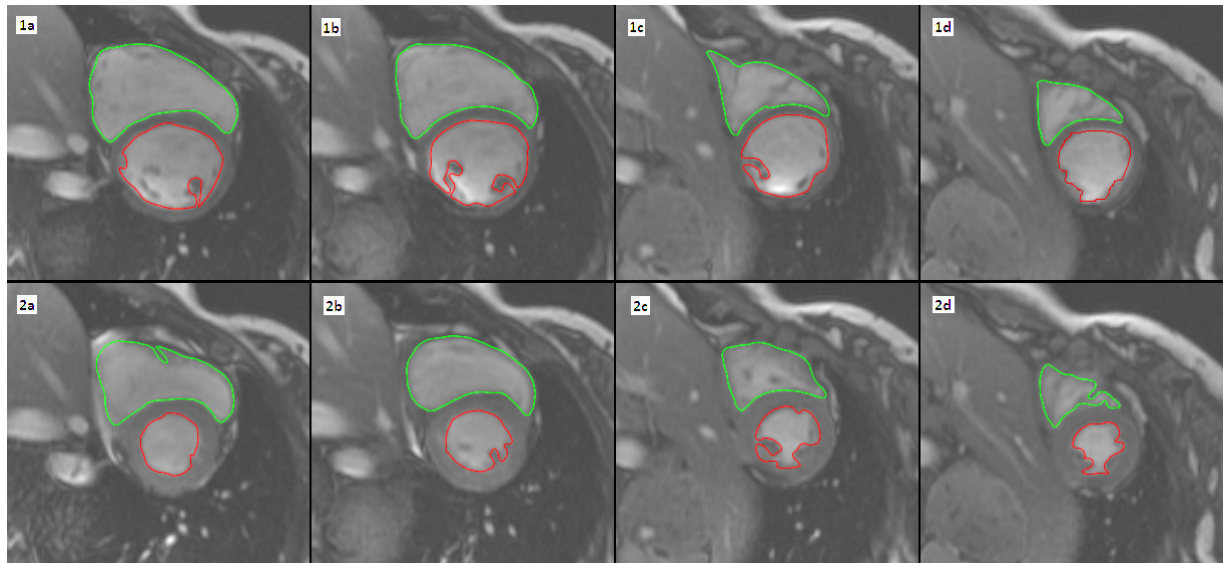
Figure 3.2.1: FIESTA bright-blood images, with right and left ventricular contours in end-diastole (top row, 1a-1d) and end-systole (bottom row, 2a-2d)

The positioning of the surface MR coils in relation to the object to be imaged, the heart, is very important. Since the homogeneity of the magnetic field decreases with increasing distance from the magnet isocentre, the centre of the heart should be placed at the isocentre. In other words, the patient should be positioned with the heart at or near the magnet isocentre. Multi-planar scout images are useful in evaluating the positioning (Saremi et al. 2008).

To reduce patient positioning errors due to breathing, it has been suggested that image acquisition should be done at end expiration, as it is more reproducible (Taylor et al. 1997). The importance of breath-holding should be explained to the patient before the imaging examination.   To optimise cardiac gating, ECG leads should be applied and the ECG waveform evaluated before image acquisition is begun (Saremi et al. 2008). An ECG signal that has poor amplitude requires repositioning of the leads.

Sequential scans provide continuity that can also aid in manual segmentation, where the observer can examine the image that follows or precedes the image to be segmented, or in slices imaged above or below the current slice image (Petitjean & Dacher 2011).

As discussed in an article by Petitjean and Dacher (2011, p. 171), former knowledge of the anatomical shape of the ventricles, their orientation with respect to each other, and their biomechanics can help with numerous segmentation problems.

Varying accuracy has been reported by different studies, and reproducibility of the manual contouring process is still a worry (Bonnemains et al. 2012). Available automatic contouring methods are not reproducible or reliable. Therefore the need arises to test the reliability and accuracy of manual segmentation by inter-observer (Bradlow et al. 2010) and inter-method variability tests (Grothues et al. 2004).

With all of the abovementioned problems and issues considered, the necessity of a preliminary study was also realised, in which the potential pitfalls could be determined with respect to the equipment and resources available locally. The standard cardiac MRI protocol was to be used.

4 ACQUISITION AND ANALYSIS OF MRI RV FUNCTIONAL PARAMETERS

From the discussions on the anatomy, physiology and different imaging options of the right ventricle in the previous chapters, a strong motivation for the use of MRI as a non-invasive technique for the evaluation of right ventricular function has developed. It was also seen that MRI is the most favourable to study RV function. It was decided that cardiac Magnetic Resonance Imaging (MRI) would be the best imaging option in this study, as there is no radiation dose to the participants, it was available through collaboration between Medical Physics and the local Radiology Department, and it enables any orientation of the anatomy to be imaged.

From a financial viewpoint, the fact that no nuclides or interventional contrast agents were needed that could otherwise incur further costs, favoured the decision for MRI, as well as no extra personnel input other than the person operating the MR scanner was necessary. The MR imaging could be done after hours as the department was open for emergency patients, thus no interference with radiology patient bookings was necessary.

The advantages of cardiac MRI outweigh the limitations, especially for the proposed clinical investigations. As the study will investigate normal healthy volunteers with no cardiac abnormalities, thus limitations such as implanted pace makers will not be a problem. There is no radiation risk associated with MRI, the technique is safe and can be repeated if necessary. MRI does not rely on geometrical assumptions, and the volumes and ventricular function derived are accurate and representative of the true ventricle.

In addition to volumetric and functionality investigations of the ventricle, MRI can also be applied in the assessment of valve function, vascular anatomy and function, myocardial scar determination, myocardial perfusion and myocardial tissue characteristics (Pitcher et al. 2011).

Also, as there was no radiation risk or intervention associated with imaging on an MRI scanner, it was anticipated that volunteers would be more at ease with participating in the study, and this simplified application for ethics approval.

Not much data on the RV based on MRI measurements in South Africa were available when the investigation was started, thus the study would contribute to the development of the method in South Africa. Some data are available in literature from studies in other countries with which to compare this study data.

As the aim of this study was to develop a manual quantification method to define cardiac functional parameters, it was important that the methods of imaging and analysis were similar for all volunteers studied (Pitcher et al. 2011; Pfisterer et al. 1985) as well as reproducible (Grothues et al. 2004).

As no clear instructions are available in the literature on quantification of cardiac volumes by contour tracing of the LV and RV and existing RV protocols show high intra- and inter-observer variability (Prakken et al. 2008), a preliminary study was first undertaken to test the available resources, determine the feasibility of the proposed method and to establish the available options. The preliminary findings are discussed in Appendix B. It was also necessary to determine the time span of such a project as manual contouring and determination of cardiac functional parameters are often time consuming (Lalande et al. 1999). The same imaging data were used in the preliminary study and in the final proposed study. Different observers were to take part in the final study.

4.1 METHODS

This work made use of an observational descriptive study method. Volunteers underwent cardiac MRI and the resulting image data were analysed. The development of the quantification method can be divided into two sections, namely data collection and data analysis.

4.1.1 POPULATION GROUP

Ethics approval was obtained through the University of the Free State Ethics Committee (ETOVS NR 56/08). To collect data for this study, 20 volunteers with no identified cardiac defects or risk factors for such anomalies were required for inclusion to undergo standard cardiac MRI.

Volunteers were selected non-randomly, as all were personnel in the Medical Physics department of Universitas Hospital. This made the logistics of the study easier in terms of availability of volunteers, their understanding of the importance of the imaging and where imaging had to be repeated. However, it might be that the study population was stratified by the non-random selection of a specific group of people. Although none of the volunteers had any known cardiac abnormalities, all of them underwent echocardiography to verify the absence of cardiac disease.

All volunteers gave informed consent, and cooperated well.

For selection of a group of twenty suitable volunteers in the study, the following inclusion criteria were applied:

1. "Normal healthy volunteers" with no known cardiac abnormalities
2. Adults in the age range 18 to 60

3. Males and females in approximately equal numbers

4. Resting heart rate of 50 to 80 beats per minute

Certain exclusion criteria were also applied as follows:

1. Smokers

2. Volunteers with a history of cardiac abnormalities or diseases, including hypertension

3. Any current medication for heart disease

4. Medication for hypertension or asthma

5. Any other absolute contraindication for Magnetic Resonance Imaging (MRI) investigation.

For collection of the required 20 normal healthy volunteers, in total 28 volunteers were entered into the study, of which 10 males and 10 females in the age range 21 to 53 were included in the analysis.

4.1.2   DATA COLLECTION

All cardiac MRI data collection scans were performed with a commercial 1.5T MRI scanner (Signa® twinspeed, GE Healthcare, Milwaukee, WI, USA) using a phased array cardiac coil and the standard clinical cardiac protocols and commercially available pulse sequences.

The Magnetic Resonance Imaging was performed in the Radiology Department of Universitas Hospital, Bloemfontein.

The standard cardiac MRI protocol that is used routinely in the Radiology Department was applied to image the participants in the study. During routine standard cardiac MRI, only one slice is imaged per 2-Chamber view and one per 4-Chamber view orientation as these slices are simply intended for positioning purposes. However, for this study, multiple image slices were acquired in each of the three orientations so as to encompass the entire volume of the heart. Full 2CV and 4CV imaging view series were done to determine whether one imaging view is better than another, if it is the best option only to rely on SA view data, or if it may be an advantage to use a combination of the imaging view data for volume and function determination.

No contrast agents were used during the imaging in this study.

By defining the scan extent of each view on the previous set of images as discussed in chapter 3, all the images were linked on a single coordinate system, which was helpful in determining the same corresponding position on each view during segmentation.

The imaging process for one volunteer, including set-up and acquisition of all views, amounted to 50 to 60 minutes per volunteer; that is if the volunteer cooperated and none of the series had to be repeated. All of the imaging was done after normal working hours.

After all imaging data were collected for a volunteer, the images were sent via a local network to the reporting workstation (GE Advantage workstation, AW 4.1) for contouring.

4.1.3 SEGMENTATION

The MR image processing was performed with a commercially available standard program for cardiac analysis (MASS ANALYSIS PLUS, software package version 5.1, Leiden, The Netherlands), which was available on the MR reporting workstation in the Radiology Department.

Software for automatic and semi-automatic contour detection of the left and right ventricles was available on the Mass Analysis Plus software, but it was not found to be reliable or reproducible at all for the right ventricle. Geometric models and software for contour detection of the right ventricle are also not widely available, thus manual segmentation was utilized.

The parameters investigated include, for both the left and right ventricles:

- end-diastolic volume (EDV),
- end-systolic volume (ESV),
- stroke volume (SV), and
- ejection fraction (EF).

On each slice through the heart, the right and left ventricles were manually contoured as regions of interest (ROIs) following the left and right endocardial borders on the 20 phase images. No smoothing was performed on the images.

Before EDV, ESV, SV and EF could be measured, manual analyses required that the frames corresponding to end-diastole and end-systole be identified (Bradlow et al. 2010). To do this, end-diastole (ED) and end-systole (ES) were defined by identifying the respective frames demonstrating the largest and smallest ventricular cavity sizes (Codella et al. 2010).

This process of contouring and identifying ED and ES frames was repeated on all slices of the three imaging views, as well as for both the left and right ventricle.

After the contouring was completed, the contour files were exported via a local network to a Windows based personal computer. The contour files could be opened in Microsoft Excel, where the area of each drawn contour was listed in the frame it was drawn, for all slices, left and right ventricles.

4.1.4   VOLUME AND FUNCTION CALCULATION

The largest contour areas (in units of cm^2) from the report files for a specific view were multiplied with the imaging slice thickness (0.9cm), and summed over all the slices to obtain the corresponding EDV, for the left and right ventricles respectively. In the same manner, the left and right ESV were calculated from the smallest contour areas. The volumetric conversion of $1cm^3$ = 1mℓ was employed to obtain volume values in mℓ.

Figure 4.1.1 illustrates the volume calculation where the drawn contours are multiplied with the slice thickness and summed to produce an estimate of the volume of the entire ventricle contoured. The illustration shows the contours on the left, the resultant slice volumes as the contour areas were multiplied with the slice thickness in the middle, and the summed volume of all the slices on the right.
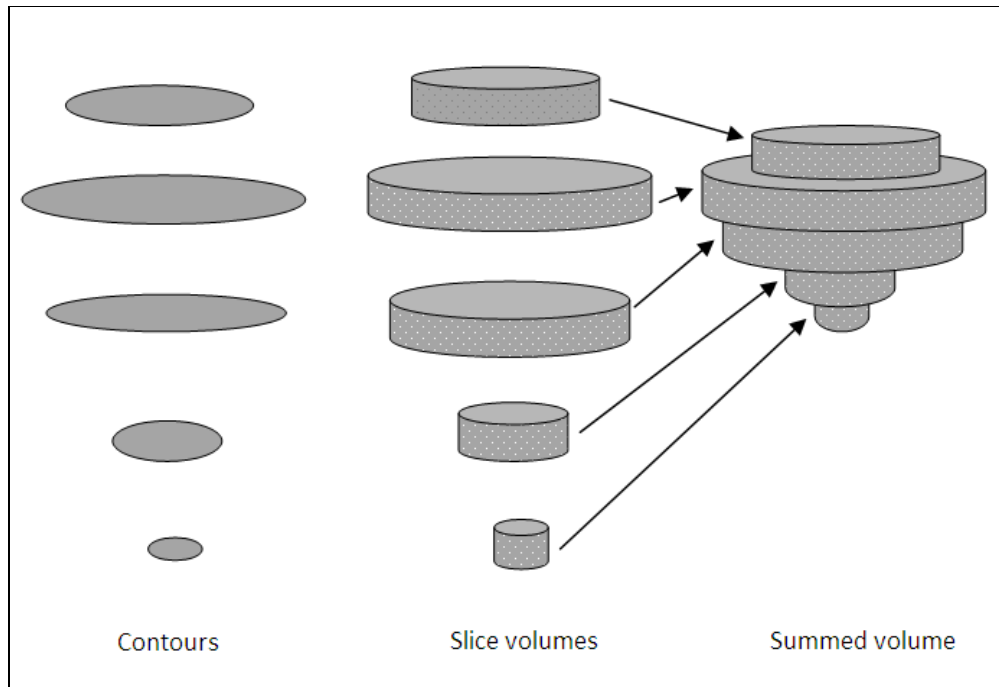
Figure 4.1.1: Illustration of volume calculation from the contours drawn on the MR images

Stroke volumes (SV) could then be derived by subtracting the ESV from the EDV values (Uribe et al. 2008), as the difference between the EDV and the ESV is the SV of the heart. Because the function of the left ventricle is related to the function of the right ventricle, the SV is equal for the left and right ventricles. Thus, when comparing volumes from the left and right ventricles, the SV is a useful point of comparison. The SV was also calculated for both left and right ventricles in units of mℓ.

The EDV and ESV were further used to calculate the ejection fraction (EF) of the heart, as in equation 4.1.1 (Meyer et al. 2002). The left and right EF were expressed as percentages.

$$EF = \frac{EDV - ESV}{EDV} \times 100\%$$

<div align="right">(4.1.1)</div>

All the abovementioned calculated volume and EF values were employed to test the integrity of the study and its method, and to list the cardiac volumes and function for the normal volunteer group.

4.2 CARDIAC MR IMAGES

4.2.1 IMAGE CHARACTERISTICS

On good quality 2CV and 4CV images, valve levels could be defined easily and segmentation was straightforward. The following figures show examples of images obtained in the three imaging views where the tricuspid and bicuspid (mitral) valves, papillary muscle and the endocardium can be clearly distinguished. Figure 4.2.1 and 4.2.2 show examples of 2CV images, first of the left and then of the right ventricle.
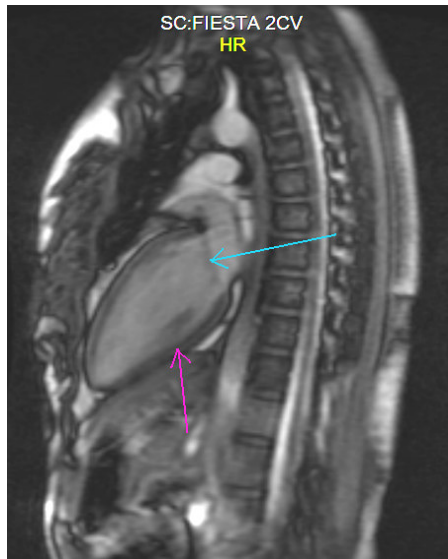
Figure 4.2.1: Example of a 2CV image of the left ventricle, where the mitral valve and endocardium surrounding the left ventricular volume are distinguished clearly, indicated by the blue and pink arrows respectively. The papillary muscle inside the volumes is also clearly visible.

Figure 4.2.2: Example of a 2CV image of the right ventricle, where the tricuspid valve is distinguished clearly, indicated by the blue arrow. The endocardium is not as marked, as it is much thinner surrounding the right ventricular volume.

On the 4CV view both ventricles are visible. In figure 4.2.3 an example can be seen, with the endocardium clearly distinguishable surrounding the left ventricle, the papillary muscle inside the ventricular volumes and the valve levels clearly marked.
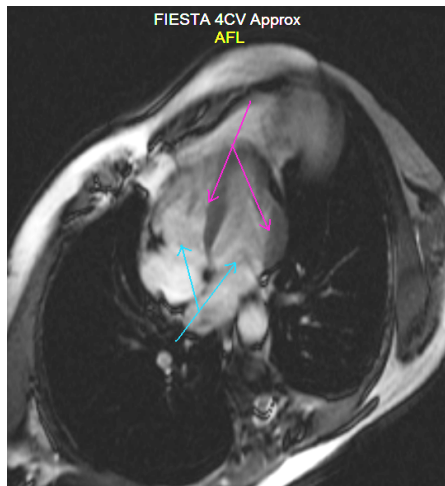
Figure 4.2.3: Example of a 4CV image of the left and right ventricles, where the mitral and tricuspid valves and endocardium surrounding the left ventricular volume are distinguished clearly, indicated by the blue and pink arrows respectively. The papillary muscle inside the volumes is also clearly visible.

On the SA view both ventricles are also visible. An example of a SA image is shown in figure 4.2.4, with the endocardium clearly distinguishable surrounding the left ventricle, and the papillary muscle inside the ventricular volumes. Delineation of the endocardial borders was good on these images, but the valve plane was again difficult to determine. A wrap-around artefact can also be seen in the image.
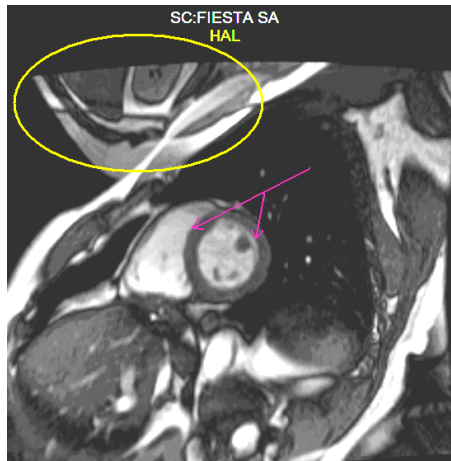
Figure 4.2.4: Example of a SA view image of the left and right ventricles, where the endocardium surrounding the left ventricular volume is indicated by the pink arrow. The papillary muscle inside the ventricular volumes is clearly visible in this view. Also note the wrap-around artefact, circled in yellow.

The gated MR imaging produced 20 phases, or images, per cardiac cycle for every slice imaged through the heart. The cardiac cycle starts at diastole, the heart contracts until end-systole, and ends again in diastole. Figure 4.2.5 demonstrates the 20 phases, imaged as one short-axis view slice, and end-diastole and end-systole were identified to be frames no. 1 and 6 respectively in this example.
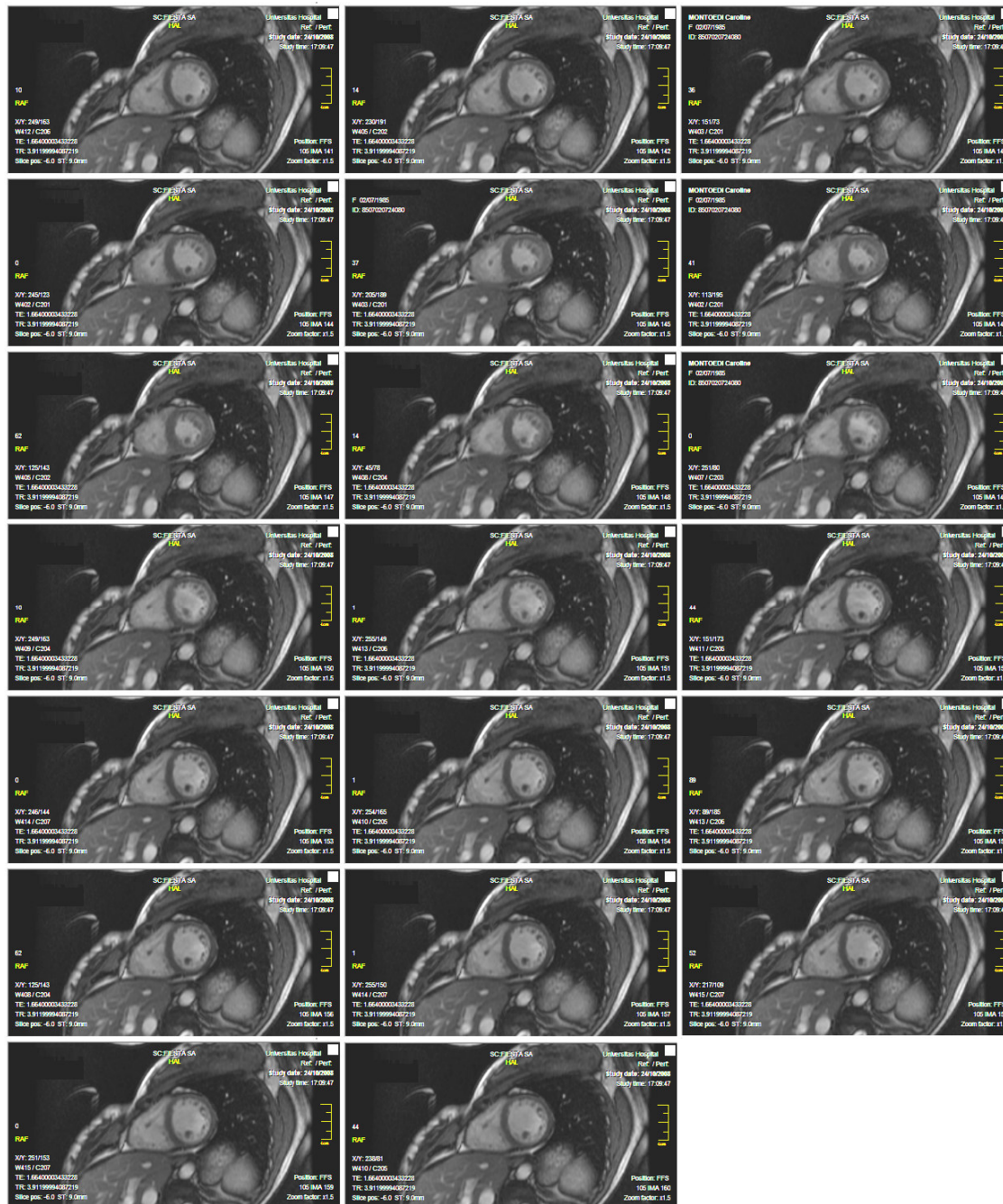
Figure 4.2.5: Example of a SA view slice imaged through the heart, with one cardiac cycle divided into 20 phase images

With the slice thickness of 9mm and no gaps between slices, the cardiac MR imaging with three imaging views produced 30 to 35 slices through the heart in total, with 20 images per slice, amounting to 600-700 images for an averaged sized heart.

Unfortunately, on many images segmentation was not as easy, due to artefacts and other factors like patient movement during imaging and a partial volume effect. The figures that follow show examples of such images. Flow artefacts and wrap-around artefacts occurred most. In some instances they interfered quite severely with ventricle edge delineation and contouring. The partial volume effect was seen in almost all imaging series, leading to uncertainty in the amount of blood actually present in an image with partial volume effect. A metal artefact was also seen. Figure 4.2.6 shows an example of a flow artefact; figure 4.2.7 the partial volume affect; figure 4.2.8 poor image quality; figures 4.2.9 and 4.2.10 wrap-around artefacts; and figure 4.2.11 a metal artefact.
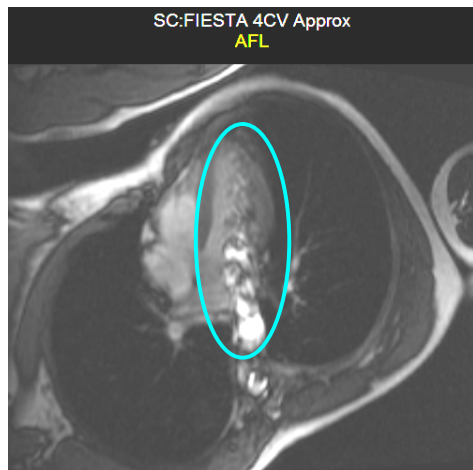
Figure 4.2.6: Example of flow artefact on 4CV image, disabling distinction of the left ventricular edges and mitral valve
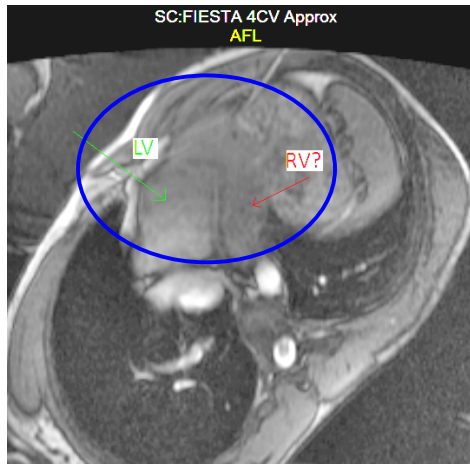
Figure 4.2.7: Example of the partial volume effect on 4CV image, creating uncertainty in the amount of RV to be included in the blood volume
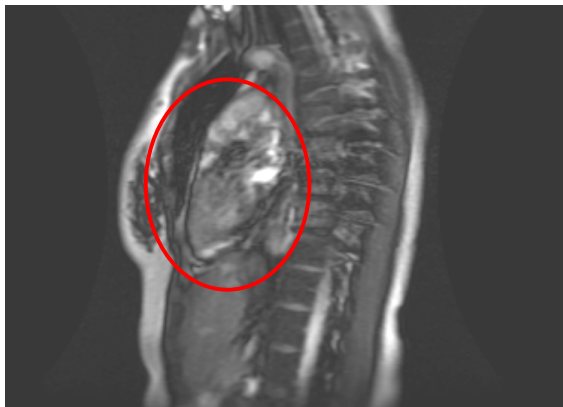
Figure 4.2.8: Example of an image with overall poor quality in the cardiac region, possibly due to patient movement or cardiac movement
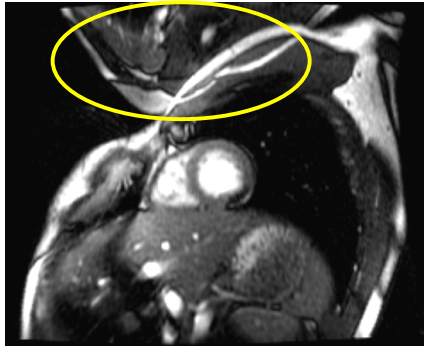
Figure 4.2.9: Example of a wrap-around artefact on SA image, although not influencing image quality or edge detection in the cardiac region
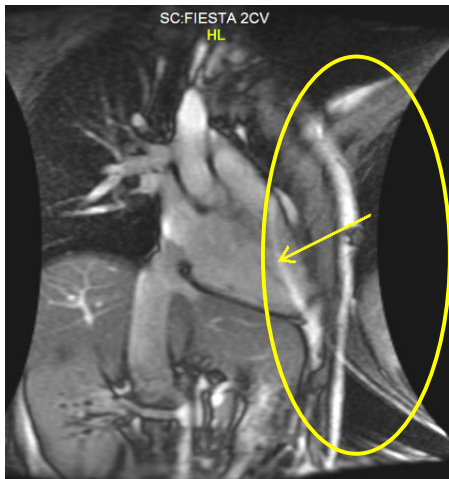
Figure 4.2.10: Example of a wrap-around artefact, influencing right ventricle volume image quality and edge detection
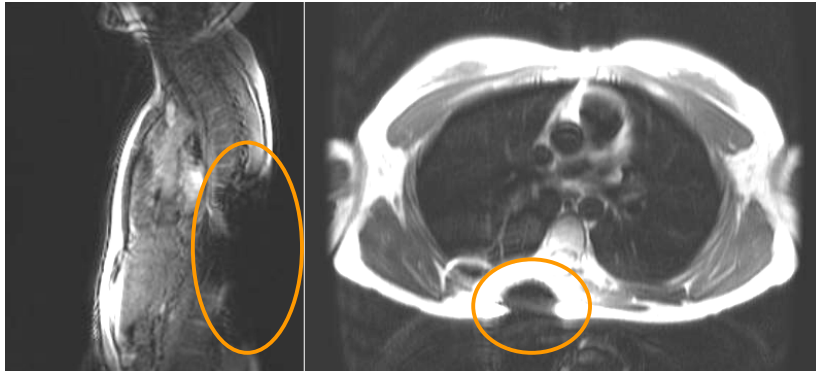
Figure 4.2.11: Example of a metal artefact, creating "holes" in the obtained images

These obtained images were then implemented for segmentation where possible. Volunteers with images that contained too many artefacts or of poor quality were not included in the study.

From the preliminary study described in Appendix C, it was seen that a certain amount of standardisation was necessary to ensure repeatable and consistent segmentation results, and it was decided that standardisation guidelines would be drafted for the study method. The standardisation guidelines will be discussed in general as well as more specific per imaging view.

4.2.2   STANDARDISATION AND GUIDELINES DERIVED FROM PRELIMINARY STUDY

Having the three sets of orientations related on a single coordinate system, assisted in linking a certain area on a slice on one orientation to the corresponding position on the other orientations. This was applied as far as possible to aid in determining positions, but due to the relatively large slice thickness of 9mm, the corresponding position could lie between slices and did not always contribute to the accuracy and certainty of delineation.

For segmentation of the cardiac ventricular volumes, it was attempted to apply standardised guidelines to keep the contours as close as possible or even equal to the anatomy. In all imaging views, for both the left and right ventricles, care was taken to exclude papillary muscle from the ventricular volume, as also suggested in the literature by Drake et al. (2007, p. 1014) and Codella et al. (2010, p. 847).

No smoothing or correction was done on slices where the partial volume effect had an effect.

Furthermore, certain guidelines were defined for each view to accomplish standardisation of the segmentation, and will be discussed as such. The example images given in the following discussion were from the same volunteer, with ED and ES identified on frames 1 and 9 respectively.

4.2.2.1   2-Chamber View segmentation guidelines

In the 2CV series, only a few slices are imaged through the volume of the ventricle, both left and right, resulting in a large ventricle area per image. With the relatively thick slice thickness of 9mm, such an arrangement lends for large errors due to the partial volume effect on slices through the myocardium. To minimise the influence of the partial volume effect, consistency had to be maintained throughout, including the same signal intensity on all slices as part of the volume.

The internal contour of the left ventricle was to be only included in the volume segmentation when it was clearly surrounded by myocardium. This minimises the influence of the partial volume effect as well as inclusion of vessel or atrial volumes that lie outside the muscular region of the ventricles. This muscular ventricular wall was noted to stop at mitral valve level on the 2CV slices.

The right ventricle was included up to the tricuspid valve and pulmonary valves. The tricuspid valve level could be distinguished rather easily. As the pulmonary semiluminar valves are quite thin, it complicated the segmentation. The guideline was to include the conus arteriosus, from which the pulmonary artery arises, up until where a tapering could be seen (see figure 4.2.13), and that was where the pulmonary valve level was estimated.

Where it was difficult to distinguish the valve levels, the phase scans could be viewed in a movie mode to aid in the contouring. It was also possible to use the linked coordinate system to see where on other imaging views the valve was positioned or moving.

Figure 4.2.12 and 4.2.13 show examples of contouring the left and right ventricles on 2CV images. The papillary muscle was excluded form the volume as far as reasonably achievable. The 9 images are all from the same 2CV slice and represent the first nine phases of the 20 phases in the cardiac cycle on that slice through the heart.
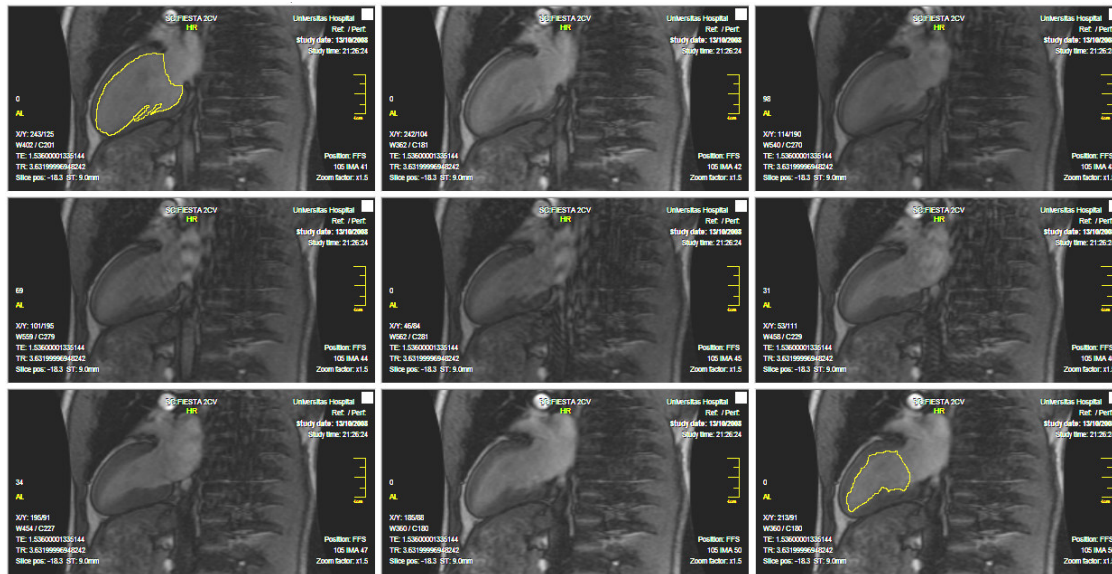
Figure 4.2.12: Segmentation of left ventricle on 2CV images, at ED (frame 1) and ES (frame 9)
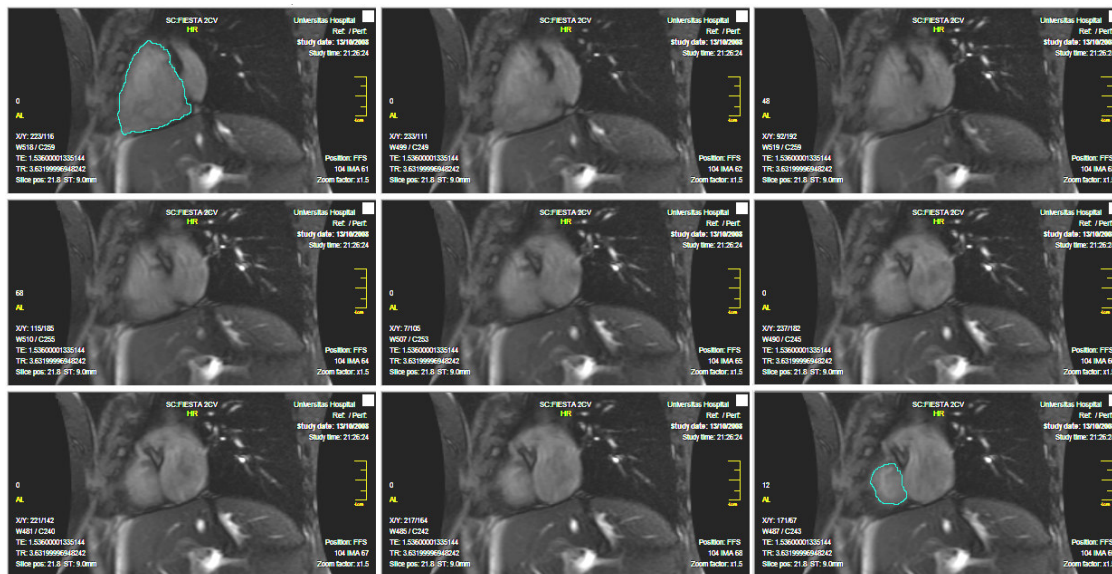
Figure 4.2.13: Segmentation of right ventricle on 2CV images, at ED (frame 1) and ES (frame 9)

4.2.2.2 4-Chamber View segmentation guidelines

The 4CV series also produced fewer slices through the two ventricles leading to larger ventricle areas per image, as the 4CV is also known as the long-axis imaging view.

In the 4CV, the partial volume effect is quite a problem on many images. The contouring is very user-dependent due to the variation in signal intensity. As with the 2CV images, the partial volume effect was minimised by means of consistency, including the same signal intensity on all slices as part of the volume.

Due to the positioning of the 4CV slices, the right and left ventricles are supposed to lie on the same level, in other words, if a 4CV slice clearly contains the left ventricle, the right ventricle is also visible in this slice, provided that the planning of the 4CV imaging was correct. Therefore, on a slice where the left ventricle is not visible anymore, and there is uncertainly whether the volume on the right belongs to the right ventricle or not, the guideline was to exclude such a volume from the right ventricular segmentation.

The mitral and tricuspid valve levels were reasonably easily identified.

Figure 4.2.14 shows an example of the left and right ventricles segmented on 4CV images. As in the 2CV example, the nine images represent nine phases of the cardiac cycle on this slice.
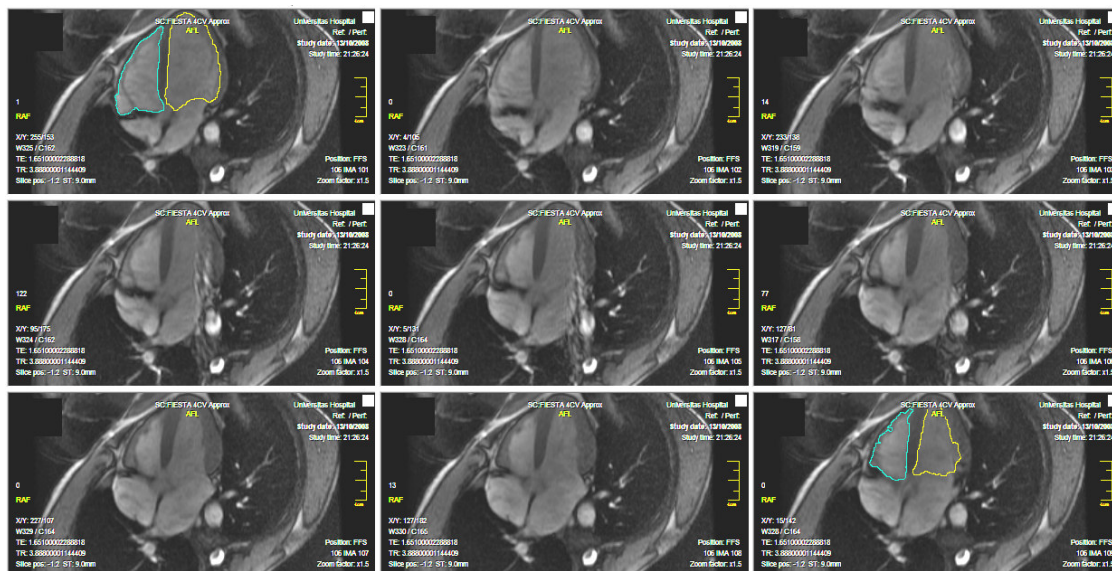
Figure 4.2.14: Segmentation of left (yellow contour) and right (green contour) ventricles on 4CV images, at ED (frame 1) and ES (frame 9)

4.2.2.3 Short-Axis view segmentation guidelines

The SA imaging view was the standard to use when clinically evaluating left ventricular function in the Radiology Department. Edge detection and segmentation of the left ventricle on SA slices were considered straightforward.

The left ventricle was to be only included in the volume segmentation when clearly surrounded by myocardium, which was relatively easy to distinguish, as the thick myocardium stopped at mitral valve level on the SA slices.

Due to the positioning of the SA slices as well, the right and left ventricles are supposed to lie on the same level, in other words, if a SA slice clearly contains the left ventricle, the right ventricle is also visible in this slice, provided that the planning of the SA imaging was correct. Therefore, on a slice where the left ventricle is not visible anymore, and there is uncertainly whether the volume on the right belongs to the right ventricle or not, the guideline was to exclude such a volume from the right ventricular segmentation. As imaging was planned to position the two valve levels in the same plane, i.e. on the same slice, contours of the two ventricles should only be included on slices where both ventricles can be delineated.

The mitral and tricuspid valve levels were overall easily identified. The valve level of the left ventricle was also only to be included in the ventricular volumes when surrounded with thick myocardium, otherwise it was considered to be atrium.

However, on the upper and left angle of the right ventricle segmentation became complex, as the transition from the conus arteriosus to the pulmonary artery was not clear.

The guideline was to include the conus arteriosus, from which the pulmonary artery arises, up until where a slight tapering could be seen, and that was where the pulmonary valve level was estimated.

Where it was difficult to distinguish the different valve levels, the phase scans could be viewed in a movie mode to aid in the segmentation. It was also possible to use the linked coordinate system to see where on other imaging views the valve was positioned or moving.

Figure 4.2.15 shows an example of the left and right ventricles segmented on SA images. As in the previous examples, the nine images represent nine phases of the cardiac cycle on this slice.
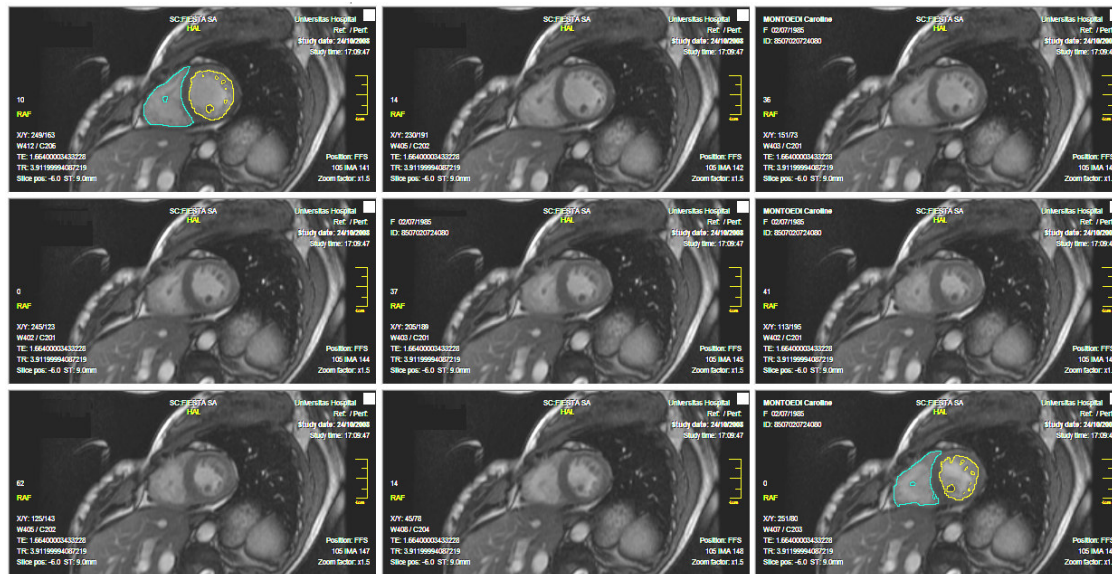
Figure 4.2.15: Segmentation of left (yellow contour) and right (green contour) ventricles on SA images, at ED (frame 1) and ES (frame 9).

4.3 VOLUME ANALYSIS

The calculation of volumes was done as described in section 4.1.4. The analysis of the data can also be divided into different sections and discussed and planned accordingly. Firstly, the volumes had to be determined from the segmented contours to create the test data. Thereafter, the inter-observer reliability, inter-method reliability and validity of the method and accompanying data had to be established. If all of these goals could be achieved, average normal values would be derived from quantification with the proposed method.

The volume and functional parameters were also compared with published values.

4.4 STATISTICAL ANALYSIS

Most statistical analyses were done by Prof. Gina Joubert of the Department of Biostatistics, University of the Free State, using the SAS system.

Three different procedures were used in the system to evaluate the data, namely the MEANS, TTEST and CORR procedures. The MEANS procedure was implemented as a first line of assessment to determine mean values, standard deviations, and minimum and maximum data values. The TTEST procedure was used to determine t values and Pr values to test for statistical significant differences, and the CORR procedure to test possible correlations by calculating Pearson correlation coefficients.

Microsoft Excel 2003 was used on a personal computer to construct graphs, plots and tables to display the data, as well as for further Student's t tests, regression analyses, box plot distributions and arbitrary calculations.

As no standard technique was available at Universitas Hospital as a reference for right ventricular function characterization, the 3 imaging views were analyzed separately as well as combined, with the right ventricular volumes compared to left ventricular volumes. The volumes were averaged for many of the tests.

The results were analysed regarding differences between observers and differences between imaging views; reliability, accuracy and statistical significance of the data; and normal values.

The statistics in the comparison of different groups of data were obtained by implementing 95% confidence levels and applying a T test to compare the differences between the separate groups. A p value < 0.05 was considered statistically significant.

4.5 CONCLUSION

With the inconsistency of the preliminary contouring results in mind, the segmentation in the final study was performed by three observers to determine and eliminate inter-observer dependency and to establish average normal values with an acceptable statistical variance.

As it has been stated that the role of cardiac MRI-trained physicists is important (Dahya & Spottiswoode 2010), it was decided that all three the observers would be medical physicists.

From the preliminary study described in Appendix B, it was seen that a certain amount of standardisation was necessary to ensure repeatable and consistent results. Therefore the three observers should get training from experts in anatomy and cardiac imaging, as it has been shown by Prakken et al. (2008, p. 110) that brief coaching of persons inexperienced in cardiac MRI, provides reliable volume and function quantification of both the cardiac ventricles. Mr. Alkie Gous and Johan Steyl of the Anatomy Department, University of the Free State, and Prof. Coert de Vries, Radiology, were asked to assist in distinguishing between the anatomical components in the cardiac images.

5 QUANTIFICATION RESULTS AND ANALYSIS

5.1 INTRODUCTION

The problems described in the previous chapter showing artefacts on the images, difficulty in segmentation and inconsistency in the preliminary results emphasise the need to test the reliability of the data.

As a primary assessment of this study, the inter-observer reliability, inter-method reliability and validity of the data collected from 20 volunteers, by 3 different observers, were to be evaluated.

Reliability is the consistency of a set of measurements, and is inversely related to random error (Meeker & Escobar, 1998). Validity refers to the extent to which a measurement is well-founded and corresponds accurately to the real world, or the true cardiac volumes in our case. However, although validity is often assessed along with reliability, reliability does not imply validity, but rather limits it. So as reliability is necessary, but not sufficient for validity, reliability had to be established first.

Therefore a data comparison was made firstly between the three observers to test inter-observer reliability of the method. As it was unknown whether one imaging view would produce better results than another, the differences between observers were tested per imaging view. Secondly the inter-method reliability was tested by comparing the data from the three imaging views.

With the necessary reliability established, validity of this study could be determined. Only then could average values for the normal group be further examined.

The calculation and analysis methods to obtain the reliability and validity of this study will be discussed accordingly.

The aim of this part of the study was to determine the reliability and validity of using cardiac MRI for the determination of RV function by applying manual contouring as suggested in the previous chapter.

5.2 METHODS

5.2.1 POPULATION

Of the 20 initial volunteers entered into the study, data of only 12 could be used, as complete results from the other volunteers were not suitable due to data acquisition problems and/or data analysis problems, such as poor ECG gating, artefacts on the images, and poor quality images. One patient withdrew from the study due to claustrophobia. For collection of the required numbers, 8 more volunteers were selected and entered. Thus of the total of 28 volunteers entered into the study, only 20, of which 10 males and 10 females in the age range 21 to 53, were included in the analysis. Volunteers included in the study all stated that they had no known cardiac problems or history thereof, and all underwent cardiac ultrasound imaging to confirm this. These volunteers also represented persons of different body mass index (BMI), body surface area (BSA) and race. Informed consent was obtained from all the volunteers.

The volunteer details and demographic data, at the time the study was undertaken, are listed in Table 5.2.1 below, and calculated according to the following equations:

The body mass index (BMI) was calculated as follows using equation 5.2.1:

$$BMI(kg.m^{-2}) = \frac{Mass(kg)}{\left(Height(m)\right)^2} \qquad (5.2.1)$$

The body surface area (BSA) was calculated with the Mosteller (1987) formula in equation 5.2.2:

$$BSA(m^2) = \sqrt{\frac{Height(cm) \times Mass(kg)}{3600}} \qquad (5.2.2)$$

Table 5.2.1: Demographics of the volunteers included in the study population

Volunteer no.	Gender	Age (y)	Height (m)	Mass (kg)	BMI (kg.m^{-2})	BSA (m^2)
CMR1	Male	23	1.79	70	21.8	1.9
CMR2	Male	53	1.79	71	22.2	1.9
CMR3	Male	26	1.78	75	23.7	1.9
CMR4	Female	27	1.50	52	23.1	1.5
CMR5	Male	27	1.68	70	24.8	1.8
CMR7	Female	28	1.74	67	22.1	1.8
CMR8	Male	26	1.76	70	22.6	1.8
CMR9	Male	49	2.05	100	23.8	2.4
CMR11	Female	23	1.70	60	20.8	1.7
CMR13	Female	25	1.73	64	21.4	1.8
CMR15	Male	30	1.92	85	23.1	2.1
CMR16	Female	40	1.75	65	21.2	1.8
CMR17	Male	28	1.69	71	24.9	1.8
CMR18	Male	33	1.83	93	27.8	2.2
CMR19	Female	25	1.56	53	21.8	1.5
CMR22	Female	22	1.58	50	20.0	1.5
CMR23	Female	23	1.78	51	16.1	1.6
CMR26	Female	28	1.61	73	28.2	1.8
CMR27	Male	21	1.68	70	24.8	1.8
CMR28	Female	22	1.63	59	22.2	1.6

Manual contours representing the EDV and ESV were drawn on cardiac MR images for the left and right ventricles, and the corresponding volumes calculated as described in chapter 4. Stroke volumes (SV) and ejection fractions (EF) were derived from the measured data. Three observers repeated the sampling process.

To assess the data, the reliability was firstly evaluated.

5.2.2   RELIABILITY OF THE DATA

To test the reliability of the method and its results, the volumes and resultant ejection fractions were compared between the three observers to test inter-observer reliability, and between the three imaging views to test inter-method reliability. T values and p values were used to determine statistical significance in the measured differences.

Two types of reliability were investigated, i.e. inter-observer reliability and inter-method reliability. Inter-observer reliability is the variation in measurements when taken by different persons, but with the same method or instruments. To determine this reliability of the study, the segmentation measurements done by the three observers on the same software and on the same data were compared. Inter-method reliability is the variation in measurements of the same target, or data set, when taken by different methods, but with the same person or when inter-observer dependency can be ruled out. To determine the reliability of the study, the segmentation measurements from the three different imaging views were compared.

To compare the data from the three observers, differences between observers were employed in the analysis. The mean differences and standard deviations were reported per category (EDV, ESV, SV, EF) for both ventricles. The differences were calculated between observer 1 and 2, between 1 and 3, and between observer 2 and 3. Paired t tests determined the statistical significance in the differences, with a 95% confidence.

Although analyses like these are most of the time based on parametric methods and normal distributions, box plots have also been employed here to demonstrate the entire distribution of the data per observer, the study being the first of its kind for Universitas Hospital.

The linear relationship between the left and right ventricular volumes was investigated by a linear regression analysis per observer as a last test for inter-observer reliability.

With inter-observer reliability established first, the data could be incorporated as an average from the three observers for further investigation. To compare the data from the three imaging views, differences between the views were employed in the analysis. The mean differences and standard deviations were again reported per category (EDV, ESV, SV and EF) for both ventricles. The differences were calculated between the 2CV and 4CV, between 2CV and SA view, and between 4CV and SA view. Paired t-tests determined the statistical significance in the differences, with a 95% confidence. Another box and whisker chart was used to display the full distribution as a comparison between the three imaging views for inter-method reliability.

Only with inter-observer and inter-method dependency in the three imaging views ruled out, the data could be affirmed as reliable, and the validity of the data was investigated.

5.2.3 VALIDITY OF THE DATA

A comparison between the left and right stroke volumes was implemented as a practical indication of validity. Since the amount of blood that enters the heart through the right atrium, should under normal circumstances be the same amount that leaves the left ventricle, the amount of blood displaced by the two ventricles should be equal. In other words, the function of the left and right ventricles is related, and therefore the stroke volumes (SV) of the left and right ventricles should be equal.

The combined average values of the three observers and the three imaging views were implemented to investigate the stroke volume comparison between left and right ventricular measurements. This analysis was used to test the overall validity of the study method.

Since there was no acceptable means of determining right ventricular function at Universitas Hospital, it was even more important to test the validity of the data as no other local values were available. Thus RV values could only be judged according to the fact that the stroke volumes from both ventricles were the same.

The average SV values over the 20 volunteers were used to determine the mean left-to-right ratio of the two ventricles' SV, the mean absolute difference between LV SV and RV SV and their standard deviations.

An additional check for validity was to compare the left cardiac volumes to right cardiac volumes, where the right ventricle is anatomically larger than the left, and the resulting RV EF smaller than LV EF. A qualitative analysis was only applied in this determination and discussion of validity, as the results have been evaluated to be true already.

5.2.4 MALE AND FEMALE SUBGROUP DATA

To further refine the statistics, the data were split into 2 groups according to gender for further investigation. Differences in the groups of demographic factors between male and female participants were investigated by means of T tests, where p values < 0.05 stated statistical significant differences.

5.2.5 COMPARISON TO AVAILABLE DATA

The data derived in the current study were also compared to available data from different authors, namely Alfakih et al. (2003), Cain et al. (2009), Grothues et al. (2004), Hudsmith et al, (2005), Mooij et al. (2008) and Tandri et al. (2006). Values from these 6 studies were employed in a comparison, where all imaging was done on 1.5 T MRI scanners, with electrocardiographic gating. Horizontal long-axis and vertical long-axis image series were acquired and applied as localizers, and volume determination were based on short-axis cine images for both the left and right ventricles. Slice thickness varied from 6mm to 10mm.

Grothues et al. and Mooij et al. studied 20 healthy normal adults, Alfakih et al. 60, Cain et al. 76, Hudsmith et al. 108 and Tandri et al. 487 subjects. Manual contouring of endocardial borders were drawn of images at end-diastolic and end-systolic permitted the calculation of EDV, ESV, SV and EF. Papillary muscles were outlined and excluded from the ventricular volumes (Alfakih et al. 2003; Grothues et al. 2004; Hudsmith et al. 2005).

In two of the studies, specific guidelines were given on the contouring method. Both Alfakih et al. (2003) and Hudsmith et al. (2005) mentioned that at the base of the left ventricle, slices were included in the volume where at least 50% of the blood volume was surrounded by myocardium. For the right ventricle, if the pulmonary valve was evident, volumes below the valve were included, but at the inflow part of the RV, the blood volume was excluded from the RV volume where the surrounding muscle was thin and not trabeculated.

With such useful information, it was quite simple to compare the current study data to the published data.

The paragraphs that follow will display the results of the abovementioned analyses of this study.

5.3 RESULTS

The results will be split into separate categories. Firstly, the inter-observer and inter-method reliability will be assessed, followed by the determination of the validity of the data, and then a comparison to other published data. All mean values were displayed as the average plus or minus one standard deviation unless stated otherwise.

5.3.1 OVERVIEW OF MEASUREMENTS

The following bar graphs in figures 5.3.1 and 5.3.2 show the cardiac left ventricular volumes of all 20 volunteers as examples from the data measured by observer 1. LV EDV values can be seen in figure 5.3.1 shown for the three imaging views (2CV, 4CV and SA), and LV ESV values in figure 5.3.2.
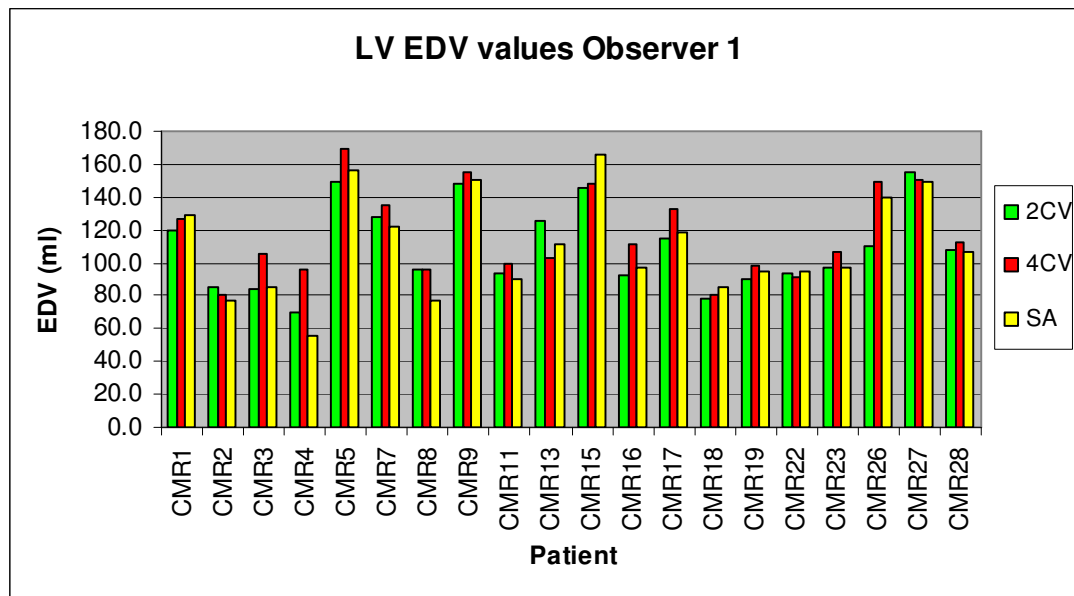
Figure 5.3.1: Left ventricle EDV values measured by observer 1, displayed per imaging view for every volunteer
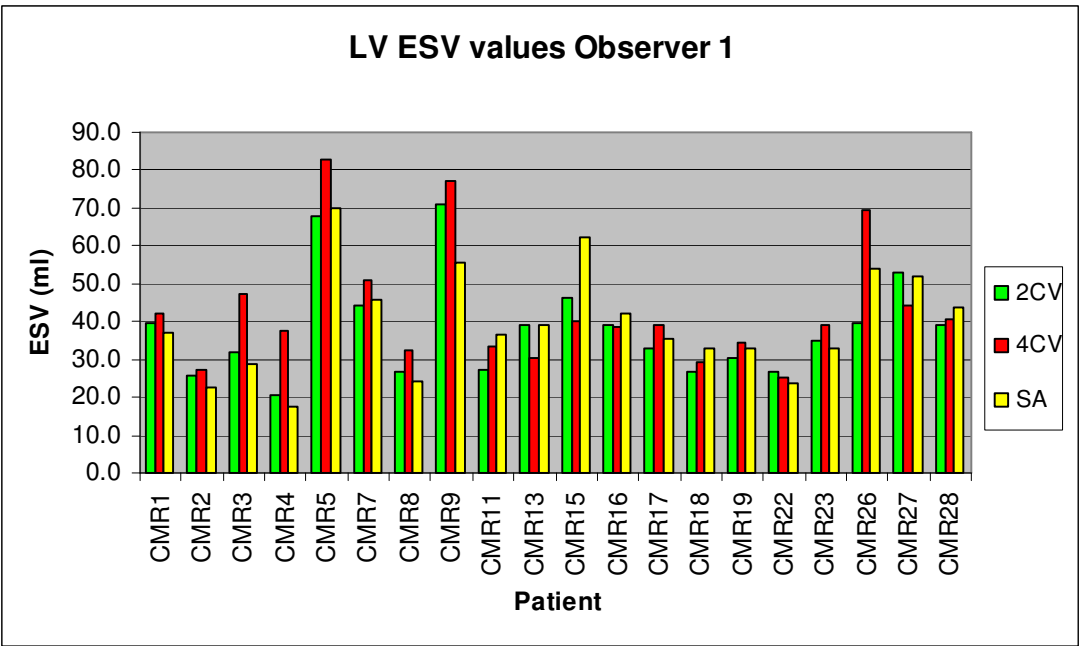
Figure 5.3.2: Left ventricle ESV values measured by observer 1, displayed per imaging view for every volunteer

Figures 5.3.3 and 5.3.4 show the cardiac right ventricular volumes of all 20 volunteers as examples from the data measured in the short-axis imaging view. RV EDV values can be seen in figure 5.3.3 shown as measured by the three observers, and RV ESV values in figure 5.3.4.
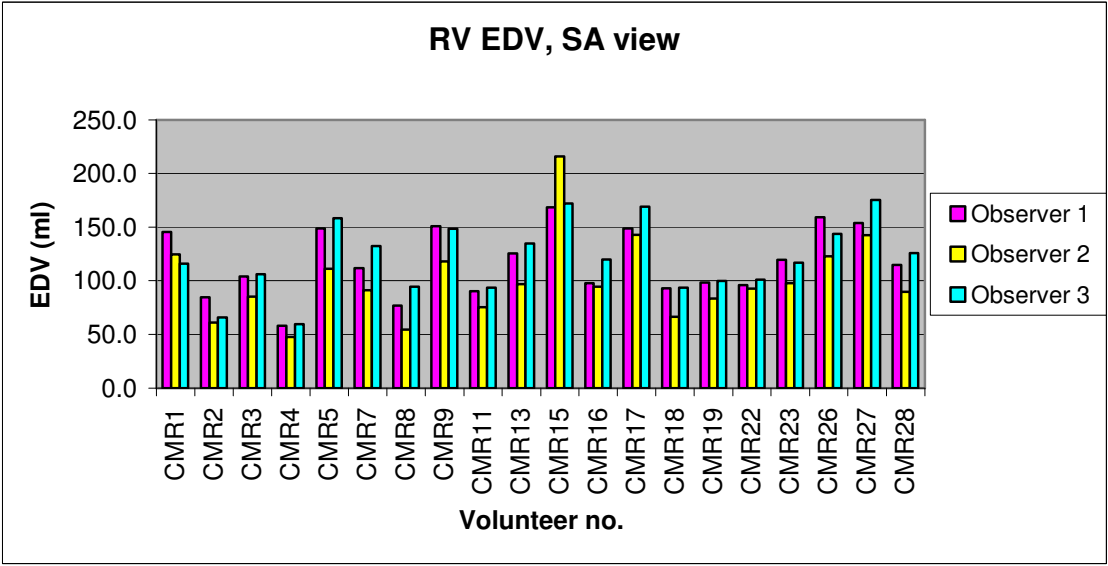
Figure 5.3.3: Right ventricle EDV values from SA view data, displayed per observer for every volunteer
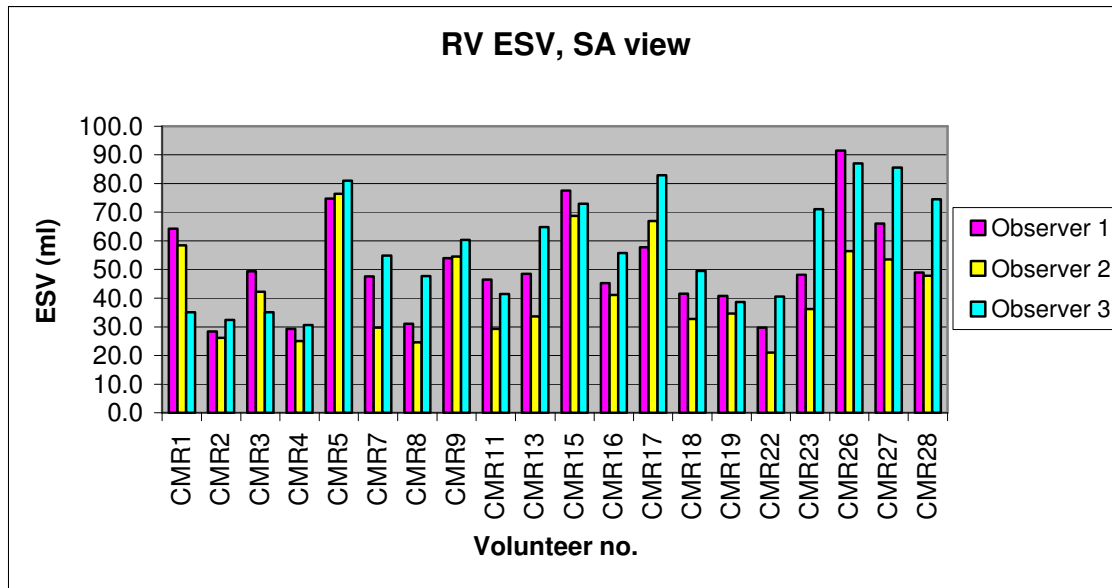
Figure 5.3.4: Right ventricle ESV values from SA view data, displayed per observer for every volunteer

Table 5.3.1 sorts the values per observer, and also includes SV and EF data. The mean volumes and ejection fractions of the whole group, averaged over the three views, are shown with their corresponding standard deviations. The values are listed first for the left ventricle, and then for the right ventricle.

Table 5.3.1: Mean values ± standard deviation for volumes and ejection fractions as determined by the 3 observers

All patients (n=20), average of 3 views

Parameter	Observer 1 Mean ± 1SD			Observer 2 Mean ± 1SD			Observer 3 Mean ± 1SD		
LV EDV (mℓ)	112.2	±	27.4	103.7	±	28.3	115.2	±	28.3
LV ESV (mℓ)	40.2	±	14.3	37.1	±	13.8	41.4	±	14.4
LV SV (mℓ)	72.0	±	16.5	66.5	±	18.2	73.7	±	18.8
LV EF (%)	64.7	±	5.8	64.5	±	6.6	64.3	±	6.9
RV EDV (mℓ)	118.3	±	28.4	102.3	±	33.1	119.2	±	31.2
RV ESV (mℓ)	48.3	±	14.4	40.6	±	14.5	51.3	±	16.7
RV SV (mℓ)	70.0	±	17.5	61.8	±	23.5	67.9	±	20.5
RV EF (%)	59.3	±	6.0	59.9	±	8.7	56.9	±	8.5

These measurements were then utilised to test firstly the inter-observer reliability of the data, then the inter-method reliability, and thirdly the validity of the obtained data.

5.3.2 INTER-OBSERVER RELIABILITY

The results in the following paragraphs will compare the segmented volumes measured by the three different observers to test the inter-observer reliability of the data.

5.3.2.1 Comparison between observers

The differences in the data from the three different observers were analysed by means of a paired t-test. The statistics in table 5.3.2 to 5.3.4 contain the mean differences between named observers, the standard deviations of the corresponding differences, and Pr values with a confidence of 95% for the three imaging views respectively. Statistical significance was acknowledged at Pr values smaller than 0.05, and are marked in bold. The parameters used in the tables are described below table 5.3.2, and all follow the same principle:

Table 5.3.2: Statistics from a T-test based on differences between the three observers in the 2-Chamber View data, where the first row data was calculated on differences in LV EDV values between observers 1 and 2. Mean differences are tabulated in units of mℓ for volumes and % for ejection fractions.

2-Chamber View data Parameter	Mean	Std dev	Pr > |t|
Left ventricle			
Diff12LVEDV	0.97	7.35	0.5625
Diff13LVEDV	-4.38	10.19	0.0695
Diff23LVEDV	-5.35	12.37	0.0680
Diff12LVESV	-2.31	4.78	**0.0433**
Diff13LVESV	-2.42	7.85	0.1833
Diff23LVESV	-0.11	8.94	0.9567
Diff12LVSV	3.28	6.96	**0.0484**
Diff13LVSV	-1.96	11.06	0.4383
Diff23LVSV	-5.24	12.06	0.0668
Diff12LVEF	2.79	4.48	**0.0118**
Diff13LVEF	1.26	6.95	0.4292
Diff23LVEF	-1.53	7.61	0.3782
Right ventricle			
Diff12RVEDV	9.85	16.86	**0.0171**
Diff13rVEDV	1.56	11.11	0.5384
Diff23RVEDV	-8.30	19.39	0.0709
Diff12RVESV	2.80	8.13	0.1404
Diff13RVESV	-2.80	9.97	0.2238
Diff23RVESV	-5.60	12.31	0.0561
Diff12RVSV	7.06	12.18	**0.0179**
Diff13RVSV	4.36	9.37	0.0512
Diff23RVSV	-2.69	14.74	0.4236
Diff12RVEF	1.20	5.61	0.3496
Diff13RVEF	3.26	7.17	0.0562
Diff23RVEF	2.06	8.21	0.2761

Diff12LVEDV: Differences between observer 1 and observer 2 in the left ventricle end-diastolic volume (EDV) values

Diff23RVSV: Differences between observer 2 and observer 3 in the right ventricle stroke volume (SV) values

From the values in table 5.3.2 above it can be seen that there were statistically significant differences in the volumes measured by the 3 observers, for example the LV ESV values in the 2CV data between observer 1 and observer 2 differed significantly with a Pr value of 0.0433.

When looking at only the 2CV data in table 5.3.2, there were statistically significant differences between the observers, but out of the three groups of imaging view data, the least differences between observers were found in the 2CV data. Only between observers 1 and 2 significant differences were seen, and then only in one instance in the EF data, where the mean difference in the LV EF data was but 2.79% with a standard deviation of 4.48%.

Table 5.3.3: Statistics from a T-test based on differences between the three observers in the 4-Chamber View data, where the first row data was calculated on differences in LV EDV values between observers 1 and 2. Mean differences are tabulated in units of mℓ for volumes and % for ejection fractions.

4-Chamber View data			
Parameter	Mean	Std dev	Pr > |t|
Left ventricle			
Diff12LVEDV	14.33	17.63	**0.0018**
Diff13LVEDV	-5.40	16.14	0.1513
Diff23LVEDV	-19.73	16.82	**<0.0001**
Diff12LVESV	4.72	8.25	**0.0192**
Diff13LVESV	-2.01	13.36	0.5094
Diff23LVESV	-6.73	12.72	**0.0288**
Diff12LVSV	9.61	14.43	**0.0077**
Diff13LVSV	-3.39	9.87	0.1412
Diff23LVSV	-13.00	15.91	**0.0017**
Diff12LVEF	0.80	5.12	0.4943
Diff13LVEF	0.04	6.53	0.9789
Diff23LVEF	-0.76	7.90	0.6720
Right ventricle			
Diff12RVEDV	21.49	18.97	**0.0001**
Diff13RVEDV	-0.10	13.92	0.9754
Diff23RVEDV	-21.59	23.93	**0.0007**
Diff12RVESV	12.24	11.01	**0.0001**
Diff13RVESV	-0.15	10.81	0.9519
Diff23RVESV	-12.39	11.82	**0.0002**
Diff12RVSV	9.25	16.67	**0.0226**
Diff13RVSV	0.05	12.90	0.9862
Diff23RVSV	-9.20	17.90	**0.0331**
Diff12RVEF	-3.04	8.61	0.1312
Diff13RVEF	0.37	7.75	0.8335
Diff23RVEF	3.41	8.23	0.0797

In the 4CV data in table 5.3.3 statistical significant differences were found between observers 1 and 2 and observers 2 and 3 in all of the volume measurements. Still, these differences did not influence the ejection fractions, as there were no significant differences ($p > 0.05$) in the 4CV left or right EF data. No significant differences were found between observers 1 and 3.

Table 5.3.4: Statistics from a T-test based on differences between the three observers in the Short Axis View data, where the first row data was calculated on differences in LV EDV values between observers 1 and 2. Mean differences are tabulated in units of mℓ for volumes and % for ejection fractions.

Short Axis view data			
Parameter	Mean	Std dev	Pr > |t|
Left ventricle			
Diff12LVEDV	10.44	6.68	**<0.0001**
Diff13LVEDV	1.03	9.07	0.6180
Diff23LVEDV	-9.42	8.90	**0.0001**
Diff12LVESV	6.92	5.68	**<0.0001**
Diff13LVESV	0.85	6.47	0.5636
Diff23LVESV	-6.07	5.62	**0.0001**
Diff12LVSV	3.53	7.37	**0.0455**
Diff13LVSV	0.18	9.58	0.9349
Diff23LVSV	-3.35	8.91	0.1092
Diff12LVEF	-3.19	4.64	**0.0062**
Diff13LVEF	-0.12	5.62	0.9219
Diff23LVEF	3.07	5.26	**0.0172**
Right ventricle			
Diff12RVEDV	16.65	18.08	**0.0006**
Diff13RVEDV	-4.04	13.81	0.2058
Diff23RVEDV	-20.70	20.48	**0.0002**
Diff12RVESV	8.09	9.13	**0.0008**
Diff13RVESV	-6.05	13.71	0.0632
Diff23RVESV	-14.14	14.64	**0.0004**
Diff12RVSV	8.57	19.27	0.0614
Diff13RVSV	2.00	11.25	0.4351
Diff23RVSV	-6.56	18.68	0.1326
Diff12RVEF	0.08	8.94	0.9684
Diff13RVEF	3.64	9.36	0.0979
Diff23RVEF	3.56	11.20	0.1709

The SA data in table 5.3.4 again show differences between observers 1 and 2 and observers 2 and 3 in the EDV and ESV values, and in the LV SV values only between observers 1 and 2. Unfortunately, there were two instances of statistical difference in the LV EF data, between observers 1 and 2 and observers 2 and 3. Still, the mean differences were only -3.19% and 3.07%.

In the rest of the data no statistical significant difference ($p > 0.05$) was found between the ejection fractions calculated by the different observers.

In all three tables, i.e. in the data from all three the imaging views, differences between the observers in the measured volumes can be noticed.

In the 4CV (table 5.3.3) and SA data (table 5.3.4), the differences in LV and RV measured volumes were between observer 1 and 2, and between 2 and 3. In the 2CV data, differences in measured volumes were only found between observer 1 and 2. Taking this into account, it was not surprising to find differences in the SV values in the same groups of data.

Some differences in EF values between the observers were significant.

The results from the three observers will be analysed further in box plot graphs to show the full distribution in the ejection fraction values.

5.3.2.2 Ejection Fraction box plots

The following Box and Whisker diagrams have boxes showing the range from first to third quartiles, with the median dividing the box into two smaller areas for the second and third quartiles. The whiskers span the first quartile, from the second quartile box down to the minimum, and the fourth quartile, from the third quartile box up to the maximum.

The spacing between the different parts of the box, and the length of the whiskers, give an indication of the degree of distribution in the data.

These three Box and Whisker charts in figure 5.3.5 to figure 5.3.7 display the EF data per observer, for both ventricles, for the 2CV, 4CV and SA imaging views respectively.
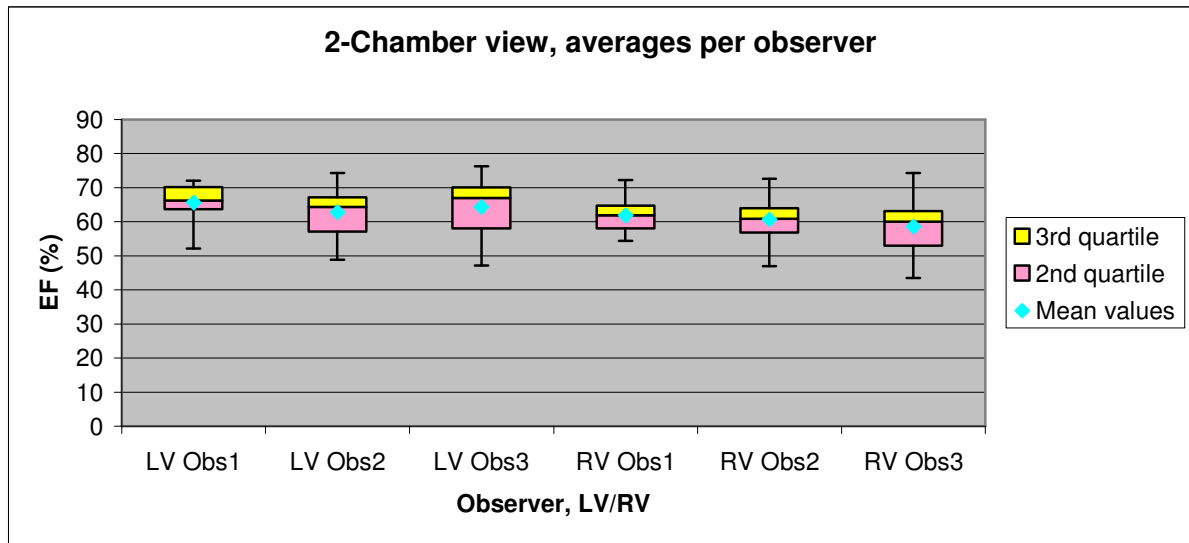
Figure 5.3.5: Boxplot of EF statistics from 2-Chamber view data, for both ventricles and for all three observers. The endpoints of the whiskers show the maximum and minimum values in the data
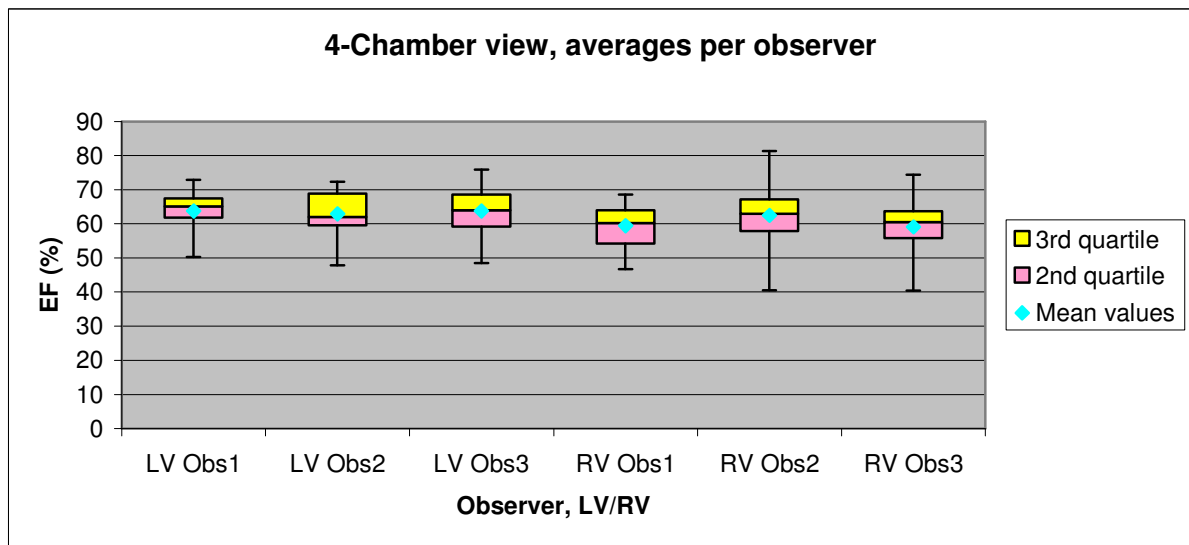
Figure 5.3.6: Boxplot of EF statistics from 4-Chamber view data, for both ventricles and for all three observers

What may look like outliers in these plots, have been declared real measured values and was kept as part of the data sets. As an example, in the 4CV data in figure 5.3.6, the whiskers of the RV EF box plot of observer 2 are reasonably longer than those of observer 1. It may be argued that the maximum and minimum EF values measured

here were outliers, but as the same plots show that the data distribution is in the form of a normal distribution, the whole range of values were maintained as the true data set.
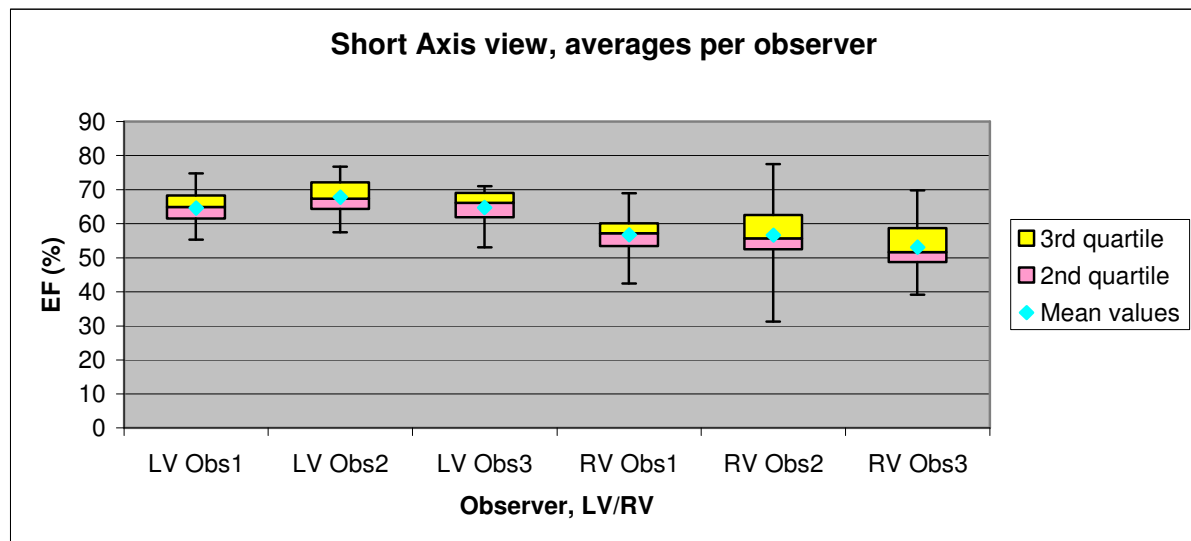
Figure 5.3.7: Boxplot of EF statistics from Short Axis view data, for both ventricles and for all three observers

To have a further comparison between the data from the three observers, box and whiskers plots were implemented here to show the full range of the data distribution.

Box and whisker plots are a simple way of displaying and comprehending the distribution in a set of data, and where the majority of data points lie in the distribution. In such a plot, the median of the data set, the full range and the width of the distribution can be found. The whiskers indicate the minimum and maximum values in the dataset. If there are outliers, they can easily be identified, as the whiskers extend to their maximum of 1.5 times the inter-quartile range. In the plots in figures 5.3.5 to 5.3.7 the mean values were also added extra to the graphs.

In the following discussion of the box plots, LV plots will be compared to LV plots and RV to RV, when data from the three observers are compared.

If figure 5.3.5 is used as an example, the plots for the 2-Chamber view data are displayed. The average LV and RV EF values for all 3 observers are shown separately. When comparing the RV data of observer 2 to that of observer 3, it can be said that the median values of the two data sets are comparable. The median of observer 2 divides the box in the middle, which means that the distribution of the data points in the second and third quartile is equal. For observer 3 the data are clustered between the median and the upper quartile. When comparing the 2CV RV

plots for the three observers, the plots overlap in the inter-quartile range, although the minimum values differ between the observers.

In the same graph, the median of the LV data of observer 1 is slightly higher than for observer 2. In this case, the data points are clustered between the median and the upper quartile for observers 2 and 3, and between the median and lower quartile for observer 1, although not as obvious. Still, all 3 LV plots overlap, with the maximum and minimum values differing slightly between observers.

5.3.2.3   Relationship between RV and LV volumes per observer

The relationship between the RV and LV data was also investigated for each observer. The following graphs are plots of the LV volumes against the RV volumes, to test whether there is a linear relationship between the volumes of the two ventricles. Figures 5.3.8 to 5.3.10 illustrates the linearity for observer 1, 2 and 3 respectively.
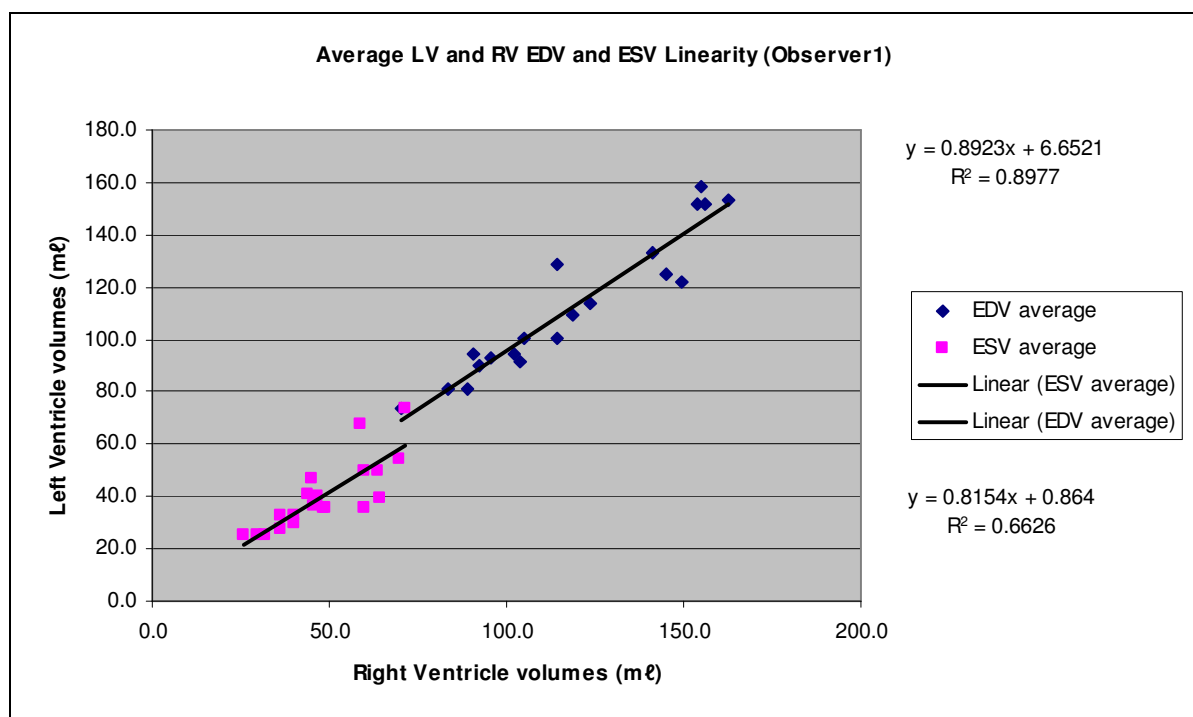
Figure 5.3.8: Linearity between left and right ventricular volumes: Average LV EDV and ESV versus average RV EDV and ESV for observer 1
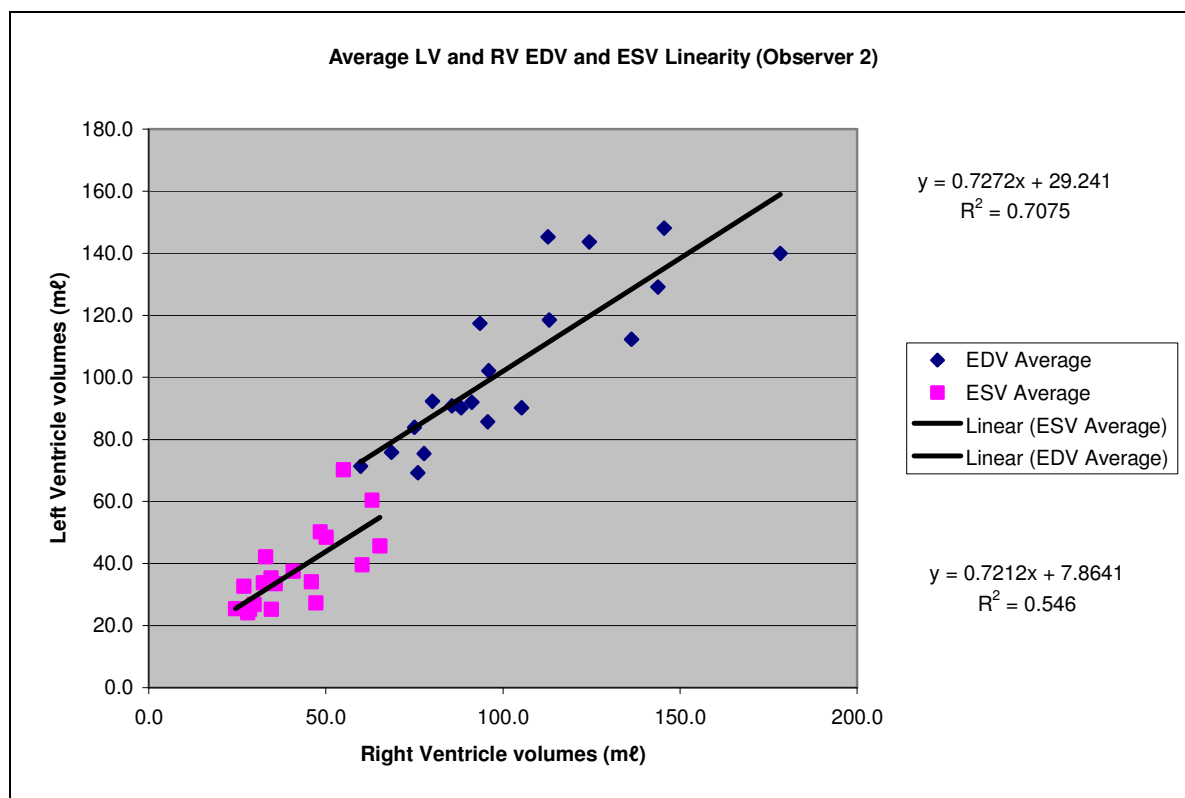
Figure 5.3.9: Linearity between left and right ventricular volumes: Average LV EDV and ESV versus average RV EDV and ESV for observer 2
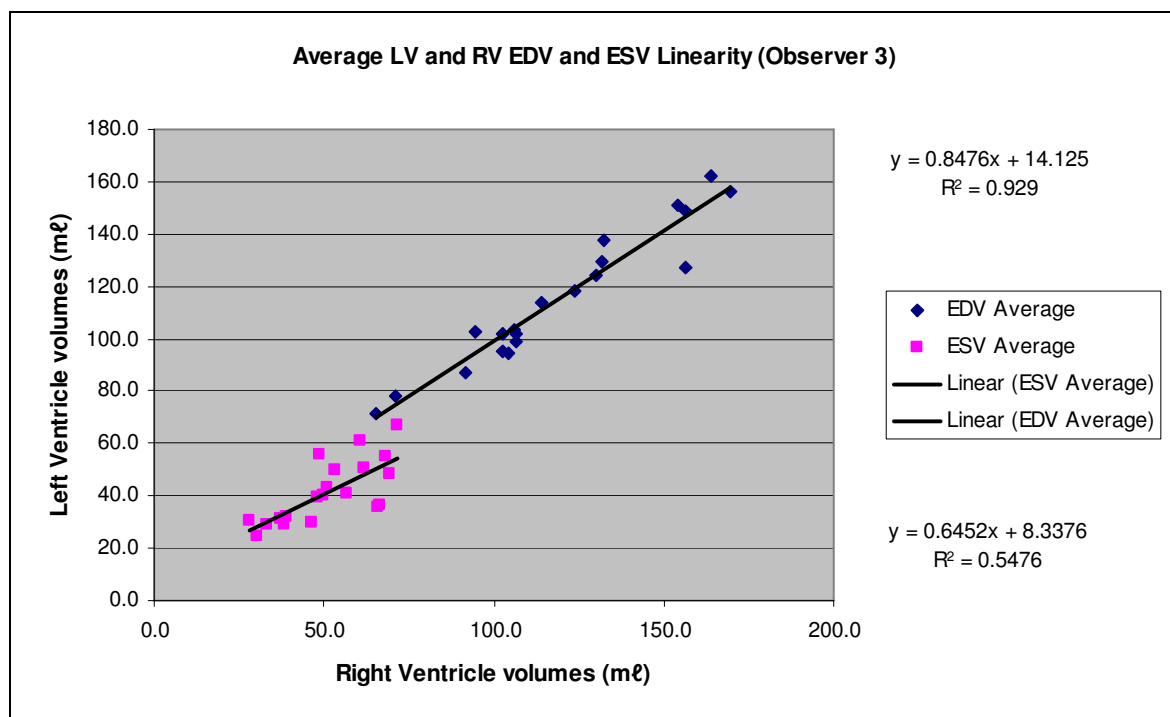
Figure 5.3.10: Linearity between left and right ventricular volumes: Average LV EDV and ESV versus average RV EDV and ESV for observer 3

Graphs of the LV volumes against the RV volumes were plotted to test whether there is a linear relationship between the volumes of the two ventricles. Figures 5.3.8 to 5.3.10 illustrated the linearity for observer 1, 2 and 3 respectively, where a linear regression line was fitted to the data and the coefficients of determination (R^2) that compares estimated and actual y-values were calculated.

Table 5.3.5 includes a summary of the regression equation values for the three observers, with errors on the parameters for the graphs in figure 5.3.8 to figure 5.3.10. The method of least squares was implemented to determine the best fit for the data, calculated with the "linest" function in Microsoft Excel. F probability distribution values can also be seen in the table, indicating whether the observed relationships between the dependent and independent variables occurred by chance. The F values and their accompanying statistics were determined with the "fdist" function in Microsoft Excel.

The slopes (m) of all 6 fitted straight lines were positive, which confirms that the one variable will increase when the other variable does. For example, in a group of data, if the LV EDV is larger for participant X than for participant Y, the RV EDV will also be larger for participant X. This was expected.

The slopes (m) of all 6 equations also had a value of less than 1, which predicts that, for the range of absolute non-zero values (volumes) measured, RV volumes are larger than LV volumes. As published data have shown that the right ventricle is indeed larger than the left, this constant again confirms the expectation of the measured data.

Table 5.3.5: Regression equations, shown with errors on parameters.

F probability distribution	Observer 1		Observer 2		Observer 3	
	EDV	ESV	EDV	ESV	EDV	ESV
m	0.892	0.815	0.727	0.721	0.848	0.645
se	0.071	0.137	0.110	0.155	0.055	0.138
b	6.652	0.864	29.241	7.864	14.125	8.338
seb	8.627	6.861	11.739	6.587	6.776	7.327
sey	8.778	8.028	14.574	8.751	7.177	8.272
R^2	0.898	0.663	0.708	0.546	0.929	0.548
F	158.0	35.3	43.5	21.6	235.5	21.8
df	18	18	18	18	18	18
ssreg	12172.5	2278.2	9248.0	1657.8	12131.8	1490.6
ssresid	1387.1	1160.2	3823.2	1378.4	927.1	1231.6
sstotal	13559.6	3438.4	13071.2	3036.2	13059.0	2722.2
Fdist	2.39E-10	1.26E-05	3.39E-06	1.98E-04	8.79E-12	1.92E-04

In table 5.3.5, the acronyms have the following meanings:

m   The slope of the straight line fitted to the data. The equation of the straight line is y = mx + b.

b   The y-intercept of the line

se   The standard error value for the coefficient m

seb   The standard error value for the constant b

sey   The standard error for the y estimate

R^2 The coefficient of determination

F	The F statistic, or the F-observed value
df	The degrees of freedom, which can be used to find F-critical values in a statistical table to determine a confidence level for the model.
ssreg	The regression sum of squares
ssresid	The residual sum of squares
Fdist	Values obtained by a Microsoft Excel function "FDIST(F,v1,v2)" to calculate the probability of a larger F value occurring by chance, where v1 = n – df – 1 and v2 = df.
n	Number of data points = 20

The smaller the residual sum of squares compared to the total sum of squares (the sum of the residual and regression sums of squares), the larger the value of the coefficient of determination (R^2), an indicator of the quality of the regression analysis.

The coefficient of determination compares estimated and actual y-values, and ranges in value from 0 to 1. If R^2 is equal to 1, there is a perfect correlation in the sample, which means that there is no difference between the actual y-values and the estimated y-values. However, if the coefficient of determination is equal to 0, the regression equation cannot be used to predict a y-value.

The F-observed values were compared to critical values for the F distribution found in published statistics tables by Filliben & Heckert (2003, p. 2 of 11). For a one-sided test, the null hypothesis is rejected when the F-observed value is greater than the tabled value. Assuming an Alpha value of 0.05 (5% significance level), the critical value for the F probability with abovementioned degrees of freedom (v1 = 1 and v2 = 18) was 4.414 as found in the abovementioned tables. All the F-observed values were higher than the critical value. This is also confirmed by the Fdist values displaying small probabilities of larger F values occurring by chance. Thus the null hypothesis is rejected, and the F distributions did not occur by chance.

The results will be further analysed as the average from the three observers, compared between the three imaging views.

5.3.3 INTER-METHOD RELIABILITY

The results in the following paragraphs will compare the volumes measured from the three different imaging views to test the inter-method reliability of the data set, where inter-observer reliability was confirmed.

5.3.3.1 Volumes measured in each imaging view

The three imaging views were investigated separately to determine whether there were analogous results from the different views. The average volumes and ejection fractions from the three observers were employed to test the data per view.

Table 5.3.6 sorts the values per imaging view. The mean volumes and ejection fractions of the whole group, averaged for the three observers, are shown with their corresponding standard deviations. The values are listed first for the left ventricle, and then for the right ventricle.

Table 5.3.6: Mean values ± standard deviation for volumes and ejection fractions as determined for the three imaging views

All patients (n=20), average of 3 observers

Parameter	2CV Mean ± 1SD			4CV Mean ± 1SD			SA Mean ± 1SD		
LV EDV (mℓ)	110.4	±	25.5	114.3	±	29.6	106.3	±	29.5
LV ESV (mℓ)	39.8	±	13.2	42.2	±	16.1	36.9	±	12.8
LV SV (mℓ)	70.7	±	16.8	72.1	±	18.4	69.5	±	19.1
LV EF (%)	64.2	±	6.8	63.5	±	6.7	65.7	±	5.4
RV EDV (mℓ)	116.0	±	30.0	110.7	±	30.4	113.1	±	34.9
RV ESV (mℓ)	45.8	±	13.4	44.0	±	15.0	50.4	±	18.3
RV SV (mℓ)	70.2	±	20.0	66.8	±	20.2	62.8	±	21.9
RV EF (%)	60.3	±	6.7	60.4	±	7.8	55.5	±	8.3

These results obtained in each imaging view will be compared to analyse the inter-method reliability.

5.3.3.2 Comparison between imaging views

The differences in the data from the three different imaging views were analysed by means of a T-test. The statistics in table 5.3.7 were obtained by implementing confidence levels of 95%. Statistical significant differences were acknowledged at Pr values smaller than 0.05, and are marked in bold. The parameters used in the tables are described below table 5.3.7, and all follow the same principle:

Table 5.3.7: Statistics from a T-test based on differences in the data from the three imaging views. Mean difference are tabulated in units of mℓ for volumes and % for ejection fractions.

Parameter	Mean	Std dev	Pr > |t|
Left ventricle			
Diff2cv4cv.LVEDV	-3.8776	14.0229	0.2313
Diff 2cvSA.LVEDV	4.1023	10.1827	0.0875
Diff4cvSA.LVEDV	7.9798	15.7810	**0.0357**
Diff2cv4cv.LVESV	-2.4263	8.9775	0.2416
Diff2cvSA.LVESV	2.9055	6.1964	**0.0496**
Diff4cvSA.LVESV	5.3317	9.5784	**0.0222**
Diff2cv4cv.LVSV	-1.4513	7.0837	0.3710
Diff2cvSA.LVSV	1.1968	7.9610	0.5095
Diff4cvSA.LVSV	2.6481	9.3554	0.2209
Diff2cv4cv.LVEF	0.7034	4.0717	0.4493
Diff2cvSA.LVEF	-1.5258	-3.5192	0.1256
Diff4cvSA.LVEF	-2.2292	4.5738	**0.0421**
Right ventricle			
Diff2cv4cv.RVEDV	5.2684	10.8889	**0.0434**
Diff 2cvSA.RVEDV	2.8894	13.0199	0.3334
Diff4cvSA.RVEDV	-2.3791	14.1226	0.4605
Diff2cv4cv.RVESV	1.8352	7.6353	0.2959
Diff2cvSA.RVESV	-4.5346	10.6746	0.0728
Diff4cvSA.RVESV	-6.3697	6.9643	**0.0006**
Diff2cv4cv.RVSV	3.4333	9.1100	0.1083
Diff2cvSA.RVSV	7.4239	9.7510	**0.0030**
Diff4cvSA.RVSV	3.9907	10.3973	0.1023
Diff2cv4cv.RVEF	-0.0135	5.3201	0.9911
Diff2cvSA.RVEF	4.8921	6.3934	**0.0029**
Diff4cvSA.RVEF	4.9056	4.0273	**<0.0001**

Diff2cv4cv.LVEDV: Differences between 2CV and 4CV data in the left ventricle end-diastolic volume (EDV) values

Diff4cvSA.RVSV: Differences between 4CV and SA data in the right ventricle stroke volume (SV) values

The average EF values will also be used in box plots to illustrate the distribution per imaging view, and to compare them.

The next Box and Whisker chart in figure 5.3.11 displays the EF data per imaging view, for both ventricles, as averages from the data of the three observers. Graphs displaying the plots for the three observers separately can be found in Appendix C.
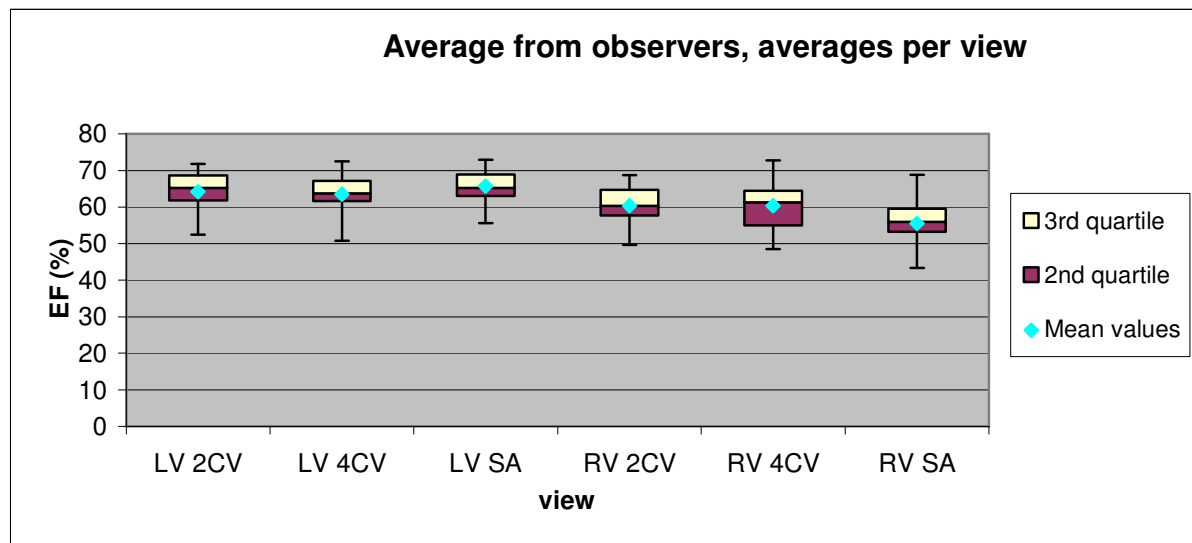
Figure 5.3.11: Boxplot of EF statistics comparison for 2CV, 4CV and SA data, from the average values of the three observers, shown for the left and right ventricles

Even if the data may be reliable from the results in the tests above, it must still be tested for validity, as reliability does not imply validity, and thus the data will be evaluated as such in the following paragraphs.

5.3.4 VALIDITY

While reliability as shown in the above results is often related to precision, validity is related to accuracy. Therefore, to further test to accuracy of the volumes and function measured, the data have to be valid as well, and will be analysed as such in the next section.

5.3.4.1 Stroke Volumes as an important point of comparison

The SV was employed as a useful point of comparison between the two ventricles to test convergent validity. The average SV values per observer (averaged over the three imaging views) are included in table 5.3.8 below, as well as the ratio of left SV to right SV and the absolute difference between LV SV and RV SV. Table 5.3.9 show the same statistics, but per imaging view (averaged over the data from the three observers). Table 5.3.10 display the results for the averaged data. Tables listing the SV for every volunteer, left and right, and per imaging view for the three observers respectively can be found in Appendix C.

Table 5.3.8: Average stroke volumes over all 20 volunteers, averaged over the data from the three views, and their ratios and absolute differences for the left and right ventricle, as measured by the three observers

Stroke volumes (SV) (mℓ)

Observer 1	Left ventricle Average	Right ventricle Average	Ratio L:R	Abs diff LV-RV (mℓ)
Mean	72.0	70.0	1.0	2.0
Std Dev	15.9	16.9	0.1	5.6
Observer 2				
Mean	66.5	61.8	1.1	4.8
Std Dev	16.2	20.4	0.2	11.1
Observer 3				
Mean	73.7	67.9	1.1	5.8
Std Dev	17.7	19.4	0.1	7.3

Table 5.3.9: Average stroke volumes over all 20 volunteers, averaged over the data from the three observers, and their ratios and absolute differences for the left and right ventricle, as measured in the three imaging views

Stroke volumes (SV) (mℓ)

| 2CV | Left ventricle | Right ventricle | Ratio | Abs diff |
	Average	Average	L:R	LV-RV (mℓ)
Mean	70.7	70.2	1.0	0.5
Std Dev	15.9	18.8	0.1	5.6

4CV

	Left ventricle	Right ventricle	Ratio	Abs diff
Mean	72.1	66.8	1.1	5.4
Std Dev	16.0	17.8	0.1	11.1

SA

	Left ventricle	Right ventricle	Ratio	Abs diff
Mean	69.5	62.8	1.1	6.7
Std Dev	18.7	19.7	0.2	7.3

The standard deviations were taken over the 20 averages per view or per observer respectively.

Table 5.3.10: Average stroke volumes over all 20 volunteers, and their ratios and absolute differences for the left and right ventricle

Stroke volumes (SV) (mℓ)

| | Left ventricle | Right ventricle | Ratio | Abs diff |
	Average	Average	L:R	LV-RV (mℓ)
Mean	70.8	66.6	1.08	4.2
Std Dev	16.2	17.9	0.09	5.3

5.3.4.2 Cardiac anatomy and function

When comparing left to right volumes in the above tables and graphs, as well as in the full data in Appendix C, it can be seen that the values behave as expected from knowledge of the anatomy of the heart (Haddad et al. 2009;

Lorenz et al. 1999). The right ventricle is slightly larger than the left ventricle, and this is confirmed in the quantification results where EDV RV > EDV LV and ESV RV > ESV LV.

Physiologically, the lower ejection fraction of the right ventricle is also confirmed in the data where EF RV < EF LV.

5.3.5 MALE AND FEMALE SUBGROUP DATA

The average data with their corresponding standard deviations for the male and female volunteer groups are shown in table 5.3.11, as well as the resultant p values per demographic factor to demonstrate statistically significant differences between the two gender groups.

Table 5.3.11: Average demographic data and standard deviations for the male and female groups, and p value per parameter indicating statistically significant differences

	Age (yr)	Height (m)	Mass (kg)	BMI (kg.m^{-2})	BSA (m^2)
Male	32 ±11	1.80 ± 0.12	78 ± 11	23.9 ± 1.7	2.0 ± 0.2
Female	26 ± 5	1.66 ± 0.09	59 ± 8	21.7 ± 3.0	1.7 ± 0.1
p	0.1906	**0.0439**	**0.0025**	**0.0313**	**0.0048**

For height, mass, BMI and BSA there were statistical significant differences between the male and female group with p values smaller than 0.05. It was thus necessary to split the group for further refining and use the male and female groups separately.

The determination of the average normal values was done on average values from the three observers and the 3 views combined. The resulting EF values with the associated standard deviations over the averages are shown in table 5.3.12, per gender group for both ventricles.

From this data it can be seen that the EF values and their corresponding standard deviations (errors) were of the same order in the male and female groups for LV and RV respectively.

Table 5.3.12: Left and right cardiac ventricle average EF values with standard deviations for the normal male and female volunteer groups studied

	Left ventricle		Right ventricle	
	EF (%)	Std Dev (%)	EF (%)	Std Dev (%)
Female	64.6	4.0	58.9	5.3
Male	64.3	5.5	58.5	4.8

5.3.6   COMPARISON TO AVAILABLE DATA

As a further confirmation of the accuracy of the obtained data, a visual comparison was made to available data from previous published studies. In the following two tables, measured EDV, ESV, SV and EF values can be seen as obtained in the present study as well as from literature. Table 5.3.13 compare left ventricle values for different studies, and table 5.3.14 right ventricle values.

All studies in the comparison used MRI as the imaging modality. The number of participants in each study (n) can be seen in both tables, as well as the relationship of male to female participants in brackets, for example 20 volunteers participated in this study, of which 10 were male and 10 female. The distribution of body surface area (BSA) in m^2 and age in years are also shown. These distributions are either shown as ranges (minimum to maximum values) or as the average value plus or minus 1 standard deviation. Where the BSA values or ranges are split, it is shown first for the male group and secondly for the female group.

The EDV, ESV and SV values are all shown in millilitres and EF in percentages, as averages values plus or minus 1 standard deviation. Where the standard deviations of the data were not available, the data were shown as ranges from minimum to maximum values, and where available both distributions were illustrated. In the study by Mooij et al. (2008) only average values were published for the volumes.

Table 5.3.13: Comparison between left ventricular volume and function value ranges and/or averages in this study and in selected published reports (Hudsmith et al. 2005; Cain et al. 2009; Alfakih et al. 2003; Mooij et al. 2008)

	Study	Present	Hudsmith et al.	Cain et al.			Alfakih et al.		Mooij et al.
	Imaging mod.	MRI	MRI	MRI			MRI TGE	MRI SSFP	MRI
	n	20(10m,10fm)	108 (63m,45fm)	76(41m,35fm)			60 (30m,30fm)		20 (12m,8fm)
	BSA (m²)	1.8±0.2	1.88±0.18	2.01±0.15 / 1.73±0.15			2.05 / 1.74 (average)		1.9±0.5
	Age group (yr)			21-81					
		29±9 (21-53)	38±12	21-30	31-40	51-60	20-65		20.6±10.7
LV EDV (mℓ)	Male	119.6±31.4	160±29	167 (115-219)	165 (113-217)	145 (94-197)	152.6±34.3	168.5±33.4	
	Female	101.1±16.1	135±26	119 (76-161)	118 (75-160)	115 (73-158)	123.0±19.7	134.9±19.3	
	Total	110.4±26.1	150±31						153.9
LV ESV (mℓ)	Male	43.2±14.9	50±16	64 (32-96)	67 (35-99)	61 (29-93)	52.7±13.8	60.8±16.0	
	Female	36.0±8.3	42±12	40 (17-63)	42 (19-64)	44 (21-67)	40.6±9.2	48.9±10.7	
	Total	39.6±12.3	47±15						64.6
LV SV (mℓ)	Male	76.4±19.7	112±19	102 (68-137)	98 (64-132)	85 (51-119)	99.9±23.0	107.7±20.7	
	Female	65.1±9.7	91±17	81 (49-112)	77 (46-108)	71 (40 -103)	82.5±13.5	86.0±12.3	
	Total	70.8±16.2	104±21						89.3
LV EF (%)	Male	64.3±5.5	69±6	66 (51-81)	65(51-80)	64 (50-79)	65.5±4.1	64.2±4.6	
	Female	64.6±4.0	69±6	70 (55-86)	70 (54-85)	69 (53-84)	67.1±4.6	64.0±4.9	
	Total	64.5±4.7	69±6						59±6

Table 5.3.14: Comparison between right ventricular volume and function value ranges and/or averages in this study and in selected published reports (Hudsmith et al. 2005; Tandri et al. 2006; Grothues et al. 2004; Alfakih et al. 2003; Mooij et al. 2008)

	Study	Present	Hudsmith et al.	Tandri et al.	Grothues et al.	Alfakih et al.		Mooij et al.
	Imaging mod.	MRI	MRI	MRI	MRI	MRI TGE	MRI SSFP	MRI
	n	20(10m,10fm)	108 (63m,45fm)	487 (219m,268fm)	20 (7m,13fm)	60 (30m,30fm)		20 (12m,8fm)
	BSA (m²)	1.8±0.2	1.88±0.18	1.96±0.01 / 1.73±0.01	1.88±0.2	2.05 / 1.74 (average)		1.9±0.5
	Age group (yr)	29±9 (21-53)	38±12	61±10	34±8 (26-57)	20-65		20.6±10.7
RV EDV (mℓ)	Male	124.4±34.5	190±33	142.2±31.1		160.4±32.6	176.5±33.0	
	Female	102.2±16.2	148±35	110.2±24		117.4±23.2	130.6±23.7	
	Total	113.3±28.6	173±39		153±34 (99-203)			155.8
RV ESV (mℓ)	Male	51.1±13.9	78±20	54.3±16.9		67.8±14.8	79.3±16.2	
	Female	42.4±10.2	56±18	35.1±12.5		44.5±9.3	52.3±9.9	
	Total	46.7±12.7	69±22		58±20 (25-88)			66.5
RV SV (mℓ)	Male	73.3±22.4	113±19	88.3±21.6		92.7±22.1	97.8±18.7	
	Female	59.8±9.0	90±19	75±17.9		72.9±16.9	78.3±16.9	
	Total	66.6±17.9	104±21		95±16 (71-119)			89.3
RV EF (%)	Male	58.5±4.8	59±6	62±10		57.6±5.4	55.1±3.7	
	Female	58.9±5.3	63±5	69±10		61.8±5.3	59.8±5.0	
	Total	58.7±4.9	61±6		63±7 (54-76)			58±5

5.4 DISCUSSION

The discussion of the aforementioned results will follow the same order as the results where applicable.

5.4.1 OVERVIEW OF MEASUREMENTS

Difficulty with segmentation produced a few problems in working according to a standard.

Some problem areas in the contouring were identified, which included:

- Difficulty in determination of the valve levels, which complicated edge detection
- Partial volume effect
- Artefacts on the images made it difficult to identify the endocardium
- Poor image quality
- If the volunteer moved during imaging, the correct volume was not included in the analysis

These problems led to observers using their own judgment in applying contouring, and differing from other observers. However, according to statistics, this only influenced the absolute cardiac volumes, and will be discussed in the paragraphs to follow.

The manual contouring procedure was just as time-consuming as the imaging, as also shown in the preliminary study in chapter 4. With the standardisation guidelines in place and followed by the observers, the contouring process on the images of one volunteer took up to an hour and a half to complete.

From the data in the bar charts in figures 5.3.1 to 5.3.4 it can be seen that there was a large distribution in cardiac size in the group of 20 participants, which was to be expected due to the variation in body size in the group. A full list of volunteer demographics can be seen table 5.2.1.

However, what is also clear from the bar graphs is that there were differences in the values measured from the data in the different imaging views (2CV, 4CV and SA) as well as a variation between the cardiac volume data as measured by the three observers. This was anticipated to some extent and can be explained by taking into account the various factors influencing judgment of where a specific contour has to be drawn, as discussed above under heading 3.2.1.

If these factors only influenced the cardiac volumes, and not the ejection fractions, the data would still be acceptable. The ejection fraction is calculated as a fraction or relation of the cardiac volumes, and thus the uncertainties and variations could be eliminated as such. A full investigation follows in the next paragraphs.

Table 5.3.1 confirms the previous arguments by displaying the mean values per observer for all the left and right ventricular parameters, with corresponding standard deviations.

However, the differences between the observers and the differences between data from the different imaging views had to be analysed further to determine the effect on the reliability of the data, and whether the differences were statistically significant.

5.4.2 INTER-OBSERVER RELIABILITY

It was important to determine the variation in measurements when taken by different observers with the same method. To establish a range of normal EF values from the measured data, consistency between different operators is significant in minimising uncertainty.

5.4.2.1 Comparison between observers

The data were analysed per imaging view as there was no clear indication yet that the data from one imaging view would produce better results than another.

When studying all three tables from the three imaging views together, it can be seen that the mean differences were overall larger between EDV values between different observers than for ESV values, although the mean differences between EF values were the lowest.

The differences between EDV and ESV values between the different observers can be attributed to the nature of manual contouring, where one observer could have argued that a certain grey level cut-off point was the epicardium surrounding the ventricular volume, and another observer used a larger or smaller border for instance. The segmentation problems, as discussed earlier in the manuscript, definitely also had an influence on these volumes, as different problems would have been handled differently by manual human action. These statistically

significant differences were however not seen as a problem, as long as the ratio of EDV to ESV stayed constant as to calculate a stable EF, and consistency was maintained throughout all manual contouring.

The smallest mean differences in stroke volumes were found between observer 1 and 3, where the differences were also not statistically significant.

It may be said that the volumes measured by observer 2 differed significantly from the data of observer 1 and 3, but as there were not as many or as large differences in the EF values, it cannot be said with certainty that the data from observer 2 has to be eliminated.

In the average data from the three imaging views, no statistical significant difference ($p > 0.05$) was found between the ejection fractions calculated by the different observers. It is difficult to draw a conclusion because of the large statistical variation in the data, but the inter-observer reliability in the data was relatively good. To implement the data further, the average values from the three observers were to be used to stabilise the data and method.

The full distribution of the EF data will be discussed with regards to the box plots.

5.4.2.2   Ejection Fraction box plots

When analysing figure 5.3.6 and 5.3.7, the separate groups of LV and RV plots also overlap in the inter-quartile range. Thus based on the data values, it cannot be said with certainty that the EF values from different observers are different.

If the plots are analysed in terms of being skew, it seems that in the 2CV plots the LV and RV data points were clustered in the upper part of the distribution (between the median and the upper quartile), which would suggest that there were more participants included in the study with an EF higher than the median. However, for the SA plots the data were clustered in the lower part of the distribution, seemingly including more participants with EF lower than the median. In the 4CV plots a conclusion on the distribution cannot really be made, which suggests that the data were more or less equally spaced.

It can however be concluded from the results that the quantification method is not very stable, and that the averages from the three observers were to be used for further calculations.

To include all outlooks on the data for inter-observer reliability, the left and right values were also compared to another for each observer.

5.4.2.3 Relationship between RV and LV volumes per observer

As a last test for inter-observer reliability, the relationship between the RV and LV data was investigated for each observer.

The coefficient of determination (R^2) was the largest for EDV data, for observer 1 (0.898) and for observer 3 (0.929) respectively, indicating a strong correlation between actual and estimated y-values. The data from observer 2 still show a correlation although not as strong. The correlation between actual and estimated ESV values are lower than for EDV values, but the F distribution test have been applied to determine the reliability of the observed correlations. The weaker R^2 correlation for ESV values can also be understood under the fact that the error on ESV values would be larger than for EDV, as there were fewer slices through the heart at end-systole.

As it can be seen from the results, all the F-observed values were higher than the critical value. From the Fdist values, it is extremely unlikely that these F values occurred by chance, or that the relationship was by chance. Thus it can be concluded that the regression equations for all three observers are useful in predicting the RV values from LV values, or visa versa.

The abovementioned tests demonstrated that in this study as well, there are differences in the manual contouring method and subsequent volume determination between observers. The following paragraphs will discuss the inter-method reliability.

5.4.3 INTER-METHOD RELIABILITY

With inter-observer reliability proved in the previous section of the results, inter-method reliability of the data was tested by employing average values obtained from data from the three observers. The volumes measured in the three different imaging views were compared to analyse the inter-method reliability.

5.4.3.1 Volumes measured in each imaging view

Table 5.3.6 show the mean values with their standard deviations measured per imaging views for all 20 volunteers, averaged over the values from the three observers. As it was seen in the comparison between the different observers, a large range of volumes were measured. This was expected, and anticipated, as participants of different body sizes were included in the study.

5.4.3.2 Comparison between imaging views

During routine cardiac MRI only one 2CV and one 4CV slice are imaged through the heart for positioning, and then a series of SA view slices imaged for volumetric calculation. All three the imaging views were used in this study to investigate if there were any differences between the data from the three views, or differences in validity and precision. With the slice slickness of 9mm used, an average heart was covered by 6 2CV slices, 8 4CV slices and 10 SA slices.

Statistical significant differences were found between almost all data sets examined in the comparison between the imaging views, both for the left and the right ventricles.

For the left ventricle the mean differences were overall larger between EDV values between different imaging views than for ESV values. The smallest mean differences in stroke volumes were found between 2CV and SA (LV), and between 2CV and 4CV (RV), where the differences were also not statistically significant.

No statistical significant difference ($p > 0.05$) was found between the ejection fractions from 2CV and 4CV or 2CV and SA (LV) and between 2CV and 4CV (RV).

A few factors contribute to the inter-method dependency observed here. The partial volume effect identified in mainly the 4CV images contribute largely to uncertainty in the segmentation on slices through the areas of the cardiac ventricles close to the endocardium. The thickness of the slices of 9mm definitely influences this as well. Unfortunately, the 9mm thickness is a compromise between image quality and the practicality of imaging patients. The slice thickness cannot be reduced, as this would increase the imaging time significantly, which will result in the patient having to lie in the MR scanner much longer than the already 45 minutes to one hour on average. As most patients undergoing cardiac imaging are already ill, increased scanning time and discomforting the patient by more breath-hold practices is not an option.

Also, as the 9mm slice thickness was already part of the standard imaging protocol, it was not principle to change it for the study, so as the employ the data and uncertainties measured in the study locally.

From this data, it cannot be concluded that one imaging view is statistically significant better or worse than another, therefore none could be rejected on these terms. To improvise and to stabilise the method, an average of the three imaging views were to be implemented for further calculations, and to set a range of normal values.

5.4.3.3   Ejection Fraction box plots

In figure 5.3.11 EF box plots are shown per imaging view, for both ventricles as averages from the data of the three observers. When comparing the LV data of the three imaging views, it can be said that the median values of the three data sets are comparable. The median of 4CV is slightly lower than for 2CV and SA, and the minimum values measured differ between the views, but overall the plots overlap well in the inter-quartile range. The 2CV data are equally spaced around the median, and the 4CV and SA data points are somewhat clustered between the median and lower quartile, but not to a large degree.

In the RV data, the median of the SA EF is lower than for 2CV and 4CV data. In this case, the data points are again fairly clustered between the median and the lower quartile for 2CV and SA data, but more between the median and upper quartile for 4CV data. Still, all 3 RV plots overlap for the most part, with the maximum and minimum values differing slightly between imaging views.

From the Box and whisker plot in figure 5.3.11, it is evident that the inter-quartile range measured for RV EF was larger than for LV EF, as the distribution of the plots are wider. There are more unknown factors for RV than for LV, for example valve levels localisation, history of RV contouring, more published data on LV segmentation, etc. Thus based only on the data values, it cannot be said with certainty that the EF values from the different imaging views are different.

5.4.4 VALIDITY

The average values from the three observers and three imaging views were used to analyse the validity of the data.

5.4.4.1 Stroke Volumes as an important point of comparison

The stroke volumes were an important point of comparison for accuracy, as it is logical that the same amount of blood that enters the heart on the right side through the right atrium, has to be equal to the amount of blood exiting the left side of the heart through the left ventricle, given that the heart is functioning normally and there is no cardiac blood leak present.

Average SV and their standard deviations from the 3 views combined, as well as for the 3 observers combined, were found to be 70.8mℓ [16.2mℓ] and 66.6mℓ [17.9mℓ] for the left and right ventricles respectively, where the standard deviations were calculated over the 20 volunteer averages per ventricle as in table 5.3.10. The average ratio between the left and right SV values was 1.08, with an average absolute difference of only 4.2mℓ.

Though the averaged data were employed in this validity test, it can be interesting to look at the data from the three observers or three imaging views in tables 5.3.8 and 5.3.9. The largest average absolute differences were found in data from observer 3 (5.8mℓ) with a LV:RV ratio of 1.1, and in the SA view data (6.7mℓ) with a LV:RV ratio of 1.1, which is still quite acceptable.

Although when looking at the data per volunteer, larger differences in SV may be found, the overall average difference in SV between the LV and RV is less than 5mℓ. This value is even lower than in the study by Alfakih et al. (2003, pp. 325-326) where the average ratios between the left and right SV values (male and female groups respectively) were 1.08 and 1.13, with average absolute differences of 7.2mℓ and 9.6mℓ. With all the artefacts and imaging difficulties taken into account, as well as the thickness of the imaging slices (9mm) and the loss in accuracy that goes hand in hand, these values are acceptable, and thus a certain degree of validity can be credited to the data.

5.4.4.2 Cardiac anatomy and function

From the separate results of the different observers and imaging views, as well as average values, it was shown that the volumes and ejection fractions correspond to the known cardiac anatomy and physiology where the right ventricle is slightly larger than the left ventricle, and the resultant RV EF is lower than the corresponding LV EF. This again confirms the validity of the data in this study.

5.4.5   MALE AND FEMALE SUBGROUP DATA

The demographic factors in table 5.2.1 were obtained at the time the study was undertaken, or calculated using equations 5.2.1 and 5.2.2. These factors were used to calculate the differences in the factors from the male and female volunteer groups. The differences between the two gender groups were statistical significant for height and mass, and the resulting BMI and BSA data, as seen in table 5.3.11. If the original demographic values in table 5.2.1 are observed again, it is obvious that there would be differences between the males and females, as the male volunteers were overall larger than the females.

Therefore, it was clearly necessary to split the volunteer group into the two gender subgroups to further test the possible correlations or state average data.

The average cardiac functional parameters stated for the 20 volunteers from Universitas Hospital were derived from the data of 10 male and 10 female normal, healthy subjects. The ranges for the two gender groups are stated in table 5.3.12 as average left and right ejection fractions, with 1 standard deviation. The standard deviations over the averages, 4.0% (LV), 5.3% (RV), 5.5% (LV) and 4.8% (RV) for the female and male EFs respectively, were found acceptable.

5.4.6 COMPARISON TO AVAILABLE DATA

When comparing the data from this study to data from other published studies, it is evident that there are obvious differences between different studies, and even when the same participants are used as in the study of Alfakih et al. (2003).

The volumes (EDV, ESV, SV) measured in this study were on average all smaller than the volumes from the other studies references in tables 5.3.13 and 5.3.14. This may either be attributed to the method being different, the average BSA of the volunteers being smaller than those of the other studies due to the non-random selection of the population group, or the age distribution differing. However, conclusions on why the volumes are smaller cannot be made with confidence from the tabulated results.

On the other hand, the ejection fraction values are overall well comparable to that from the published studies, thus contributing to the reliability and validity of this study's measured data.

However, it has been evident from some of these published studies that cardiac volumes and function may very well vary with age, gender and/or BSA (Tandri et al. 2006; Hudsmith et al. 2005; Mooij et al. 2008).

As the importance for gender and age specific ranges of cardiac volumes and ejection fractions has been suggested (Cain et al. 2009), the need to further refine the measured results from this study was realised. The data will be further investigated in tests to determine its dependency on and correlation with age, BMI, BSA and gender.

5.5   CONCLUSION

From the results discussed in this chapter, it may be said that although the inter-observer reliability and inter-method reliability were good enough not to exclude any results from the analysis, the quantification method was still somewhat unstable.

Although there were significant differences in the respective volumes, in the average data, no statistical significant differences were found between the ejection fractions of the different observers, which also indicate that the functional results were reliable.

More differences were observed between the imaging views, but still not enough to conclude that one imaging view is better or worse than another or to conclude that the data from one imaging view should be excluded from the analysis.

Thus, overall the results were reliable as far as the average values were employed to establish comparisons and estimations.

The results were valid and followed the prediction from the anatomy that the right ventricle should be larger than the left, the stoke volumes equal, and the resulting RV EF lower then LV EF.

From the above results, it is evident that the group of volunteers were too small and too uniformly distributed, with the distribution of the group maybe being too narrow in terms of too few volunteers of the same body size or age. Taking all this into account, it seems that the group of volunteers used were a too narrowly selected group of people, especially within a specific age group for the females.

However, the functional results also compared well overall with available data from publications on MR cardiac data.

Thus to conclude this chapter, with the resources at hand, this study delivered acceptably reliable and valid results. Furthermore, the method is still at an early stage, and was first investigation for Universitas Hospital.

6   CONCLUSION

Cardiac Magnetic Resonance Imaging provides accurate, high-resolution detail of the anatomy of the heart in any plane, and these images can also be applied to determine ventricular functionality. MRI can also overcome many of the imaging difficulties associated with the right ventricle. The assessment of ventricular volumes and function are essential, as even the right ventricular function is an important prognostic factor for many heart diseases.

The proposed method to quantify right and left ventricular function by manual contouring of normal ventricles on cardiac Magnetic Resonance images, yielded results for EDV, ESV, SV and EF values for both ventricles of the twenty normal healthy volunteers included in the study. The manual contouring procedure was quite time-consuming, as well as the imaging.

The fact that only 20 of the total of 28 volunteers entered into the study were included in the analysis, might predict problems for using this method on patients, as movement during imaging, inability to hold their breath, and poor ECG signal due to irregular heart beat are pertaining to patients with cardiac disease.

The three observers conducting the contouring process were all medical physicists, and acquired a lot of knowledge on the anatomy and contouring throughout the study. When comparing data from the three different imaging views, it could not be concluded that one imaging view was statistically significant better or worse than another. Although it was difficult to draw a definite conclusion due to the large statistical variation in the data, the degree of inter-observer reliability and inter-method reliability was deemed relatively good.

The measured data also followed predictions from cardiac anatomy and physiology, i.e. the right ventricle is larger during both end-diastole and end-systole; in a normal heart the SV should be equal for left and right ventricles; and the RV EF should resultantly be smaller than LV EF. With all the artefacts and imaging difficulties taken into account, as well as the thickness of the imaging slices (9mm) and the loss in accuracy that goes hand in hand, the obtained values were deemed acceptable. A degree of validity was therefore established by the equivalent stroke volumes from the left and right ventricles, and further by the comparison to published data in the literature.

Although there were errors and uncertainty in the data, the results were relatively good and valid for the normal population studied, as long as the average data from the three observers and three imaging views were used. The accuracy of measured average ejection fractions, 4.0% (LV), 5.3% (RV), 5.5% (LV) and 4.8% (RV) for the female and male groups respectively, were found acceptable.

From the box and whisker plot in figure 5.3.11, it was seen that the distribution of the RV EF plot was wider than the LV EF plot, which confirms that there are more unknown factors for RV than for LV. Overall there were large

distributions in the data, as the overall distribution of the volunteer group was wide, including males with a large body size as well as females with very small bodies. Data points that seemingly looked like outliers were treated as true values of the measured data set.

It was obvious from the results that the group of volunteers were too small and too uniformly distributed in some demographic subgroups (In the female subgroup, 7 of the volunteers had approximately the same body size and type) to show significant correlations with demographic factors, and were therefore not adjusted according to age, BMI or BSA to set normal values from this data, for a population. Rather, a range of average cardiac functional parameters for the normal volunteer group studied could be determined with acceptable accuracy.

However, it may also be noted that it might not be so much the number of participants in the group, but more importantly their distribution. Other studies have used groups of 22 healthy subjects with a mean age of 26 ± 4.2 years (Prakken et al. 2008) or 15 patients with repaired tetralogy of Fallot, compared with 8 normal subjects (Sheehan et al. 2008).

Thus, a larger normal group might improve the statistics of the data, but not without a wider and more even distribution considering demographic factors.

In essence the aim of this study was to assess the segmentation method using cardiac MRI. The method as it was used was not very stable, and might need a few adjustments to improve it. In the first place, a better knowledge of the anatomy and biomechanics will help in determining endocardial borders and valve levels to improve ventricular volume accuracy. More cooperation and sharing of knowledge amongst physicists, cardiologists and radiologists would contribute a great deal to the issue.

The slice thickness of 9mm had a great contribution to the partial volume effect; therefore either the inclusion or exclusion of a slice had a dramatic effect on the resulting volume. The partial volume effect may be overcome or at least reduced by imaging with a thinner slice thickness, producing an increased axial resolution. However, this will also lead to a decrease in signal-to-noise ratio and a proportional increase in imaging time, where the increase in imaging time may become intolerable for ill patients, especially with the breath-hold technique. Coping with the imaging time was already challenging for the normal, healthy volunteers.

Another solution to inaccuracies in contouring could be to automate the contouring process, excluding uncertainties due to human error.

This study as a first investigation for Universitas Hospital delivered reliable and valid results. Further implementation of the data obtained in the study is already active, wherein the contouring results are employed to construct automated edge detection software.

7   APPENDICES

Appendix A: Ethics approval and study documentation

Proof of approval from The Ethics Committee of the University of the Free State and further letters of approval after changes in the protocol can be found on the next 3 pages. Initial ethics approval was granted at the meeting held on 15 April 2008. Letters on 25 July 2008 and 30 October 2008 stipulate approval in terms of extension of the study duration time and amendments to the protocol.

Examples of the Volunteer information document and the Consent form are also included. The information document was given to all study volunteers and informed written consent obtained before imaging.

UNIVERSITEIT VAN DIE VRYSTAAT
UNIVERSITY OF THE FREE STATE
YUNIVESITHI YA FREISTATA

Direkteur: Fakulteitsadministrasie / Director: Faculty Administration
Fakulteit Gesondheidswetenskappe / Faculty of Health Sciences

Research Division
Internal Post Box G40
☎ (051) 4052812
Fax nr (051) 4444359

E-mail address: gndkhs.md@mail.uovs.ac.za

Ms H Strauss

2008-04-21

MS N WILLEMSE
DEPT OF MEDICAL PHYSICS
FACULTY OF HEALTH SCIENCES
UFS

Dear Ms Willemse

ETOVS NR 56/08
MS N WILLEMSE   **DEPT OF MEDICAL PHYSICS**
PROJECT TITLE: **QUANTIFICATION OF NORMAL RIGHT AND LEFT VENTRICULAR FUNCTION AS EVALUATED USING CARDIAC MAGNETIC RESONANCE IMAGING.**

- You are hereby informed that The Ethics Committee approved the above-mentioned study at the meeting on 15 April 2008.

- Committee guidance documents: Declaration of Helsinki, ICH, GCP and MRC Guidelines on Bio Medical Research. Clinical Trial Guidelines 2000 Department of Health RSA; Ethics in Health Research: Principles Structure and Processes Department of Health RSA 2004; the Constitution of the Ethics Committee of the Faculty of Health Sciences and the Guidelines of the SA Medicines Control Council as well as Laws and Regulations with regard to the Control of Medicines.

- Any amendment, extension or other modifications to the protocol must be submitted to the Ethics Committee for approval.

- The Committee must be informed of any serious adverse event and/or termination of the study.

- A progress report should be submitted within one year of approval of long-term studies and a final report at completion of both short term and long term studies.

- Kindly refer to the ETOVS reference number in correspondence to the Ethics Committee secretariat.

Yours faithfully

for   **PROF BB HOEK**
        CHAIR: ETHICS COMMITTEE

CC: Dr W Rae, Dept Medical Physics, UFS

✉ 339, Bloemfontein 9300, RSA   ☎ (051) 405 2812   🖱 gndkhs.md@ufs.ac.za
Republiek van Suid-Afrika / Republic of South Africa

UNIVERSITEIT VAN DIE VRYSTAAT
UNIVERSITY OF THE FREE STATE
YUNIVESITHI YA FREISTATA

Direkteur: Fakulteitsadministrasie / Director: Faculty Administration
Fakulteit Gesondheidswetenskappe / Faculty of Health Sciences

Research Division
Internal Post Box G40
☎ (051) 4052812
Fax nr (051) 4444359

E-mail address: gndkhs.md@mail.uovs.ac.za

Ms H Strauss

2008-07-25

MISS N WILLEMSE
DEPT OF MEDICAL PHYSICS
FACULTY OF HEALTH SCIENCES
UFS

Dear Ms Willemse

ETOVS NR 56/08
PROJECT TITLE: QUANTIFICATION OF NORMAL RIGHT AND LEFT VENTRICULAR
FUNCTION AS EVALUATED USING CARDIAC MAGNETIC RESONANCE IMAGING.

- You are hereby informed that at the meeting held on 22 July 2008 The Ethics Committee approved the following:

- *Extension of the duration of the study until the end of 2009*
- *Study will be undertaken to obtain a Master's Degree under supervision of Dr W Rae of the Dept of Medical Physics.*

- Committee guidance documents: Declaration of Helsinki, ICH, GCP and MRC Guidelines on Bio Medical Research. Clinical Trial Guidelines 2000 Department of Health RSA; Ethics in Health Research: Principles Structure and Processes Department of Health RSA 2004; Dept of Health: Guidelines for Good Practice in the Conduct of Clinical Trials with Human Participants in South Africa, Second Edition 2006; the Constitution of the Ethics Committee of the Faculty of Health Sciences and the Guidelines of the SA Medicines Control Council as well as Laws and Regulations with regard to the Control of Medicines.

- Any amendment, extension or other modifications to the protocol must be submitted to the Ethics Committee for approval.

- The Committee must be informed of any serious adverse event and/or termination of the study.

- A progress report should be submitted within one year of approval of long term studies and a final report at completion of both short term and long term studies.

✉ 339, Bloemfontein 9300,RSA   ☎ (051) 405 2812   🖰 gndkhs.md@ufs.ac.za
Republiek van Suid-Afrika / Republic of South Africa

UNIVERSITEIT VAN DIE VRYSTAAT
UNIVERSITY OF THE FREE STATE
YUNIVESITHI YA FREISTATA

Direkteur: Fakulteitsadministrasie / Director: Faculty Administration
Fakulteit Gesondheidswetenskappe / Faculty of Health Sciences

Research Division
Internal Post Box G40
☎(051) 4052812
Fax nr (051) 4444359

E-mail address: gndkhs.md@mail.uovs.ac.za

Ms H Strauss

2008-10-30

MS N WILLEMSE
DEPT OF MEDICAL PHYSICS
FACULTY OF HEALTH SCIENCES
UFS

Dear Ms Willemse

ETOVS NR 56/08
PROJECT TITLE: QUANTIFICATION OF NORMAL RIGHT AND LEFT VENTRICULAR FUNCTION AS EVALUATED USING CARDIAC MAGNETIC RESONANCE IMAGING.

- You are hereby kindly informed that at the meeting on 27 October 2008, the Ethics Committee approved the following:

- ***Amendments to the protocol***

- Committee guidance documents: Declaration of Helsinki, ICH, GCP and MRC Guidelines on Bio Medical Research. Clinical Trial Guidelines 2000 Department of Health RSA; Ethics in Health Research: Principles Structure and Processes Department of Health RSA 2004; Dept of Health: Guidelines for Good Practice in the Conduct of Clinical Trials with Human Participants in South Africa, Second Edition 2006; the Constitution of the Ethics Committee of the Faculty of Health Sciences and the Guidelines of the SA Medicines Control Council as well as Laws and Regulations with regard to the Control of Medicines.

- Any amendment, extension or other modifications to the protocol must be submitted to the Ethics Committee for approval.

- The Committee must be informed of any serious adverse event and/or termination of the study.

- A progress report should be submitted within one year of approval of long term studies and a final report at completion of both short term and long term studies.

- Kindly refer to the ETOVS reference number in correspondence to the Ethics Committee secretariat.

Yours faithfully

....
PROF WH KRUGER
CHAIR: ETHICS COMMITTEE

✉ 339, Bloemfontein 9300,RSA   ☎ (051) 405 2812   gndkhs.md@ufs.ac.za
Republiek van Suid-Afrika / Republic of South Africa

Volunteer information document

Study title: Quantification of Normal Right and Left Ventricular Function, as Evaluated using Cardiac Magnetic Resonance Imaging

Ethics Approval Number: ETOVS NR 56/08

Good day! Would you be willing to help us in our research?

We, Nanette Willemse, Dr William Rae, and our collaborators, are doing research on the quantification of normal right and left ventricular function, as evaluated using cardiac magnetic resonance imaging (MRI). To do this we need MRI images of the right and left ventricles of normal, healthy hearts, as well as Ultrasound (US) images for comparison.

Invitation to participate: We request your permission to image your heart using both MRI and US.

What is involved in the study: The study is being done at Universitas Hospital. We intend to image twenty healthy volunteers (10 male and 10 female) with no known cardiac abnormalities. Volunteers will be in the age range 18 to 60, and with a heart rate of 50 to 80 beats per minute. Exclusion criteria will comprise: Smokers; people with history of cardiac abnormalities or disease, including hypertension; any current medication for heart disease, hypertension or asthma; any contraindication for doing MRI or US investigation. You will be imaged on MRI as well as US. An electrocardiogram (ECG) will be used to monitor your heart rate while the images are being obtained. The ECG electrodes will be attached to the skin of your chest. The parameters investigated will include, for both left and right ventricles: end-diastolic volume, end-systolic volume, stroke volume, and ejection fraction. These values will be used to benchmark normal values for right ventricular function, which will be important in the clinical service to patients with right heart failure.

No risks are associated with involvement in the study above those expected for US imaging. No ionizing radiation will be used and no substances such as contrast medium will be given. No adverse effects are foreseen.

No benefits are expected for those participating in the study, as subject heart images will only be used for benchmarking of right ventricular function.

Participation is voluntary, and refusal to participate will involve no penalty and you may also discontinue participation at any time without penalty.

No reimbursements will be made, as this study involves no costs to you or additional costs to the hospital.

Confidentiality: Efforts will be made to keep personal information confidential. Absolute confidentiality cannot be guaranteed. Personal information may be disclosed if required by law. Organisations that may inspect and/or copy your research records for quality assurance and data analysis include groups such as the Ethics Committee for Medical Research and the Medicines Control Council where appropriate. Publication of results is anticipated, but no individual identification should occur. If any abnormality is found in your heart during the examination, you will be informed professionally, and the information will be kept confidential.

To contact researchers: for further information or reporting of study-related information, contact:

Nanette Willemse, Department of Medical Physics, Faculty of Health Sciences, (G68), University of the Free State, Bloemfontein, 9301

Tel: 051 405 3156, Fax: 051 444 3822, E-mail: nwillemse2005@yahoo.com

To contact the Research Ethics Committee Secretariat and Chair: for reporting of complaints or problems contact:

Ms Henriette Strauss, Research Division (Ethics Committee), Block D, Dean's Division, Room D115, Faculty of Health Sciences, (G40), University of the Free State, Bloemfontein, 9300

Tel: 051 405 2812, Fax: 051 444 4359 E-mail: gndkhs.md@mail.uovs.ac.za

Consent form

Volunteer reference number: _____

You have been asked to participate in a research study with the title "Quantification of Normal Right and Left Ventricular Function, as Evaluated using Cardiac Magnetic Resonance Imaging", and been informed about the study by _____.

Feel free to contact Nanette Willemse at the Department of Medical Physics, Faculty of Health Sciences, UFS, Bloemfontein (tel.: 051 405 3156) at any time, should you enquire any information regarding this study. You may also contact the secretary of the Ethics Committee, Faculty of Health Sciences, UFS, Bloemfontein (tel.: 051 405 2812) if you have any queries about your rights as healthy research volunteer.

Your involvement in this study is voluntary, and you will therefore not be penalized in any way if you decide not to participate in the study and/or end your involvement with the study.

If, for some reason, the images of your heart are not suitable to be included in this study, your participation in the study will be ended and your information will not be used further. If any abnormality is noted on the images you will be advised appropriately.

There is no cost to you associated with this study, and you will not receive any remuneration for your participation.

If you agree to take part in this study, you will receive a signed copy of this document, as well as the Participant information document, which is a summary of this research study.

Are you aware of any cardiac abnormalities?

Yes	No

If yes, please provide a description of the abnormality. _____
_____

Have you ever experienced any heart problems before?

Yes	No

If yes, please provide details. _____
_____

Are you on any medication?

Yes	No

If yes, please provide details. _____
_____

Are you a | Smoker | Non-smoker | ?

The research study and the above information have been explained to me orally. I understand what my involvement in this study implies and I voluntarily agree to participate.

_____   _____
Signature of participant   Date

A description of the two-dimensional FIESTA pulse sequence used in the cine cardiac Magnetic Resonance Imaging in the study is given in the following paragraphs.

B.1. 2D FIESTA pulse sequence and ECG gating

FIESTA is an acronym in the GE Healthcare MRI software that stands for **F**ast **I**maging **E**mploying **ST**eady-state **A**cquisition. It is a fully balanced steady-state coherent pulse sequence aiming to produce high signal-to-noise ratio (SNR) images at very short repetition times (TRs) (General Electric Company 2001a).

According to Bushberg et al. (2002, p. 405), steady-state precession with short TRs of less than 50msec, refers to balancing of the longitudinal and transverse magnetization from one pulse to another in an image acquisition sequence. In standard imaging techniques (e.g. spin echo, inversion recovery, generic GRE sequences), partial saturation occurs due to the repetition time TR of the radiofrequency (RF) pulses being too short to allow recovery of longitudinal magnetization equilibrium. When this steady-state partial saturation occurs, the same longitudinal magnetization is present for each following pulse. However, for very short TR, which are less than the T2* decay constant, there is a constant transverse magnetization as well. During each repeated pulse sequence, a part of the transverse magnetization is converted to longitudinal magnetization, as well as a part of the longitudinal magnetization converted to transverse magnetization. In a situation like this, there is at all times a coexistence of steady-state longitudinal and transverse magnetization elements in a dynamic equilibrium.

While most other fast scan techniques use phase spoiling to eliminate phase coherence, the 2D FIESTA technique uses balanced gradients, designed to maintain phase coherence of the transverse magnetization at each RF excitation. The short TRs are essential to maintain spin phase coherence in the FIESTA pulse sequence (General Electric Company 2001a, p. 7-3).

In steady-state imaging, the user-defined factors that determine the amount of transverse magnetization created, and the image contrast, include TR, TE and flip angle. Steady-state imaging is practical only with short and very short TR, where the flip angle has the most important impact on the contrast "weighting" of the resultant images (Bushberg et al. 2002).

The FIESTA pulse sequence employed by GE uses flip angles typically in the order of 40-45 degrees, which is categorized by Bushberg et al. (2002, p.406) as a moderate flip angle. With flip angles between 30 and 60 degrees, a larger longitudinal magnetization creates a larger transverse magnetization, and tissues with a long T1 have more signal saturation, which produces some T1 weighting. For the same reason, tissues with long T2* produce a higher signal amplitude. Because in most tissues T1 and T2 are correlated (i.e., long T1 implies long T2), the contrast will depend on the difference in the T2/T1 ratios between the tissues.

Thus 2D FIESTA imaging can be applied in clinical situations that take advantage of the differentiation of contrast between tissues of low T2/T1 ratios and high T2/T1 ratios. This type of acquisition sequence can be practical in the imaging of, but not limited to, structures in motion such as the heart, which needs an evident delineation between blood (high signal intensity) and myocardium (tissue with low signal intensity). The improved blood/myocardium contrast allows for better definition of the myocardial boundaries and therefore enhances and accelerates the determination of the ventricular volumes. (General Electric Company 2001a, p.7-6 - 7-7)

Furthermore, the 2D FIESTA pulse sequence is a fast-ECG-gated cardiac triggered data acquisition. Triggering synchronises the data acquisition (imaging) with the ECG cycle of the heart. Thus for each slice, the image data are consistently acquired at the start of the same phase on the ECG cycle (General Electric Company 2001b, p. 2-7).

The R wave of the ECG waveform is used as a trigger to start the gated imaging. In the imaging sequence used, 20 cardiac phases will be reconstructed for each ECG waveform and on each slice imaged through the heart. When using ECG gating, it is advisable to use the lead that provides the best signal (General Electric Company 2001b, p. 2-7).

Figure B.1.1 is an illustration of the ECG waveform, showing the P, Q, R, S, and T waves of the cardiac cycle. The QRS complex represents the depolarisation of the right and left ventricles and results in systole of the ventricles. End-diastole occurs at the R-wave. The R-wave is used for triggering because of its strong electrical signal and correlation of the muscle activity of the heart. Each R-R interval represents one cardiac cycle. The T-wave represents re-polarisation of the ventricles and results in diastole of the ventricles. End-systole occurs after the T-wave. Thus when one cardiac cycle is acquired during one R-R interval, the 20 gated images will contain the cardiac area from end-diastole, through systole, end-systole, through diastole until end-diastole again.

The functional cardiac imaging with 2D FIESTA is acquired with no spacing between slices, thus it is acquired sequentially: one slice at a time and with multiple cardiac phases.
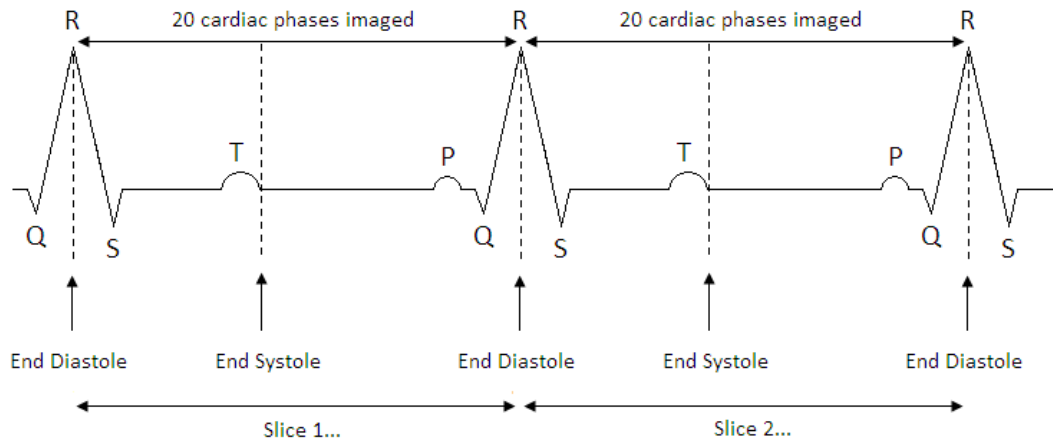
Figure B.1.1: Representation of gating and triggering of cardiac imaging of 2 prescribed slices on an ECG waveform (General Electric Company 2001b, p. 2-7, 2-10; Meyer et al. 2002, p. 13.15).

There are several benefits to the 2D FIESTA pulse sequence that may be considered (General Electric Company 2001a, p. 7-4):

• 		High signal-to-noise ratio images can be obtained

• 		Excellent contrast between soft tissues and fluids is achieve

• 		Reduced repetition times are used, which minimises motion artefacts

• 		Inherent flow compensation, which minimises artefacts due to blood flow

Therefore the 2D FIESTA pulse sequence is an excellent choice for functional cardiac MRI.

B.2. Imaging set-up

Patients are scanned in the cardiac coil, positioned supine, with the feet in the direction of the MR scanner ("feet first"). The patient is positioned on top of the posterior component of the cardiac coil. The anterior component of the cardiac coil is placed on the anterior surface of the thorax of the patient, and aligned with the posterior

component, such that the centre of the coil is positioned over the mid chest. It is important that the centre of both the anterior and posterior surface coils should be well aligned with the centre of the heart.

Four ECG electrodes are arranged around the cardiac area, and attached, using standard MRI compatible contacts, onto the skin. The arrangement of the electrodes are in the form of a square; 2 electrodes above the heart, left and right, and 2 electrodes below the heart, left and right. Due to interference of the radiofrequency pulses of the MRI system, the electrodes are positioned rather close to each other so as to minimize interference from the RF signal. The ECG monitoring is not used for diagnostic purposes, but only to achieve gating and triggering.

With the set-up complete, the zero position is set corresponding to the centre of the coil, ensuring the heart being in the isocentre of the magnet.

To minimise movement of the heart or thorax during imaging and consequently reduce motion-induced artefacts, a breath-hold technique is usually implemented during imaging. Patients are asked to hold their breath at expiration during imaging of each slice through the cardiac area. This is communicated to the patient via an intercom, prior to each image. The reduction in movement should improve accuracy, as long as the heart is in the same spatial position with every breath.

This technique is general practice for standard cardiac MRI in the department. With the set-up complete and positioning confirmed with multi-planar localizer scout images, the imaging process can be initiated.

B.2.1. Imaging to determine general positioning

From the coronal localizer, the area over which the axial scan for positioning is to be acquired is defined. The axial scan includes the area of the heart from the aortic arch to the apex, so as to include the entire volume of all four chambers of the heart. The selection of the length of the lines placed on the planning images is critical, as when these lines are too short, significant wrap-around occurs because the acquired image is too small, and if they are too long, the image of the heart becomes relatively small in relation to the size of the acquired image.

A rough estimate for a practical length of the positioning lines is that they should be twice the length of the heart (the object of interest) and just shorter than half of the patient's diameter.

In figure B.2.1 the positioning of the axial scan on the coronal localizer image can be seen, with an example of an axial image through the body, showing the position of the heart.
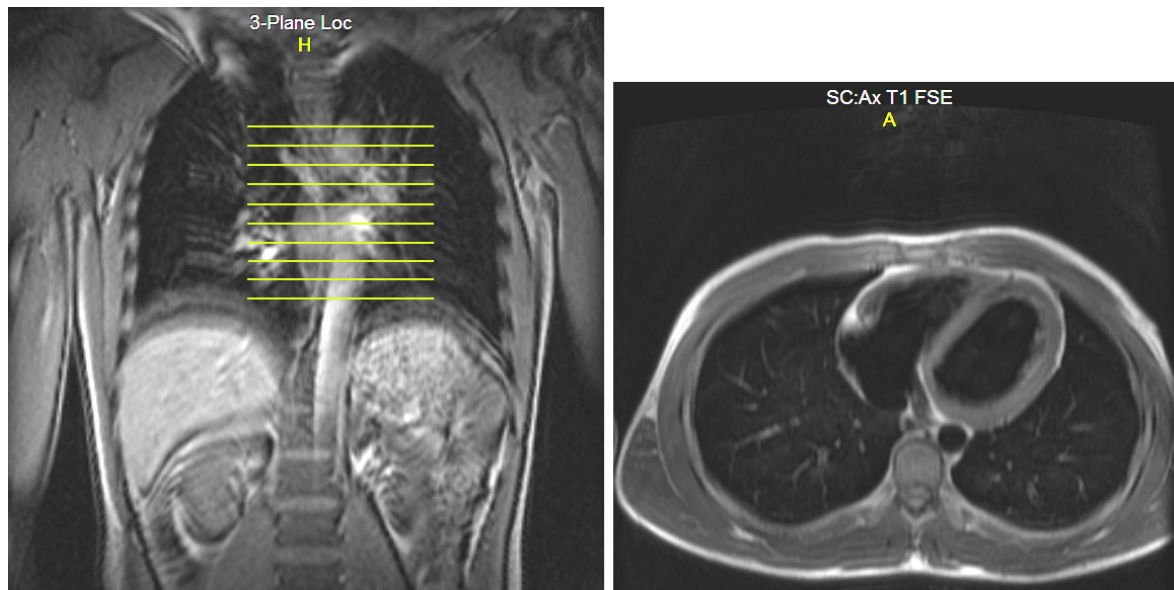
Figure B.2.1: Positioning of axial image slices on the coronal localizer image (left image) and an example of an axial image slice through the body (right image). The axial scans include the entire volume of the heart, from the aortic arch to the apex.

B.2.2. Volumetric imaging planning

The imaging views for the volumetric calculations are planned on the preceding image sets, and discussed below.

2-Chamber View

From the Axial views imaged, the 2-Chamber View (2CV) scan angle and extent are defined. Planning is done on the axial image where the bicuspid valve can be best identified. The 2CV scan is planned parallel to the ventricular septum, including both ventricles, as can be seen in figure B.2.2.
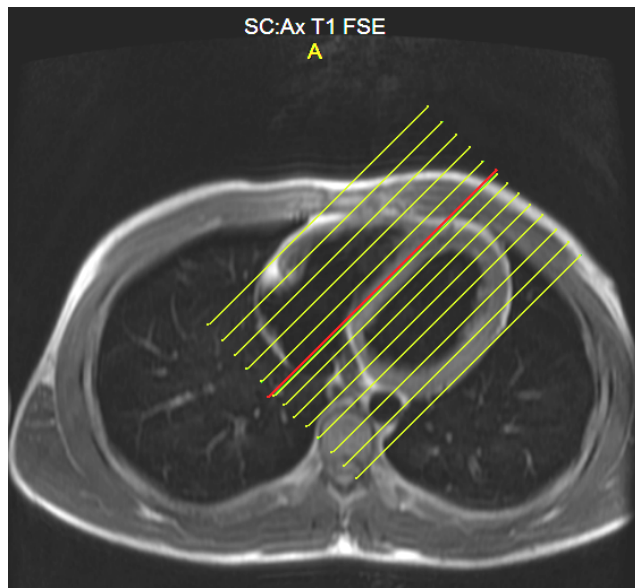
Figure B.2.2: Positioning of 2CV image slices on an axial image. Slices are positioned parallel to the ventricular septum

4-Chamber View

The 4-Chamber View (4CV) scan angle and extent is in turn defined on the 2CV image which best represents the centre of the left ventricle, which is where the mitral valve can be seen most clearly. The 4CV slices are positioned perpendicular to the LV aortic valve plane, as illustrated in figure B.2.3, where the valve level is indicated by the red line and the slices perpendicular to it in green.

Figure B.2.3: Positioning of 4CV image slices on a 2CV image. Slices (in green) are positioned perpendicular to the valve level (indicated by red line)

Short-Axis View

The Short Axis (SA) view scan angle and extent are finally defined on a 4CV image. On the image where the septum between the ventricles is clearly visible, the SA slices are positioned perpendicular to the septum, and parallel to the valve levels, so as to position the tricuspid and mitral valves on the same imaging slice or plane. This is illustrated in figure B.2.4 below.
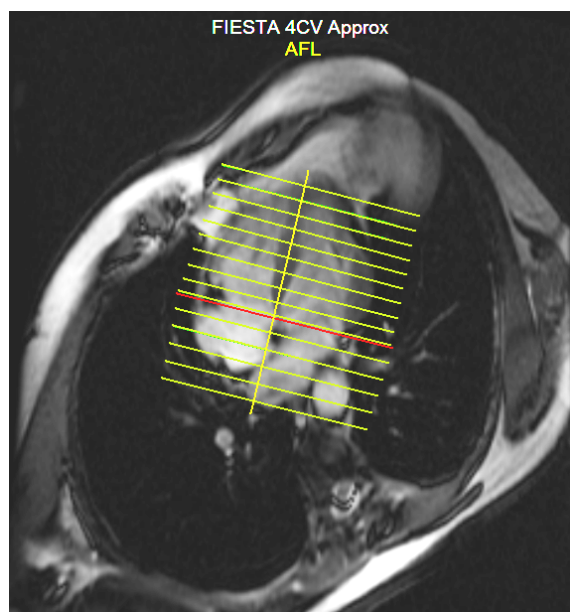
Figure B.2.4: Positioning of SA view image slices on a 4CV image. Slices (in green) are positioned perpendicular to the septum (yellow line) and parallel to the valve level (indicated by red line).

B.3. PRELIMINARY STUDY

As discussed in the manuscript, a preliminary study was undertaken to test the existing resources, determine the practicability of the proposed method and to establish the options at hand. In the preliminary study, manual contouring was done by the first observer on all the available cardiac MR images, and to regulate the method it was utilized for both the left and right ventricles. Contours were drawn on the 20 cardiac phase images, on all slices imaged through the heart with all three imaging views. The only experience the first observer had was from literature, anatomy textbooks and nuclear medicine cardiac imaging.

Many existent and potential problems were identified during the preliminary study that needed attention and solutions. As a primary concern, time constraints were a big issue. The availability of the MRI scanner was limited, as patients were booked until late in the day. Volunteers could therefore only be scanned after the patients have been finished after hours. The availability of the MR workstation with the Mass Analysis plus software was also limited, as this was the primary reporting workstation.

The manual contouring of the left and right ventricles was quite time-consuming. To complete the process for one volunteer on all three imaging views, up to 2 hours were needed for the more difficult cases. Therefore, as imaging and contouring were mainly carried out after hours, the availability of radiologists' and cardiologists' help was just as limited.

Artefacts on the cardiac MR images were a large hindrance that made contouring difficult. It was also noted that if a volunteer's/patient's breathing became shallower or deeper during imaging, the position of the heart changed, and that would increase the error in volume determination. A few volunteers were rescanned to correct some of these problems, or replaced by new volunteers.

The most important factor contributing to the problems and difficulties associated with the proposed method, was the uncertainty in the anatomy in the cardiac images, especially concerning the right ventricle. In the images below in figures B.3.1 and B.3.2, some of these areas of uncertainty are highlighted. It was not clear whether these areas in question had to be included or excluded from the right ventricular volume, but in reality, the question mark in figure B.3.2 corresponds to the RV inflow tract.

Figure B.3.1: Example of 2CV image with uncertainty in contouring of part of the right ventricle, indicated by the red arrow and question mark
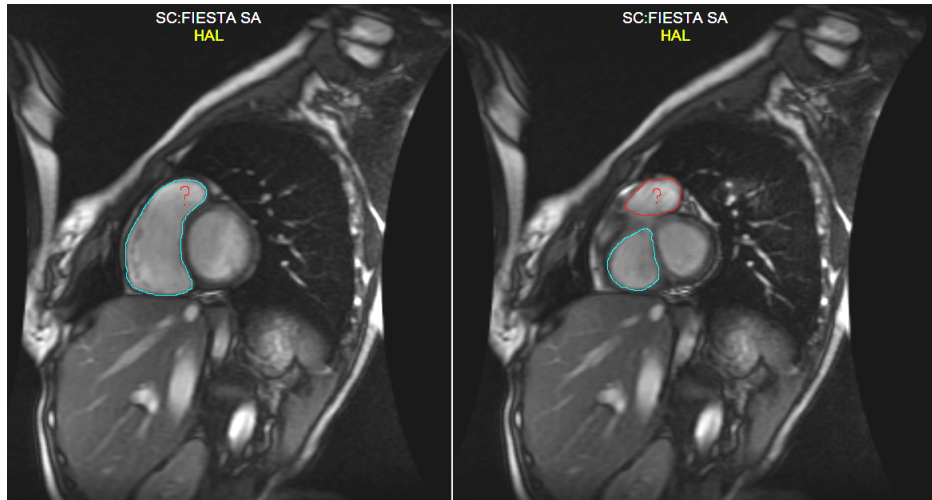
Figure B.3.2: Example of SA image with uncertainty in contouring of part of the right ventricle, indicated by the red question mark. In the image on the left it seems that the area in question is part of the right ventricle, but in the image on the right the area seems obviously removed from the ventricle, indicating the RV inflow tract.

The initial segmentation results from the preliminary study produced volumes that were inconsistent. This was mostly due to the problem associated with the difficulty of determining the valve level between the right ventricle and its outflow (near the conus arteriosus). The main reasons for the uncertainties were the facts that the endocardium around the right ventricle is not as clearly distinguishable, and that the valves were just not easily visible.

Table B.3.1 Initial results from the preliminary study for an example volunteer: stroke volumes for LV and RV not close to equal, and RV not larger than LV as per anatomy

	Left ventricle				Right ventricle			
	EDV (mℓ)	ESV (mℓ)	SV (mℓ)	EF (%)	EDV (mℓ)	ESV (mℓ)	SV (mℓ)	EF (%)
2CV	148.5	71.1	77.3	52.1%	159.5	67.4	92.1	57.8%
4CV	154.9	77.1	77.8	50.2%	151.0	54.5	96.4	63.9%
SA	150.8	55.3	95.5	63.3%	150.9	53.9	97.0	64.3%

Table B.3.1 display the initial measured results from an example volunteer. The stroke volumes from the 2CV and 4CV data differ with more than 15mℓ between the left and right ventricles, where it is supposed to be equal. According to the anatomy, the right ventricle is slightly larger than the left, and this fact is also not demonstrated in the results from the 4CV EDV data, or in any of the ESV data, which might be the reason behind the stroke volume inconsistencies.

It was decided that to eliminate errors as described above, and to standardise the contouring method, basic guidelines had to be set to formulate an acceptable reproducible manual contouring method, and to educate and instruct the different observers. It was also hoped that the guidelines would reduce the contouring time.

The volumetric results from the preliminary study would not be included in the statistical analyses of the final study.

C.1. FULL RESULTS TABLES

All calculated volumes and ejection fractions for each volunteer are shown in the following tables, as determined by the three observers, in all three imaging views. Averages over the values from the 3 imaging views with corresponding standard deviations are also shown for each volunteer in both ventricles. Average standard deviations were calculated over the 60 values measured for the 20 volunteers in the three imaging views for a specific ventricle.

C.1.1 End Diastolic Volumes

Table C.1.1: EDV values for the 20 volunteer participants as measured by observer 1, for all three imaging views and both ventricles, with added averages and standard deviations

Observer 1   End Diastolic Volumes (EDV) (mℓ)

Volunteer no.	Left ventricle					Right ventricle				
	2CV	4CV	SA	Average	St dev	2CV	4CV	SA	Average	St dev
CMR1	120.0	126.3	128.7	125.0	4.5	148.3	141.6	145.7	145.2	3.4
CMR2	85.6	80.3	76.4	80.8	4.6	88.0	77.3	84.7	83.3	5.5
CMR3	83.6	105.0	85.5	91.4	11.8	107.6	99.7	104.2	103.8	4.0
CMR4	70.1	95.3	55.6	73.7	20.1	80.6	71.9	58.1	70.2	11.4
CMR5	149.1	169.1	156.8	158.3	10.1	156.1	160.1	148.8	155.0	5.8
CMR7	128.4	135.4	122.5	128.8	6.4	114.4	116.8	111.6	114.3	2.6
CMR8	96.4	96.3	77.6	90.1	10.8	99.7	100.9	76.8	92.4	13.6
CMR9	148.5	154.9	150.8	151.4	3.2	159.5	151.0	150.9	153.8	5.0
CMR11	93.1	99.6	90.2	94.3	4.8	93.4	88.1	90.1	90.5	2.7
CMR13	125.7	103.1	111.5	113.4	11.4	123.6	121.7	125.5	123.6	1.9
CMR15	146.2	148.1	166.3	153.6	11.1	158.8	160.9	168.6	162.8	5.2
CMR16	92.5	111.1	96.7	100.1	9.7	108.9	108.1	97.8	104.9	6.2
CMR17	115.4	133.0	118.4	122.3	9.4	152.3	147.7	148.9	149.6	2.4
CMR18	78.5	80.1	84.7	81.1	3.3	82.4	92.4	93.0	89.3	6.0
CMR19	90.1	98.6	94.6	94.4	4.3	104.5	103.2	98.2	102.0	3.3
CMR22	93.0	90.7	94.4	92.7	1.8	94.1	96.4	96.0	95.5	1.2
CMR23	96.6	107.1	96.6	100.1	6.0	108.6	115.0	119.5	114.4	5.4
CMR26	109.6	149.3	139.6	132.8	20.7	132.0	131.6	159.2	140.9	15.8
CMR27	155.2	149.9	149.2	151.4	3.3	157.4	157.3	153.7	156.1	2.1
CMR28	108.1	112.4	106.9	109.1	2.9	125.9	115.7	114.9	118.8	6.1
Average	109.3	117.3	110.1	112.2	27.4	119.8	117.9	117.3	118.3	28.4

Table C.1.2: EDV values for the 20 volunteer participants as measured by observer 2, for all three imaging views and both ventricles, with added averages and standard deviations

Observer 2   End Diastolic Volumes (EDV) (mℓ)

Volunteer no.	Left ventricle					Right ventricle				
	2CV	4CV	SA	Average	St dev	2CV	4CV	SA	Average	St dev
CMR1	120.4	147.8	119.2	129.1	16.2	165.8	141.0	124.6	143.8	20.7
CMR2	86.9	76.3	64.2	75.8	11.4	76.3	68.2	61.0	68.5	7.6
CMR3	87.6	106.0	76.8	90.2	14.8	97.3	81.9	85.2	88.1	8.1
CMR4	80.5	94.6	51.1	75.4	22.2	101.6	83.9	47.7	77.7	27.5
CMR5	153.9	142.5	139.3	145.3	7.7	139.2	87.9	111.0	112.7	25.6
CMR7	115.6	123.7	112.7	117.4	5.7	91.5	98.1	91.0	93.5	4.0
CMR8	92.6	95.0	64.0	83.9	17.2	87.6	82.9	54.6	75.0	17.8
CMR9	161.7	140.5	128.9	143.7	16.7	123.8	131.5	118.0	124.4	6.8
CMR11	96.0	96.6	84.4	92.3	6.9	77.3	87.6	75.3	80.0	6.6
CMR13	114.7	90.1	101.6	102.1	12.3	110.5	80.2	97.0	95.9	15.2
CMR15	145.4	117.9	156.5	139.9	19.9	186.7	132.3	215.9	178.3	42.4
CMR16	87.4	82.8	86.8	85.7	2.5	107.8	84.6	94.7	95.7	11.6
CMR17	105.1	118.0	113.8	112.3	6.6	129.0	137.3	142.6	136.3	6.9
CMR18	67.4	67.7	78.9	71.3	6.5	52.6	60.5	66.4	59.9	6.9
CMR19	83.2	42.2	82.2	69.2	23.4	95.2	49.2	83.5	76.0	23.9
CMR22	89.0	85.3	98.1	90.8	6.6	82.0	82.1	92.8	85.6	6.2
CMR23	93.5	97.7	84.7	92.0	6.6	85.3	90.9	97.6	91.3	6.1
CMR26	111.7	132.5	111.2	118.5	12.2	112.1	104.6	122.6	113.1	9.0
CMR27	163.9	139.4	140.9	148.1	13.7	142.7	151.4	142.4	145.5	5.1
CMR28	109.9	62.1	98.5	90.2	24.9	134.8	91.4	89.5	105.2	25.7
Average	108.3	102.9	99.7	103.7	28.3	110.0	96.4	100.7	102.3	33.1

Table C.1.3: EDV values for the 20 volunteer participants as measured by observer 3, for all three imaging views and both ventricles, with added averages and standard deviations

Observer 3   End Diastolic Volumes (EDV) (mℓ)

Volunteer no.	Left ventricle					Right ventricle				
	2CV	4CV	SA	Average	St dev	2CV	4CV	SA	Average	St dev
CMR1	120.6	183.6	108.9	137.7	40.2	144.0	136.8	116.1	132.3	14.5
CMR2	92.7	77.4	63.9	78.0	14.4	85.5	62.1	65.7	71.1	12.6
CMR3	104.4	126.9	73.8	101.7	26.7	115.2	98.1	106.2	106.5	8.6
CMR4	67.5	85.5	62.1	71.7	12.3	59.4	77.4	59.4	65.4	10.4
CMR5	139.5	168.3	145.8	151.2	15.1	129.6	174.6	158.4	154.2	22.8
CMR7	117.0	126.0	129.6	124.2	6.5	126.0	131.4	132.3	129.9	3.4
CMR8	99.0	109.8	75.6	94.8	17.5	98.1	120.6	94.5	104.4	14.1
CMR9	135.9	163.8	145.8	148.5	14.1	155.7	165.6	148.5	156.6	8.6
CMR11	106.2	112.5	90.0	102.9	11.6	96.3	93.6	93.6	94.5	1.6
CMR13	110.7	106.2	125.1	114.0	9.9	114.3	92.7	135.0	114.0	21.2
CMR15	153.9	156.6	158.4	156.3	2.3	176.4	161.1	171.9	169.8	7.9
CMR16	101.3	96.3	99.0	98.9	2.5	122.6	78.3	119.7	106.9	24.8
CMR17	128.7	126.9	125.1	126.9	1.8	161.1	138.6	169.2	156.3	15.9
CMR18	77.4	96.3	86.4	86.7	9.5	82.8	99.0	93.6	91.8	8.2
CMR19	103.5	96.3	85.5	95.1	9.1	99.0	108.0	99.9	102.3	5.0
CMR22	102.6	103.5	99.0	101.7	2.4	94.5	112.5	100.8	102.6	9.1
CMR23	111.6	98.1	99.9	103.2	7.3	99.0	101.7	117.0	105.9	9.7
CMR26	116.1	139.5	133.0	129.5	12.1	117.9	134.1	144.0	132.0	13.2
CMR27	165.6	163.8	156.6	162.0	4.8	161.1	154.8	175.5	163.8	10.6
CMR28	119.2	116.3	118.9	118.1	1.6	126.5	118.3	125.9	123.6	4.6
Average	113.7	122.7	109.1	115.2	28.3	118.2	118.0	121.4	119.2	31.2

C.1.2. End Systolic Volumes

Table C.1.4: ESV values for the 20 volunteer participants as measured by observer 1, for all three imaging views and both ventricles, with added averages and standard deviations

Observer 1   End Systolic Volumes (ESV) (mℓ)

Volunteer no.	Left ventricle					Right ventricle				
	2CV	4CV	SA	Average	St dev	2CV	4CV	SA	Average	St dev
CMR1	39.6	42.3	36.9	39.6	2.7	63.4	64.4	64.2	64.0	0.5
CMR2	25.6	27.4	22.8	25.3	2.3	24.5	24.3	28.4	25.7	2.3
CMR3	31.9	47.1	29.0	36.0	9.8	49.1	46.2	49.4	48.2	1.8
CMR4	20.6	37.6	17.7	25.3	10.7	36.7	29.6	29.2	31.8	4.2
CMR5	68.1	82.7	70.0	73.6	8.0	65.5	74.4	74.7	71.5	5.2
CMR7	44.2	51.1	45.7	47.0	3.6	40.9	47.0	47.6	45.2	3.7
CMR8	27.0	32.4	23.9	27.8	4.3	39.4	37.7	31.1	36.1	4.4
CMR9	71.1	77.1	55.3	67.9	11.3	67.4	54.5	53.9	58.6	7.6
CMR11	27.1	33.7	36.5	32.4	4.8	31.9	30.7	46.5	36.4	8.8
CMR13	39.1	30.3	39.3	36.2	5.1	43.9	44.9	48.5	45.8	2.4
CMR15	46.5	40.1	62.3	49.6	11.4	57.5	55.6	77.6	63.6	12.1
CMR16	39.3	38.8	42.4	40.2	1.9	43.6	50.7	45.3	46.5	3.7
CMR17	32.8	39.0	35.6	35.8	3.1	58.0	63.1	57.7	59.6	3.0
CMR18	27.0	29.3	32.7	29.7	2.9	34.2	43.8	41.6	39.9	5.0
CMR19	30.2	34.3	32.8	32.4	2.1	39.8	40.5	40.7	40.4	0.5
CMR22	26.8	25.2	23.8	25.3	1.5	29.1	30.5	29.8	29.8	0.7
CMR23	35.1	38.9	32.9	35.6	3.0	46.9	52.2	48.2	49.1	2.8
CMR26	39.8	69.5	53.8	54.4	14.8	47.2	70.1	91.5	69.6	22.2
CMR27	52.8	44.4	52.1	49.8	4.7	54.8	58.6	66.0	59.8	5.7
CMR28	39.1	40.6	43.5	41.1	2.3	42.5	41.3	48.9	44.2	4.1
Average	38.2	43.1	39.4	40.2	14.3	45.8	48.0	51.0	48.3	14.4

Table C.1.5: ESV values for the 20 volunteer participants as measured by observer 2, for all three imaging views and both ventricles, with added averages and standard deviations

Observer 2   End Systolic Volumes (ESV) (mℓ)

Volunteer no.	Left ventricle					Right ventricle				
	2CV	4CV	SA	Average	St dev	2CV	4CV	SA	Average	St dev
CMR1	39.9	40.9	37.7	39.5	1.6	71.5	50.8	58.5	60.2	10.5
CMR2	30.7	29.8	14.9	25.1	8.9	28.3	28.7	26.2	27.7	1.3
CMR3	42.0	43.5	27.0	37.5	9.1	45.5	34.6	42.3	40.8	5.6
CMR4	26.0	36.3	13.4	25.2	11.5	44.0	35.0	25.0	34.7	9.5
CMR5	65.8	57.3	58.0	60.4	4.7	60.6	52.3	76.4	63.1	12.2
CMR7	42.7	45.4	38.3	42.1	3.6	31.7	37.5	29.8	33.0	4.0
CMR8	27.6	27.1	17.4	24.1	5.7	35.5	23.9	24.6	28.0	6.5
CMR9	82.7	73.2	54.8	70.2	14.2	63.2	47.1	54.6	55.0	8.0
CMR11	30.8	34.6	32.6	32.6	1.9	22.1	29.2	29.2	26.8	4.1
CMR13	37.9	27.6	36.0	33.8	5.5	40.4	23.1	33.5	32.3	8.7
CMR15	48.3	46.8	41.8	45.6	3.4	67.9	59.2	68.7	65.3	5.2
CMR16	39.1	32.1	29.2	33.5	5.1	35.5	30.6	41.1	35.7	5.2
CMR17	34.9	34.3	33.3	34.2	0.8	45.4	25.6	66.9	46.0	20.6
CMR18	30.2	27.9	22.2	26.8	4.1	27.9	28.5	32.7	29.7	2.6
CMR19	34.1	17.3	24.1	25.2	8.4	35.5	15.4	34.7	28.5	11.4
CMR22	26.2	25.2	24.7	25.4	0.8	32.4	20.1	20.9	24.5	6.9
CMR23	40.3	34.6	31.1	35.3	4.6	33.0	34.5	36.2	34.6	1.6
CMR26	43.2	61.9	40.3	48.5	11.7	45.4	48.4	56.5	50.1	5.7
CMR27	59.0	52.2	39.4	50.2	9.9	39.0	52.8	53.4	48.4	8.1
CMR28	28.2	19.4	34.2	27.3	7.4	55.5	38.1	47.9	47.2	8.7
Average	40.5	38.4	32.5	37.1	13.8	43.0	35.8	42.9	40.6	14.5

Table C.1.6: ESV values for the 20 volunteer participants as measured by observer 3, for all three imaging views and both ventricles, with added averages and standard deviations

Observer 3　　End Systolic Volumes (ESV) (mℓ)

Volunteer no.	Left ventricle					Right ventricle				
	2CV	4CV	SA	Average	St dev	2CV	4CV	SA	Average	St dev
CMR1	35.1	94.5	37.8	55.8	33.5	64.8	46.8	35.1	48.9	15.0
CMR2	43.2	28.8	18.9	30.3	12.2	29.7	22.5	32.4	28.2	5.1
CMR3	43.2	46.8	27.9	39.3	10.0	64.8	45.0	35.1	48.3	15.1
CMR4	22.5	32.4	18.9	24.6	7.0	28.8	31.5	30.6	30.3	1.4
CMR5	63.9	67.5	68.4	66.6	2.4	49.5	84.6	81.0	71.7	19.3
CMR7	35.1	41.4	43.2	39.9	4.3	45.0	50.4	54.9	50.1	5.0
CMR8	27.9	35.1	23.4	28.8	5.9	25.2	42.3	47.7	38.4	11.7
CMR9	59.4	74.7	49.5	61.2	12.7	59.4	63.0	60.3	60.9	1.9
CMR11	25.2	39.6	27.9	30.9	7.7	36.0	34.2	41.4	37.2	3.7
CMR13	58.5	43.2	46.8	49.5	8.0	56.7	38.7	64.8	53.4	13.4
CMR15	54.0	45.9	45.9	48.6	4.7	68.4	66.6	72.9	69.3	3.2
CMR16	47.2	39.6	42.3	43.0	3.8	64.5	32.4	55.8	50.9	16.6
CMR17	36.9	30.6	42.3	36.6	5.9	66.6	50.4	82.8	66.6	16.2
CMR18	25.2	32.4	32.4	30.0	4.2	46.8	43.2	49.5	46.5	3.2
CMR19	34.2	28.8	33.3	32.1	2.9	36.9	41.4	38.7	39.0	2.3
CMR22	30.6	26.1	30.6	29.1	2.6	29.7	28.8	40.5	33.0	6.5
CMR23	36.9	40.5	45.9	41.1	4.5	41.4	58.5	71.1	57.0	14.9
CMR26	45.0	68.4	51.5	55.0	12.1	54.9	63.0	87.0	68.3	16.7
CMR27	52.2	48.6	50.4	50.4	1.8	51.3	49.5	85.5	62.1	20.3
CMR28	35.9	37.0	34.6	35.8	1.2	52.0	70.4	74.5	65.6	12.0
Average	40.6	45.1	38.6	41.4	14.4	48.6	48.2	57.1	51.3	16.7

C.1.3. Stroke Volumes

For the stroke volume values tabulated in the following three tables, the left-to-right ratios of the average SV over the three imaging views are shown, as well as the absolute differences between the average left and right SV for each volunteer.

Table C.1.7: SV values for the 20 volunteer participants as measured by observer 1, for all three imaging views and both ventricles, with added averages and standard deviations

Observer 1   Stroke volumes (SV) (mℓ)

| Volunteer no. | Left ventricle | | | | Right ventricle | | | | Ratio | Abs diff |
	2CV	4CV	SA	Average	2CV	4CV	SA	Average	L:R	LV-RV (mℓ)
CMR1	80.4	84.0	91.8	85.4	84.8	77.2	81.5	81.2	1.1	4.2
CMR2	60.0	52.9	53.6	55.5	63.5	53.0	56.3	57.6	1.0	-2.1
CMR3	51.7	57.8	56.6	55.3	58.5	53.5	54.8	55.6	1.0	-0.2
CMR4	49.5	57.8	37.9	48.4	43.9	42.3	28.9	38.4	1.3	10.0
CMR5	81.0	86.3	86.8	84.7	90.6	85.7	74.1	83.5	1.0	1.2
CMR7	84.2	84.3	76.9	81.8	73.6	69.7	64.0	69.1	1.2	12.7
CMR8	69.4	63.9	53.6	62.3	60.3	63.2	45.6	56.4	1.1	5.9
CMR9	77.3	77.8	95.5	83.5	92.1	96.4	97.0	95.2	0.9	-11.6
CMR11	66.1	65.9	53.7	61.9	61.5	57.4	43.6	54.2	1.1	7.7
CMR13	86.6	72.8	72.3	77.2	79.7	76.8	77.1	77.9	1.0	-0.6
CMR15	99.7	108.0	104.0	103.9	101.2	105.2	91.1	99.2	1.0	4.7
CMR16	53.2	72.3	54.3	59.9	65.3	57.4	52.5	58.4	1.0	1.5
CMR17	82.7	94.0	82.8	86.5	94.3	84.6	91.2	90.0	1.0	-3.5
CMR18	51.5	50.8	52.0	51.4	48.2	48.6	51.5	49.4	1.0	2.0
CMR19	59.9	64.3	61.8	62.0	64.7	62.7	57.5	61.6	1.0	0.4
CMR22	66.3	65.5	70.6	67.5	65.0	65.8	66.3	65.7	1.0	1.8
CMR23	61.5	68.2	63.7	64.5	61.7	62.7	71.3	65.2	1.0	-0.8
CMR26	69.8	79.8	85.8	78.5	84.9	61.5	67.7	71.4	1.1	7.1
CMR27	102.4	105.5	97.1	101.7	102.6	98.7	87.7	96.4	1.1	5.3
CMR28	69.0	71.8	63.4	68.0	83.4	74.4	66.1	74.6	0.9	-6.6
Mean				72.0				70.0	1.0	2.0
Std Dev				15.9				16.9	0.1	5.6

Table C.1.8: SV values for the 20 volunteer participants as measured by observer 2, for all three imaging views and both ventricles, with added averages and standard deviations

Observer 2   Stroke volumes (SV) (mℓ)

Volunteer no.	Left ventricle				Right ventricle				Ratio	Abs diff LV-RV
	2CV	4CV	SA	Average	2CV	4CV	SA	Average	L:R	(mℓ)
CMR1	80.5	106.9	81.5	89.6	94.3	90.2	66.1	83.6	1.1	6.1
CMR2	56.2	46.6	49.3	50.7	48.0	39.5	34.8	40.8	1.2	9.9
CMR3	45.7	62.5	49.8	52.7	51.8	47.3	42.9	47.3	1.1	5.3
CMR4	54.5	58.3	37.8	50.2	57.6	48.9	22.7	43.1	1.2	7.1
CMR5	88.1	85.2	81.3	84.9	78.6	35.7	34.7	49.6	1.7	35.2
CMR7	72.9	78.3	74.5	75.2	59.8	60.7	61.1	60.5	1.2	14.7
CMR8	65.0	67.9	46.6	59.8	52.0	59.0	30.0	47.0	1.3	12.8
CMR9	79.0	67.3	74.1	73.5	60.6	84.4	63.4	69.5	1.1	4.0
CMR11	65.2	62.0	51.8	59.7	55.2	58.4	46.1	53.2	1.1	6.4
CMR13	76.8	62.5	65.6	68.3	70.1	57.2	63.5	63.6	1.1	4.7
CMR15	97.1	71.1	114.7	94.3	118.8	73.1	147.3	113.1	0.8	-18.7
CMR16	48.2	50.7	57.6	52.2	72.3	54.0	53.6	60.0	0.9	-7.8
CMR17	70.1	83.8	80.6	78.2	83.6	111.6	75.7	90.3	0.9	-12.1
CMR18	37.2	39.9	56.7	44.6	24.7	32.0	33.7	30.1	1.5	14.4
CMR19	49.1	24.8	58.0	44.0	59.7	33.8	48.8	47.4	0.9	-3.4
CMR22	62.8	60.1	73.4	65.4	49.6	62.0	71.8	61.2	1.1	4.3
CMR23	53.2	63.2	53.6	56.7	52.3	56.4	61.4	56.7	1.0	0.0
CMR26	68.5	70.6	71.0	70.0	66.7	56.2	66.1	63.0	1.1	7.0
CMR27	105.0	87.2	101.5	97.9	103.7	98.6	89.0	97.1	1.0	0.8
CMR28	81.7	42.7	64.3	62.9	79.3	53.3	41.6	58.1	1.1	4.8
Mean				66.5				61.8	1.1	4.8
Std Dev				16.2				20.4	0.2	11.1

Table C.1.9: SV values for the 20 volunteer participants as measured by observer 3, for all three imaging views and both ventricles, with added averages and standard deviations

Observer 3   Stroke volumes (SV) (mℓ)

| Volunteer no. | Left ventricle | | | | Right ventricle | | | | Ratio | Abs diff LV-RV |
	2CV	4CV	SA	Average	2CV	4CV	SA	Average	L:R	(mℓ)
CMR1	85.5	89.1	71.1	81.9	79.2	90.0	81.0	83.4	1.0	-1.5
CMR2	49.5	48.6	45.0	47.7	55.8	39.6	33.3	42.9	1.1	4.8
CMR3	61.2	80.1	45.9	62.4	50.4	53.1	71.1	58.2	1.1	4.2
CMR4	45.0	53.1	43.2	47.1	30.6	45.9	28.8	35.1	1.3	12.0
CMR5	75.6	100.8	77.4	84.6	80.1	90.0	77.4	82.5	1.0	2.1
CMR7	81.9	84.6	86.4	84.3	81.0	81.0	77.4	79.8	1.1	4.5
CMR8	71.1	74.7	52.2	66.0	72.9	78.3	46.8	66.0	1.0	0.0
CMR9	76.5	89.1	96.3	87.3	96.3	102.6	88.2	95.7	0.9	-8.4
CMR11	81.0	72.9	62.1	72.0	60.3	59.4	52.2	57.3	1.3	14.7
CMR13	52.2	63.0	78.3	64.5	57.6	54.0	70.2	60.6	1.1	3.9
CMR15	99.9	110.7	112.5	107.7	108.0	94.5	99.0	100.5	1.1	7.2
CMR16	54.1	56.7	56.7	55.8	58.1	45.9	63.9	56.0	1.0	-0.1
CMR17	91.8	96.3	82.8	90.3	94.5	88.2	86.4	89.7	1.0	0.6
CMR18	52.2	63.9	54.0	56.7	36.0	55.8	44.1	45.3	1.3	11.4
CMR19	69.3	67.5	52.2	63.0	62.1	66.6	61.2	63.3	1.0	-0.3
CMR22	72.0	77.4	68.4	72.6	64.8	83.7	60.3	69.6	1.0	3.0
CMR23	74.7	57.6	54.0	62.1	57.6	43.2	45.9	48.9	1.3	13.2
CMR26	71.1	71.1	81.6	74.6	63.0	71.1	57.0	63.7	1.2	10.9
CMR27	113.4	115.2	106.2	111.6	109.8	105.3	90.0	101.7	1.1	9.9
CMR28	83.3	79.3	84.3	82.3	74.5	47.8	51.4	57.9	1.4	24.4
Mean				73.7				67.9	1.1	5.8
Std Dev				17.7				19.4	0.1	7.3

C.1.4. Ejection Fractions

Table C.1.10: EF values for the 20 volunteer participants as measured by observer 1, for all three imaging views and both ventricles, with added averages and standard deviations

Observer 1   Ejection fractions (EF) (%)

Volunteer no.	Left ventricle					Right ventricle				
	2CV	4CV	SA	Average	St dev	2CV	4CV	SA	Average	St dev
CMR1	67.0	66.5	71.3	68.3	2.7	57.2	54.5	55.9	55.9	1.4
CMR2	70.1	65.9	70.2	68.7	2.4	72.2	68.6	66.5	69.1	2.9
CMR3	61.8	55.1	66.1	61.0	5.6	54.4	53.7	52.6	53.5	0.9
CMR4	70.6	60.6	68.1	66.5	5.2	54.5	58.9	49.7	54.4	4.6
CMR5	54.3	51.1	55.3	53.6	2.2	58.1	53.5	49.8	53.8	4.1
CMR7	65.6	62.3	62.7	63.5	1.8	64.3	59.7	57.4	60.5	3.5
CMR8	72.0	66.4	69.1	69.2	2.8	60.5	62.6	59.5	60.9	1.6
CMR9	52.1	50.2	63.3	55.2	7.1	57.8	63.9	64.3	62.0	3.7
CMR11	70.9	66.2	59.6	65.6	5.7	65.8	65.2	48.4	59.8	9.9
CMR13	68.9	70.6	64.8	68.1	3.0	64.5	63.1	61.4	63.0	1.6
CMR15	68.2	72.9	62.5	67.9	5.2	63.8	65.4	54.0	61.1	6.2
CMR16	57.5	65.1	56.2	59.6	4.8	60.0	53.1	53.7	55.6	3.8
CMR17	71.6	70.7	69.9	70.7	0.9	61.9	57.3	61.2	60.1	2.5
CMR18	65.6	63.4	61.4	63.5	2.1	58.5	52.6	55.3	55.5	2.9
CMR19	66.5	65.2	65.3	65.7	0.7	61.9	60.7	58.5	60.4	1.7
CMR22	71.2	72.2	74.8	72.7	1.8	69.1	68.3	69.0	68.8	0.4
CMR23	63.7	63.7	66.0	64.4	1.3	56.8	54.6	59.7	57.0	2.6
CMR26	63.6	53.5	61.5	59.5	5.4	64.3	46.7	42.5	51.2	11.5
CMR27	66.0	70.4	65.1	67.1	2.8	65.2	62.8	57.1	61.7	4.2
CMR28	63.8	63.9	59.3	62.3	2.6	66.3	64.3	57.5	62.7	4.6
Average	65.6	63.8	64.6	64.7	5.8	61.8	59.5	56.7	59.3	6.0

Table C.1.11: EF values for the 20 volunteer participants as measured by observer 2, for all three imaging views and both ventricles, with added averages and standard deviations

Observer 2   Ejection fractions (EF) (%)

Volunteer no.	Left ventricle					Right ventricle				
	2CV	4CV	SA	Average	St dev	2CV	4CV	SA	Average	St dev
CMR1	66.9	72.4	68.3	69.2	2.8	56.9	64.0	53.1	58.0	5.5
CMR2	64.6	61.0	76.8	67.5	8.3	63.0	57.9	57.1	59.3	3.2
CMR3	52.1	58.9	64.9	58.6	6.4	53.2	57.7	50.4	53.8	3.7
CMR4	67.7	61.6	73.9	67.7	6.1	56.7	58.3	47.6	54.2	5.7
CMR5	57.2	59.8	58.4	58.5	1.3	56.5	40.6	31.2	42.8	12.8
CMR7	63.0	63.3	66.0	64.1	1.7	65.3	61.8	67.2	64.8	2.7
CMR8	70.2	71.4	72.8	71.5	1.3	59.4	71.2	54.9	61.8	8.4
CMR9	48.9	47.9	57.5	51.4	5.3	49.0	64.2	53.8	55.6	7.8
CMR11	67.9	64.2	61.4	64.5	3.3	71.4	66.7	61.2	66.4	5.1
CMR13	67.0	69.4	64.6	67.0	2.4	63.5	71.2	65.4	66.7	4.0
CMR15	66.8	60.3	73.3	66.8	6.5	63.6	55.2	68.2	62.4	6.6
CMR16	55.2	61.2	66.4	60.9	5.6	67.1	63.8	56.6	62.5	5.3
CMR17	66.7	71.0	70.8	69.5	2.4	64.8	81.3	53.1	66.4	14.2
CMR18	55.1	58.9	71.8	61.9	8.8	46.9	52.9	50.8	50.2	3.0
CMR19	59.0	58.9	70.6	62.8	6.8	62.7	68.7	58.5	63.3	5.1
CMR22	70.5	70.4	74.8	71.9	2.5	60.5	75.5	77.4	71.2	9.3
CMR23	56.9	64.6	63.2	61.6	4.1	61.3	62.0	62.9	62.1	0.8
CMR26	61.3	53.3	63.8	59.5	5.5	59.5	53.7	53.9	55.7	3.3
CMR27	64.0	62.6	72.0	66.2	5.1	72.7	65.1	62.5	66.8	5.3
CMR28	74.3	68.7	65.3	69.5	4.5	58.8	58.3	46.5	54.5	7.0
Average	62.8	63.0	67.8	64.5	6.6	60.6	62.5	56.6	59.9	8.7

Table C.1.12: EF values for the 20 volunteer participants as measured by observer 3, for all three imaging views and both ventricles, with added averages and standard deviations

Observer 3   Ejection fractions (EF) (%)

| Volunteer no. | Left ventricle | | | | | Right ventricle | | | | |
	2CV	4CV	SA	Average	St dev	2CV	4CV	SA	Average	St dev
CMR1	70.9	48.5	65.3	61.6	11.6	55.0	65.8	69.8	63.5	7.6
CMR2	53.4	62.8	70.4	62.2	8.5	65.3	63.8	50.7	59.9	8.0
CMR3	58.6	63.1	62.2	61.3	2.4	43.8	54.1	66.9	54.9	11.6
CMR4	66.7	62.1	69.6	66.1	3.8	51.5	59.3	48.5	53.1	5.6
CMR5	54.2	59.9	53.1	55.7	3.7	61.8	51.5	48.9	54.1	6.8
CMR7	70.0	67.1	66.7	67.9	1.8	64.3	61.6	58.5	61.5	2.9
CMR8	71.8	68.0	69.0	69.6	2.0	74.3	64.9	49.5	62.9	12.5
CMR9	56.3	54.4	66.0	58.9	6.3	61.8	62.0	59.4	61.1	1.4
CMR11	76.3	64.8	69.0	70.0	5.8	62.6	63.5	55.8	60.6	4.2
CMR13	47.2	59.3	62.6	56.4	8.1	50.4	58.3	52.0	53.5	4.2
CMR15	64.9	70.7	71.0	68.9	3.4	61.2	58.7	57.6	59.2	1.9
CMR16	53.4	58.9	57.3	56.5	2.8	47.4	58.6	53.4	53.1	5.6
CMR17	71.3	75.9	66.2	71.1	4.9	58.7	63.6	51.1	57.8	6.3
CMR18	67.4	66.4	62.5	65.4	2.6	43.5	56.4	47.1	49.0	6.6
CMR19	67.0	70.1	61.1	66.0	4.6	62.7	61.7	61.3	61.9	0.8
CMR22	70.2	74.8	69.1	71.3	3.0	68.6	74.4	59.8	67.6	7.3
CMR23	66.9	58.7	54.1	59.9	6.5	58.2	42.5	39.2	46.6	10.1
CMR26	61.2	51.0	61.3	57.8	6.0	53.4	53.0	39.6	48.7	7.9
CMR27	68.5	70.3	67.8	68.9	1.3	68.2	68.0	51.3	62.5	9.7
CMR28	69.9	68.2	70.9	69.7	1.4	58.9	40.4	40.8	46.7	10.5
Average	64.3	63.7	64.8	64.3	6.9	58.6	59.1	53.1	56.9	8.5

C.2.1. Bar graphs

The measured EDV and ESV are displayed in bar charts in the following figures. Figures C.2.1 to C.2.4 show left ventricle EDV and ESV data from observers 2 and 3, which were not included in the Results section. Figures C.2.5 to C.2.8 show right ventricle EDV and ESV data as determined in the 2CV and 4CV data, which were not included as examples in the Results section. The average measured EDV and ESV are displayed in bar charts in figures C.2.9 to C.2.12 showing the volumes determined by the 3 observers for each volunteer, as well as for left and right ventricles separately.
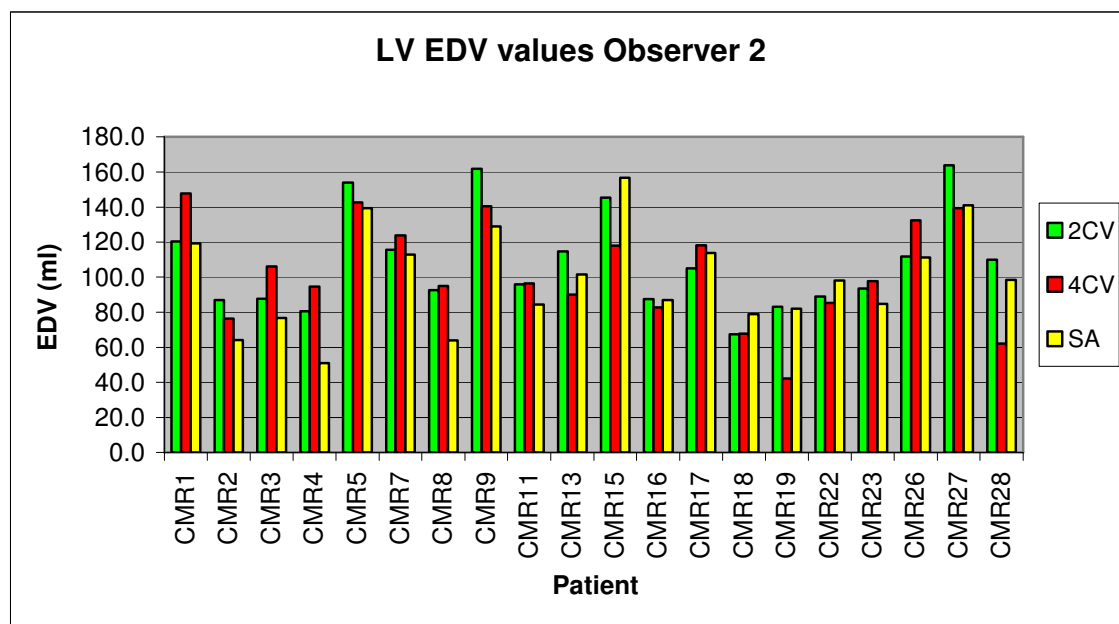
Figure C.2.1: Left ventricle end-diastolic volumes for all 20 volunteers, as measured by observer 2 in the three imaging views
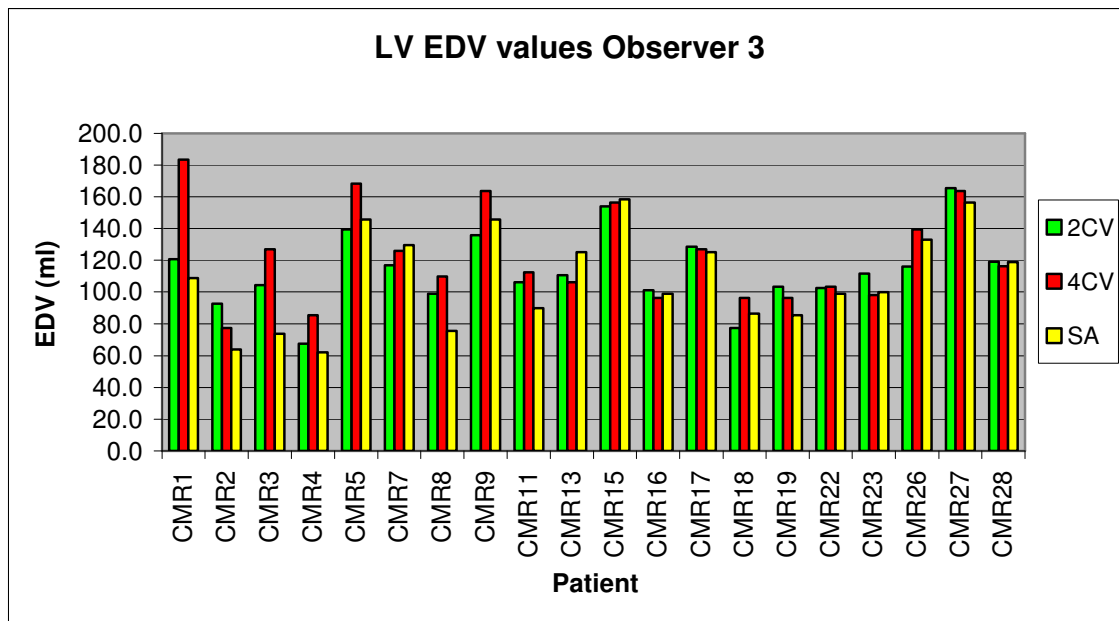
Figure C.2.2: Left ventricle end-diastolic volumes for all 20 volunteers, as measured by observer 3 in the three imaging views
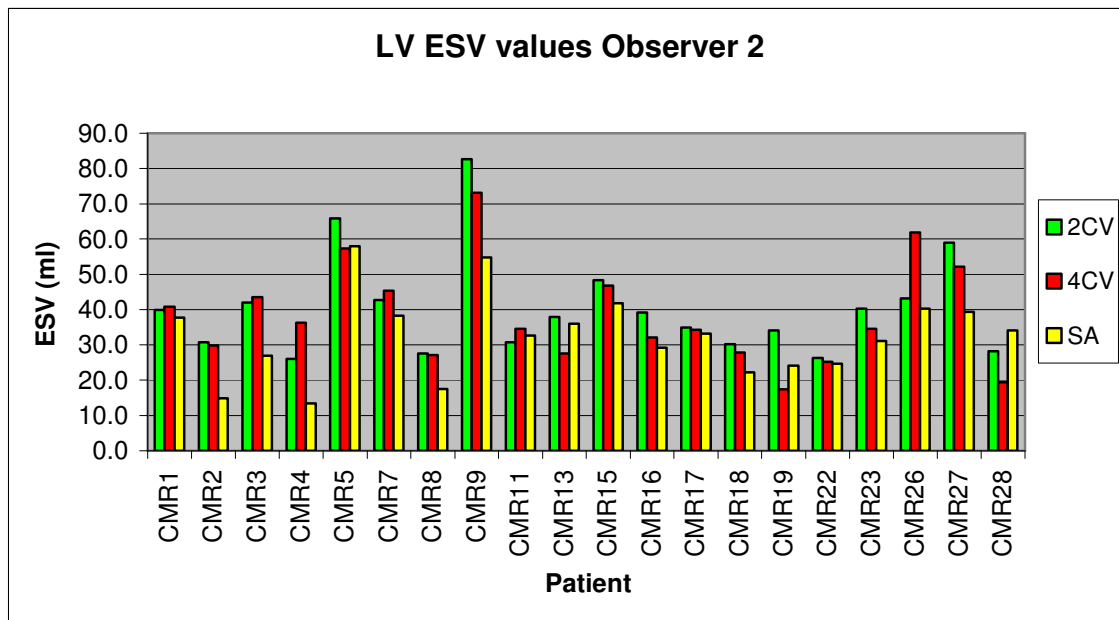
Figure C.2.3: Left ventricle end-systolic volumes for all 20 volunteers, as measured by observer 2 in the three imaging views
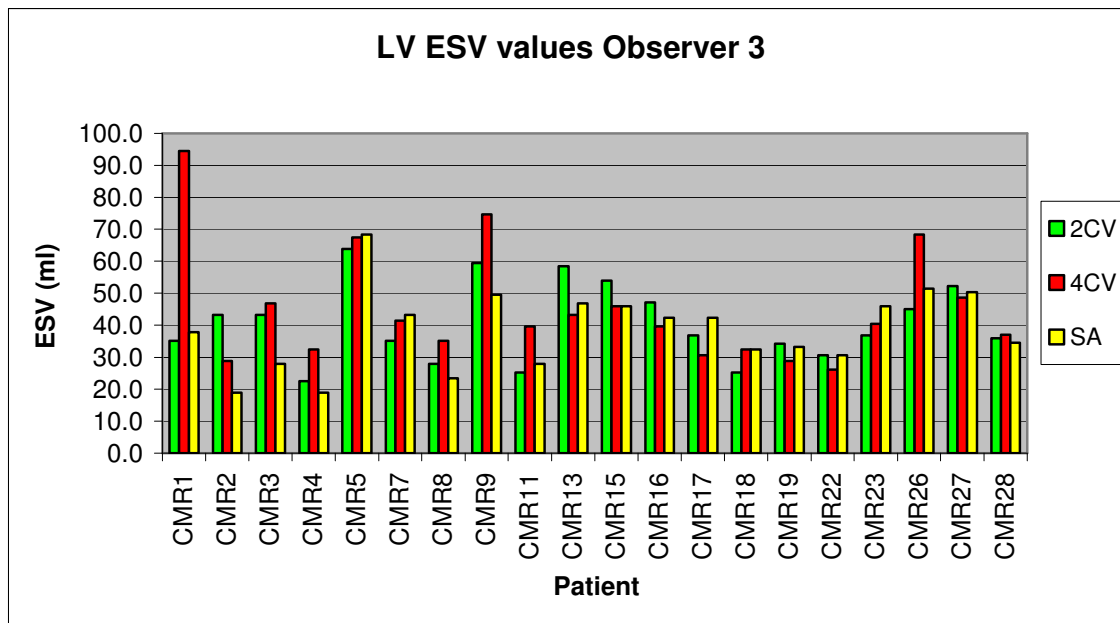
Figure C.2.4: Left ventricle end-systolic volumes for all 20 volunteers, as measured by observer 3 in the three imaging views
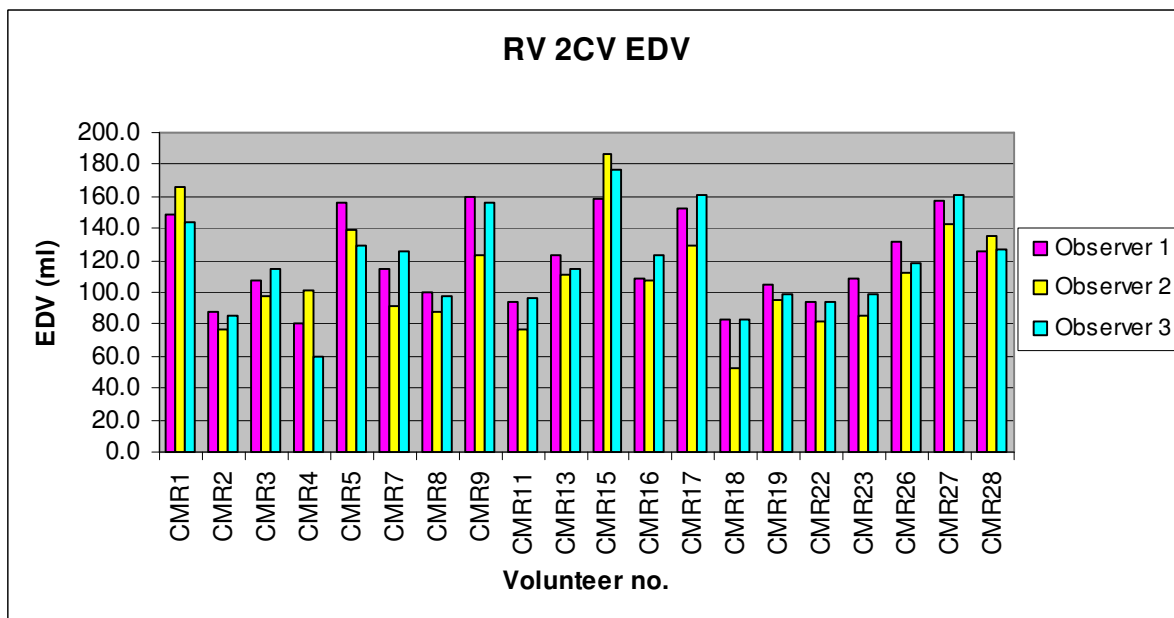
Figure C.2.5: Right ventricle end-diastolic volumes for all 20 volunteers, as measured by the 3 observers on the 2CV data
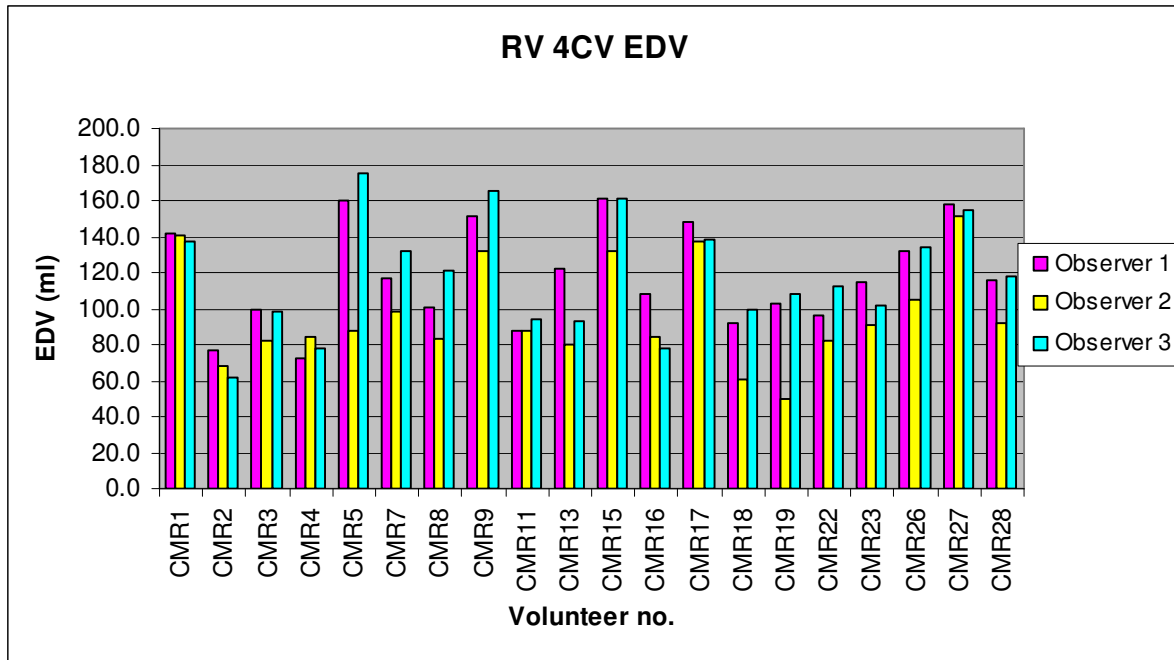
Figure C.2.6: Right ventricle end-diastolic volumes for all 20 volunteers, as measured by the 3 observers on the 4CV data
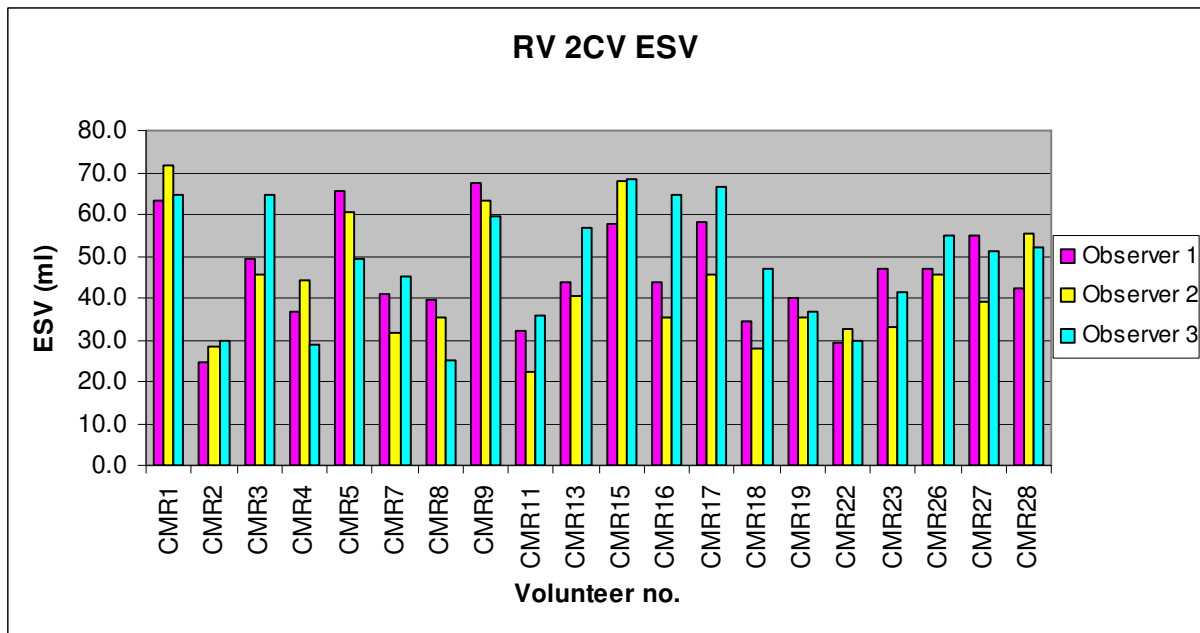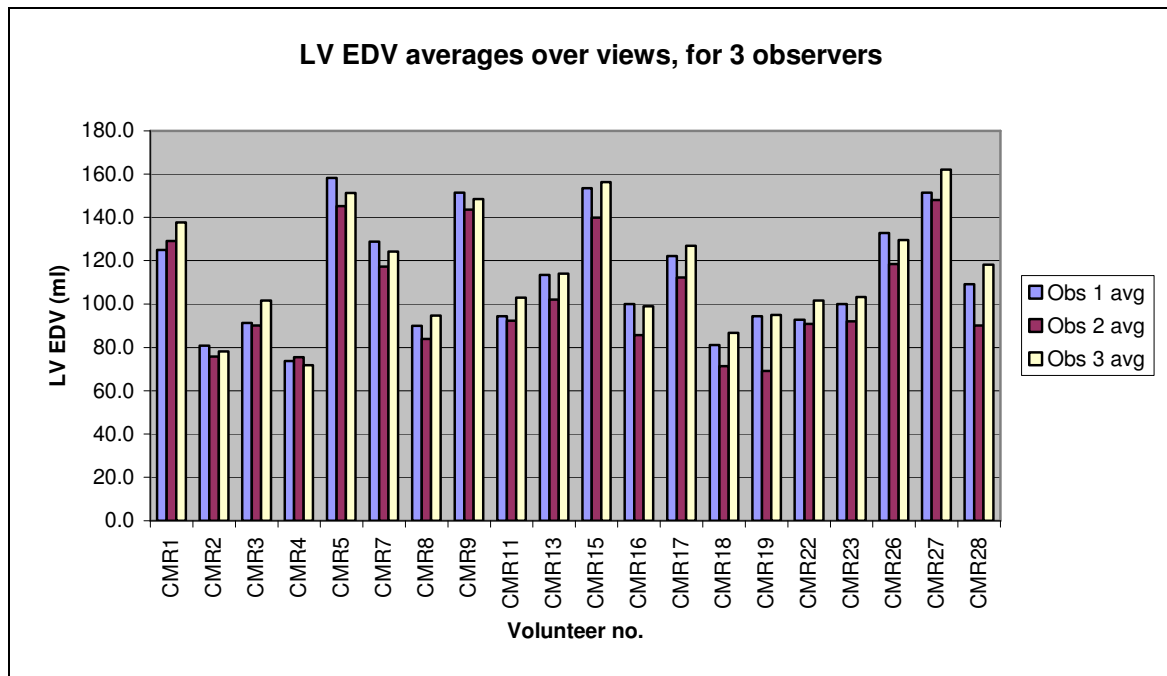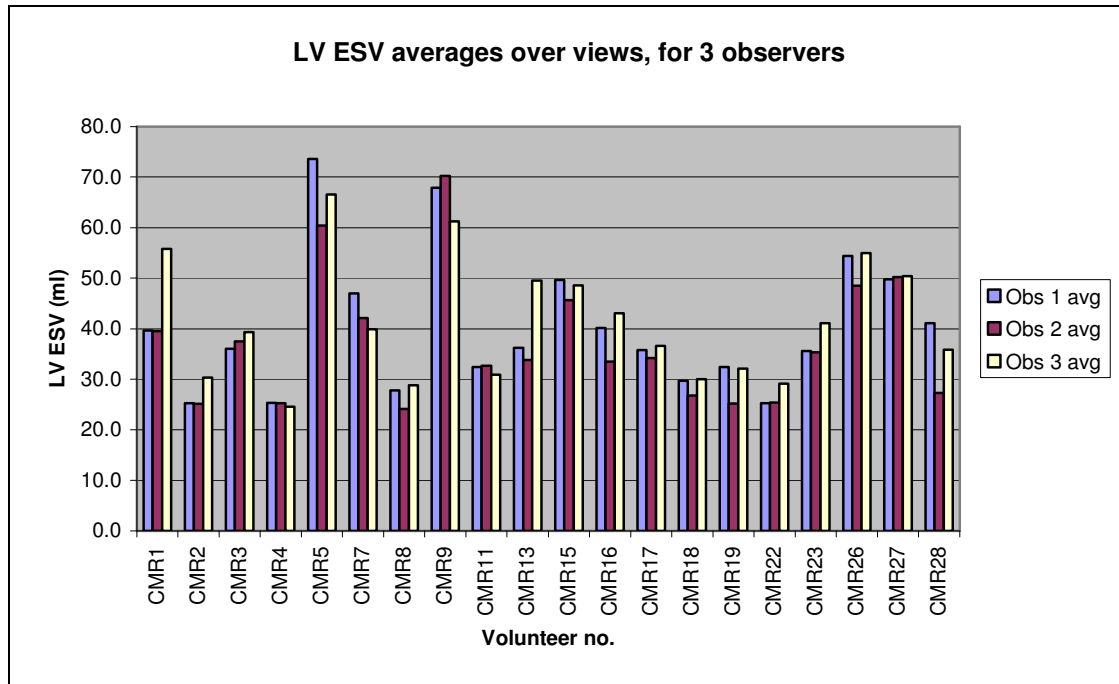

Figure C.2.7: Right ventricle end-systolic volumes for all 20 volunteers, as measured by the 3 observers on the 2CV data
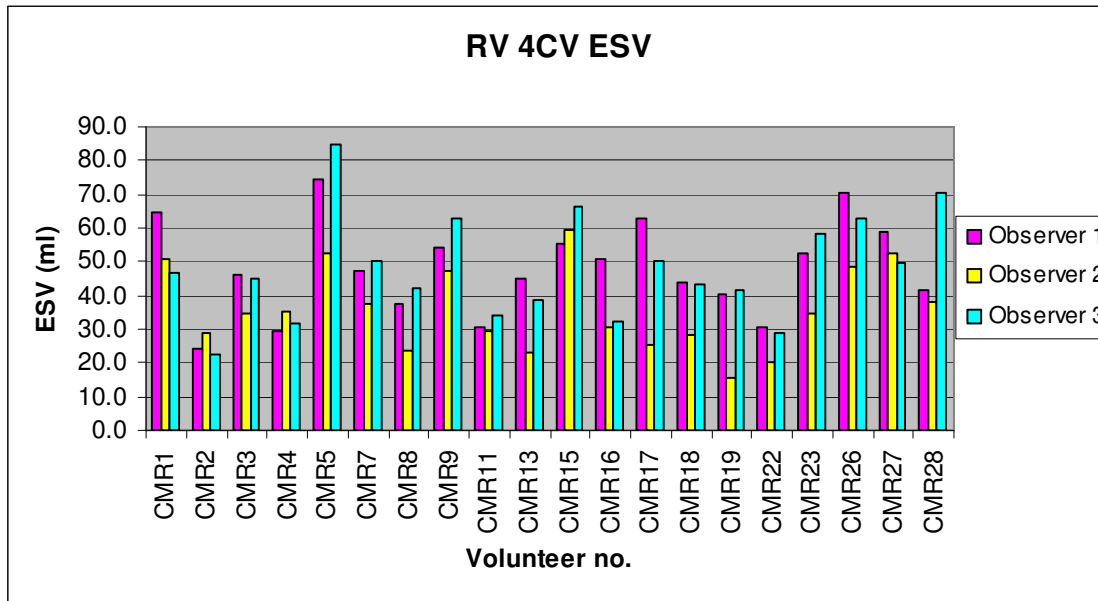
Figure C.2.8: Right ventricle end-systolic volumes for all 20 volunteers, as measured by the 3 observers on the 4CV data

Figure C.2.9: Average left ventricle end-diastolic volumes for all 20 volunteers, as measured by the 3 observers

Figure C.2.10: Average left ventricle end-systolic volumes for all 20 volunteers, as measured by the 3 observers
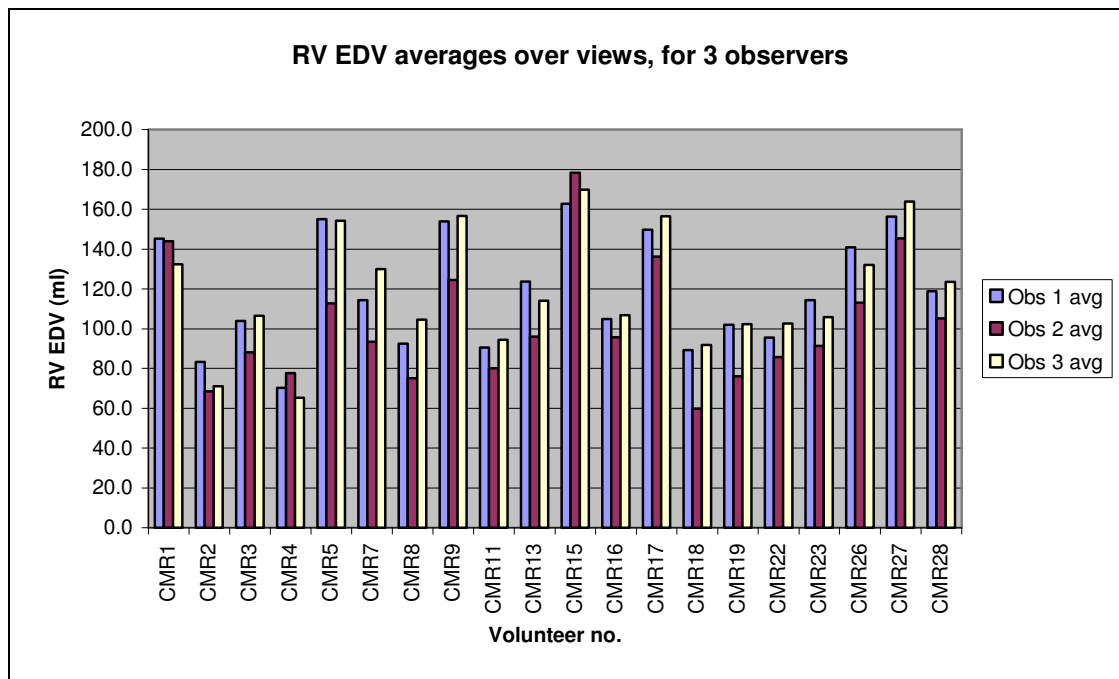

Figure C.2.11: Average right ventricle end-diastolic volumes for all 20 volunteers, as measured by the 3 observers
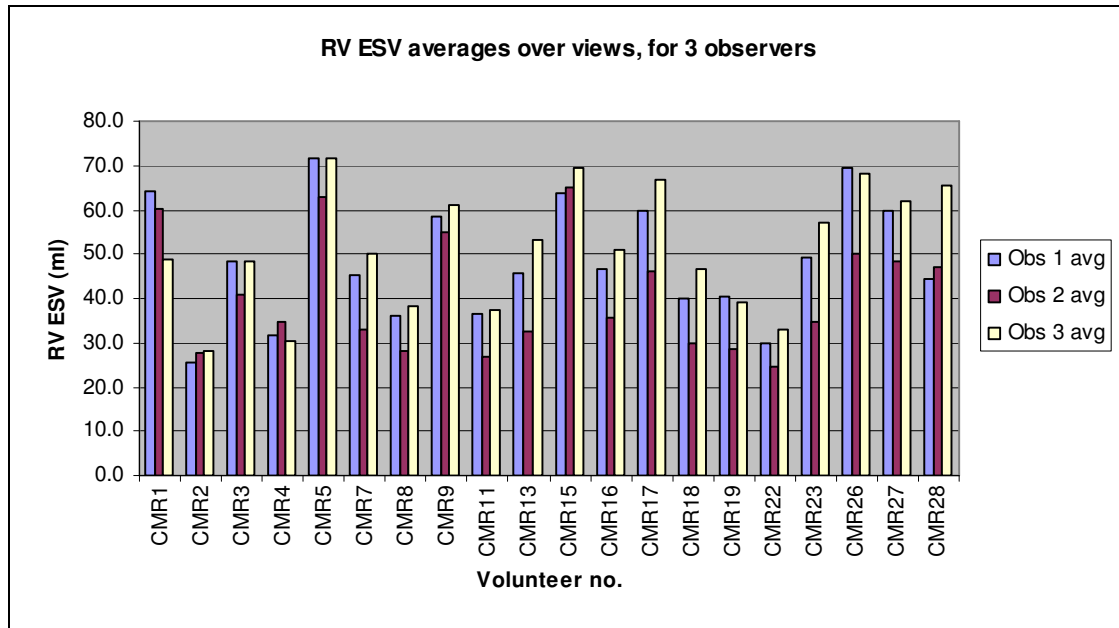
Figure C.2.12: Average right ventricle end-systolic volumes for all 20 volunteers, as measured by the 3 observers

The following three Box and Whisker charts in figure C.2.13 to figure C.2.15 display the EF data per imaging view, for both ventricles, for observer 1, 2 and 3 respectively.
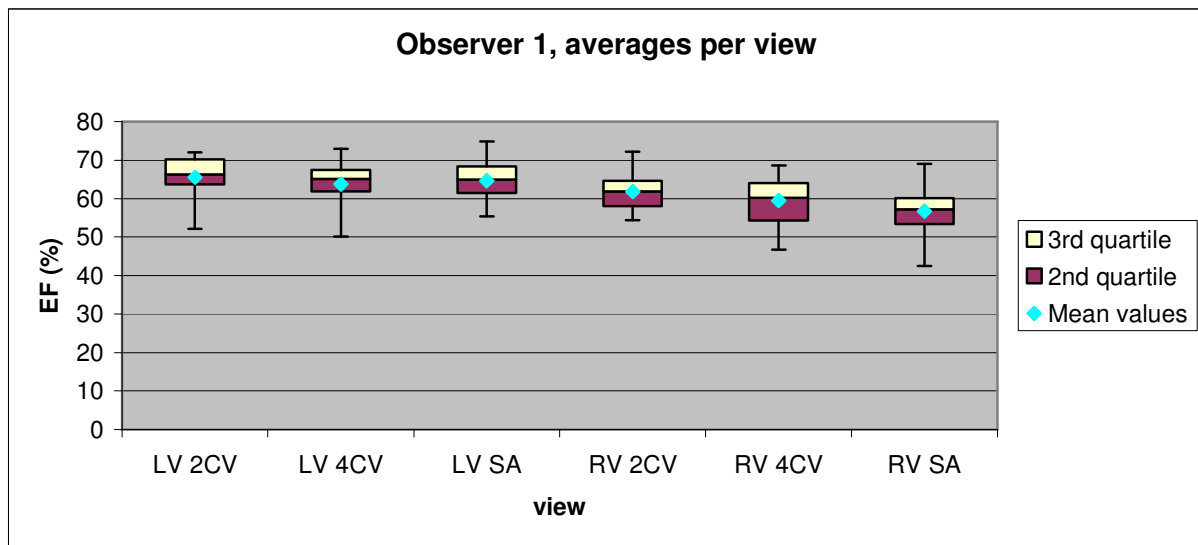

Figure C.2.13: Boxplot of EF statistics from the results of observer 1, for both ventricles. The endpoints of the whiskers show the maximum and minimum values in the data.
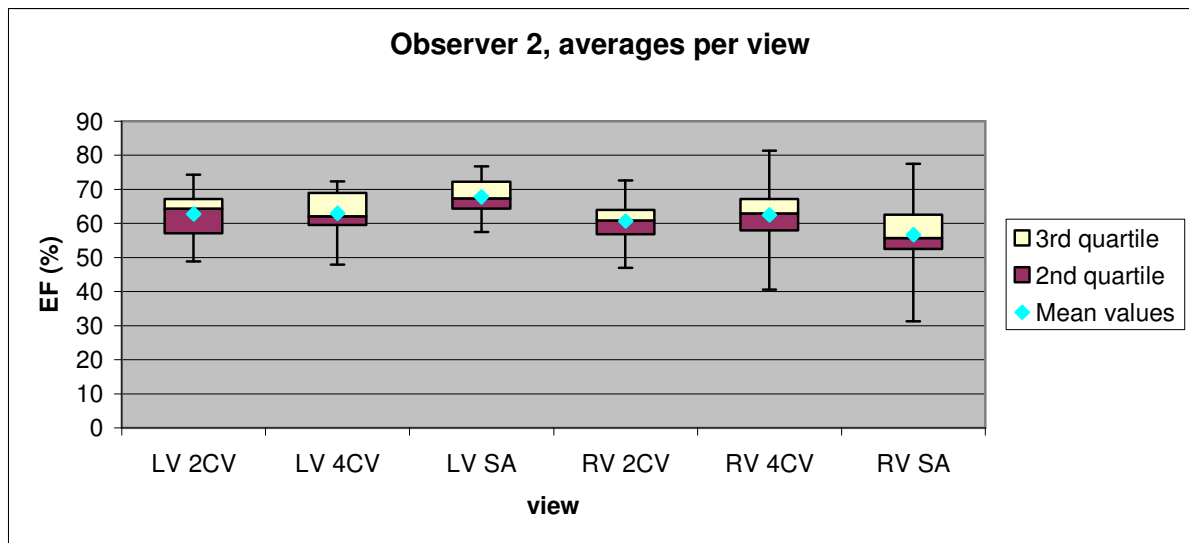
Figure C.2.14: Boxplot of EF statistics from the results of observer 2, for both ventricles. The endpoints of the whiskers show the maximum and minimum values in the data.
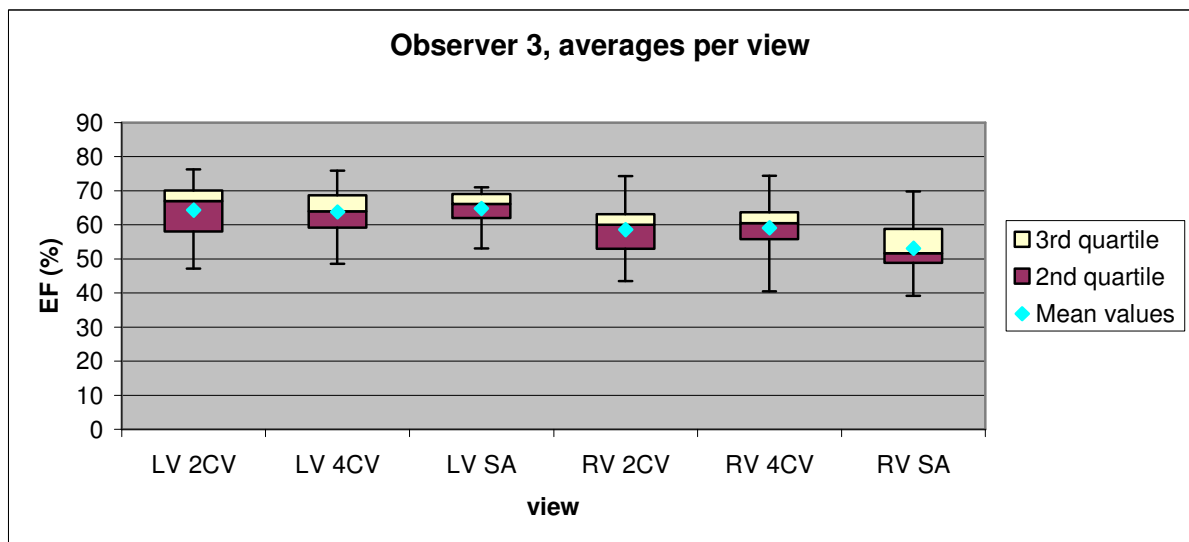

Figure C.2.15: Boxplot of EF statistics from the results of observer 3, for both ventricles. The endpoints of the whiskers show the maximum and minimum values in the data.

The study has been presented at various events during development of the method. Abstracts submitted and published for the different meetings are presented below.

D.1. School of Medicine Faculty Forum 2008

QUANTIFICATION OF NORMAL RIGHT AND LEFT VENTRICULAR FUNCTION, AS EVALUATED USING CARDIAC MAGNETIC RESONANCE IMAGING

N Willemse, WID Rae, CP Herbst

Introduction and Aim: Until recently, left ventricular function has been widely investigated and utilised in diagnostic radiology and nuclear medicine. Right ventricular function, however, has only recently been studied and has become of clinical importance as recent studies have shown that right ventricular function is an important determinant of prognosis in patients with myocardial infarction and other cardiac pathologies. The aim of this study was the benchmarking of normal values for right ventricular function at Universitas Hospital.

Material and Methods: Twenty healthy normal male and female volunteers in the age range 22 to 54, with no known cardiac abnormalities were included in the study. The evaluation was based on multislice imaging in three imaging planes (2-Chamber View, 4-Chamber View and Short Axis View) of both the ventricles using standard cardiac Magnetic Resonance (MR) imaging. This was performed in the Radiology Department, Universitas Hospital. End-diastolic volumes (EDV) and end-systolic volumes (ESV) were measured, and the stroke volumes (SV) and ejection fractions (EF) calculated for both the left and right ventricles. Regions of interest were drawn manually on all the slices intersecting the ventricles. These volumes were compared for the three different imaging planes of the heart.

Results: The average ejection fractions for the 2-Chamber View, 4-Chamber View and Short Axis View were found to be 69%, 66% and 63% respectively for the left ventricle, and 56%, 56% and 44% for the right ventricle.

Conclusion: Ejection fractions are as expected for the sample group studied. As the volume calculation for the different views were not consistent, further investigation will be carried out. It is suggested that images from the 2-Chamber View and 4-Chamber View imaging planes be used for quantification of right ventricular function.

INTER-OBSERVER VARIATION IN MANUAL CONTOURING OF VENTRICULAR FUNCTION CALCULATION USING CARDIAC MAGNETIC RESONANCE IMAGING

N Willemse, WID Rae, CP Herbst

Introduction and Aim: Until recently, left ventricular function has been widely investigated and utilised in diagnostic radiology and nuclear medicine. Right ventricular function has however only recently been studied and has become of clinical importance as recent studies have shown that right ventricular function is an important determinant of prognosis in patients with myocardial infarction and other cardiac pathologies. The aim of this study was the development of an acceptable manual contouring method and the inter-observer variation when using this method at Universitas Hospital, Bloemfontein.

Methodology: 27 subjects were entered into the study, of which 20 healthy normal male and female volunteers in the age range 22 to 54, with no known cardiac abnormalities, were included in the study. Informed consent was obtained from all the volunteers. The evaluation was based on multi-slice imaging in three imaging planes (2-Chamber View, 4-Chamber View and Short Axis View) of both ventricles using standard cardiac Magnetic Resonance imaging (MRI). This was performed in the Radiology Department, Universitas Hospital. End-diastolic volumes (EDV) and end-systolic volumes (ESV) were measured using a manual contouring method performed by three independent observers on all three imaging planes, and the stroke volumes (SV) and ejection fractions (EF) were calculated for both the left and right ventricles.

Results: Typical values from one observer for the average stroke volumes and ejection fractions for the 2-Chamber View, 4-Chamber View and Short Axis View were found to be 71.2mℓ, 65.6%, 74.2mℓ, 63.8% and 70.7mℓ, 64.6% respectively for the left ventricle, and 73.6mℓ, 61.7%, 70.1mℓ, 59.4% and 65.8mℓ, 56.2% for the right ventricle. Average values from the three observers were 72.0mℓ, 64.7%, 66.5mℓ, 64.5% and 76.4mℓ, 63.6% for the left ventricle, and 69.8mℓ, 59.1%, 61.8mℓ, 59.9% and 69.8mℓ, 53.5% for the right ventricle. The values from the three observers were compared, and relative maximum differences in the stroke volumes and ejection fractions were found to be 6.4mℓ, 2.1% and 6.7mℓ, 6.8% for the left and right ventricles respectively.

Conclusion: Ejection fractions and stroke volumes are as expected for the normal healthy adult volunteers studied. The variation between the three observers was thought to be acceptable. Problems encountered with the drawing of the contours included the uncertainty in the determination of valve levels, partial volume effect, image quality and movement. The variation between observers can be attributed to the problems encountered, but the technique is thought to be useful and is being investigated further.

ACCURACY AND VALIDITY OF A MANUAL CONTOURING METHOD FOR QUANTIFICATION OF NORMAL RIGHT AND LEFT VENTRICULAR FUNCTION ON CARDIAC MRI

N Willemse, WID Rae, CP Herbst, G Joubert

Introduction and aim: Imaging determined left ventricular function has been widely investigated and is clinically useful. Recent studies have shown that right ventricular function is also an important prognosticator in patients with cardiac pathologies. The aim of this study was the assessment of quantification of normal right and left ventricular ejection fractions (RVEF and LVEF) as done using manual contouring on cardiac Magnetic Resonance Imaging (MRI) images at Universitas Hospital, Bloemfontein.

Material and Methods: The study was conducted on 10 male and 10 female healthy normal volunteers (age 22 – 53 years) with no known cardiac abnormalities. All volunteers gave informed consent. Multi-slice MR images in three imaging planes (2-Chamber 4-Chamber and Short Axis views) were acquired using the standard cardiac MRI protocol. Left and right ventricular end-diastolic volumes (LVEDV and RVEDV) and end-systolic volumes (LVESV and RVESV) were determined using a manual contouring method performed by three independent observers on all planes. The stroke volumes (LVSV and RVSV) and ejection fractions were calculated. Average indices were compared using T-tests

Results: LVEDV and LVESV as well as RVEDV and RVESV values differed significantly ($p < 0.05$) between two observers. No statistically significant difference ($p > 0.05$) was found between EFs calculated by different observers. Average is LVEF = 64.6 ± 4.0%, RVEF = 58.9 ± 5.3%.

Conclusion: The degree of observer dependence was thought acceptable. EFs and SVs are as expected for the study group. Variations and errors were attributed to uncertainty in determination of valve levels, partial volume effects, slice thickness, image quality and movement artefacts. This manual technique is thought to be acceptable and valid.

QUANTIFICATION OF NORMAL RIGHT AND LEFT VENTRICULAR FUNCTION USING MANUAL CONTOURING ON CARDIAC MRI

N Willemse, WID Rae, CP Herbst

Introduction and Aim: Until recently, left ventricular function has been widely investigated in diagnostic radiology and nuclear medicine and has been found to be clinically useful. Right ventricular function has however only recently been studied and has become of clinical importance. Recent studies have shown that right ventricular function is an important determinant of prognosis in patients with myocardial infarction and other cardiac pathologies. The aim of this study was the assessment of quantification of normal right and left ejection fractions as done using cardiac Magnetic Resonance Imaging and a manual contouring method at Universitas Hospital, Bloemfontein.

Methodology: 27 healthy normal volunteers with no known cardiac abnormalities were entered into the study, of which 10 males and 10 females in the age range 22 to 53 were included in the analysis. Informed consent was obtained from all the volunteers. The evaluation was based on multi-slice imaging in three imaging planes (2-Chamber View, 4-Chamber View and Short Axis View) of both ventricles using standard cardiac Magnetic Resonance imaging. End-diastolic volumes and end-systolic volumes (ESV) were measured using a manual contouring method performed by three independent observers on all three imaging planes, and the stroke volumes and ejection fractions were calculated for both the left and right ventricles. Possible correlation between the right and left volumes, and the gender, age, body mass index (BMI) and body surface area (BSA), was investigated.

Results: No statistical significant difference was found between the ejection fractions of the different observers, although there were significant differences in the respective volumes. The average ejection fractions and their standard deviations from the 2-Chamber View, 4-Chamber View and Short Axis Views combined, were found to be 64.5% [4.7%] and 58.7% [4.9%] for the left and right ventricles respectively. There was no correlation between ejection fraction and BMI or age. However, in the female volunteers, a correlation between ventricle volumes and BSA was found. The average ejection fractions and their standard deviations for female volunteers were 64.6% [3.9%] and 58.9% [5.3%] for the left and right ventricle respectively. The average ejection fractions and their standard deviations for male volunteers were 64.3% [5.5%] and 58.5% [4.8%] for the left and right ventricle respectively

Conclusion: The degree of observer dependency was thought to be acceptable. Ejection fractions and stroke volumes are as expected for the normal healthy volunteers included in the study. Variations and errors are attributed to the uncertainty in the determination of valve levels, partial volume effect, slice thickness, image

quality and movement artefacts. However, this manual technique is thought to be reliable and reproducible, and is being utilised to assess an automated contouring method currently under development.

FINAL REMARKS ON MANUAL QUANTIFICATION FOR RIGHT VENTRICULAR FUNCTION USING CARDIAC MRI: OPTIMIZATION OF THE METHOD

N Willemse, WID Rae, CP Herbst

Introduction and Aim: Until recently, the right ventricle (RV) was deemed unimportant in cardiac health. Lately, RV dysfunction has been recognized as a prognostic factor in many cardiovascular diseases. However, RV geometry and location complicate evaluation using traditional imaging methods. The aim of this study was the optimization of manual quantification for RV functional parameters using standard cardiac MRI as a non-invasive tool at Universitas Hospital, Bloemfontein.

Methodology: 28 volunteers with no known cardiac abnormalities were entered into the study, of which 10 males and 10 females were included in the analysis. The evaluation was based on multi-slice imaging in three imaging planes. Manual contours representing end-diastole and end-systole were sampled on cardiac MR images for LV and RV by three observers, and EDV, ESV, stroke volumes and ejection fractions (EF) derived. Cardiac parameters were compared to published data, and tested for correlations with demographics (gender, age, BMI, BSA). Optimization methods included: use SSFP sequences, early ECG evaluation, breath-hold at end-expiration, position heart at magnet isocentre, use sequential scans, reduce slice thickness, obtain knowledge and develop guidelines, test reliability and validity of segmentation, do pilot studies.

Results: Results followed anatomical predictions. With all factors considered, the data were acceptable and valid. No correlation was found between EF and demographics, and no adjustments were made; the group was too uniform. Average EFs for normal female volunteers were 64.6% and 58.9% for LV and RV respectively, and 64.3% and 58.5% for the male group. EF values compared well with published values. Averages from three observers and three imaging views were implemented to optimize the method.

Conclusion: The proposed study as a first investigation for Universitas Hospital delivered reliable and valid results. Optimization reduced errors, but may further refine the technique. EF values derived in the study were offered as average cardiac functional parameters for the normal group studied.

REFERENCES

Alfakih, K, Plein, S, Thiele, H, Jones, T, Ridgway, JP & Sivananthan, MU 2003, 'Normal human left and right ventricular dimensions for MRI as assessed by turbo gradient echo and steady-state free precession imaging sequences', *Journal of Magnetic Resonance Imaging*, vol. 17, pp. 323-329.

Al-Shafei, AIM, Wise, RG, Grace, AA, Carpenter, TA, Hall, LD & Huang, CLH 2001, 'MRI analysis of right ventricular function in normal and spontaneously hypertensive rats', *Magnetic Resonance Imaging*, vol. 19, pp. 1297-1304.

Antoni, ML, Scherptong, WC, Atary, JZ, Boersma, E, Holman , ER, van der Wall, EE, Schalij, MJ & Bax, JJ 2010, 'Prognostic value of right ventricular function in patients after acute myocardial infarction treated with primary percutaneous coronary intervention', *Circulation: Cardiovascular Imaging*, vol. 3, no. 3, pp. 264-271.

Bartlett, ML, Srinivasan, G, Barker, WC, Kitsiou, AN, Dilsizian, V & Bacharach, SL 1996, 'Left ventricular ejection fraction: Comparison of results from planar and SPECT gated blood-pool studies', *The Journal of Nuclear Medicine*, vol. 37, no. 11, pp. 1795-1799.

Bonnemains, L, Mandry, D, Marie, PY, Micard, E, Chen, B & Vuissoz, PA 2012, 'Assessment of right ventricle volumes and function by cardiac MRI: Quantification of the regional and global interobserver variability', *Magnetic Resonance in Medicine*, vol. 67, no. 6, pp. 1740-1746.

Bradlow, WM, Hughes, ML, Keenan, NG, Bucciarelli-Ducci, C, Assomull, R, Gibbs, JSR & Mohiaddin, RH 2010, 'Measuring the heart in pulmonary arterial hypertension (PAH): Implications for trial study size', *Journal of Magnetic Resonance Imaging*, vol. 31, pp. 117-124.

Bueno, H, Lopez-Palop, R, Bermejo, J, Lopez-Sendon, JL & Delcan, JL 1997, 'In-hospital outcome of elderly patients with acute inferior myocardial infarction and right ventricular involvement', *Circulation*, vol. 96, no. 2, pp. 436-441.

Bushberg, JT, Seibert, JA, Leidholdt, EM & Boone, JM 2002, *The essential physics of medical imaging,* Lippincott Williams & Wilkins, Philadelphia.

Cain, PA, Ahl, R, Hedstrom, E, Ugander, M, Allansdotter-Johnsson, A, Friberg, P & Arheden, H 2009, 'Age and gender specific normal values of left ventricular mass, volume and function for gradient echo magnetic resonance imaging: a cross sectional study', *BMC Medical Imaging*, vol. 9, no. 2, doi: 10.1186/1471-2342-9-2.

Carr, JC, Simonetti, O, Bundy, J, Li, D, Pereles, S & Finn, JP 2001, 'Cine MR angiography of the heart with segmented true fast imaging with steady-state precession', *Radiology*, vol. 219, no. 3, pp. 828-834.

Chin, BB, Bloomgarden, DC, Xia, W, Kim, HJ, Fayad, ZA, Ferrari, VA, Berlin, JA, Axel, L & Alavi, A 1997, 'Right and left ventricular volume and ejection fraction by tomographic gated blood-pool scintigraphy', *Nuclear Cardiology*, vol. 38, no. 6, pp. 942-948.

Codella, NCF, Cham, MD, Wong, R, Chu, C, Min, JK, Prince, MR, Wang, Y & Weinsaft, JW 2010, 'Rapid and accurate left ventricular chamber quantification using a novel CMR segmentation algorithm: A clinical validation study', *Journal of Magnetic Resonance Imaging*, vol. 31, pp. 845-853.

Dahya, V & Spottiswoode, BS 2010, 'Cardiovascular magnetic resonance imaging – a pictorial review', *South African Journal of Radiology*, vol. 14, no. 4, pp. 92-96.

Dilsizian, V, Rocco, TP, Bonow, RO, Fischman, AJ, Boucher, CA & Strauss, HW 1990, 'Cardiac blood-pool imaging II: Applications in noncoronary heart disease'. *The Journal of Nuclear Medicine*, vol. 31, no. 1, pp. 10-22.

Drake, D, Gupta, R, Lloyd, SG & Gupta, H 2007, 'Right ventricular function assessment: Comparison of geometric and visual method to short-axis slice summation method', *Echocardiography: A Journal of CV Ultrasound & Allied Tech.*, vol. 24, no. 10, pp. 1013-1019.

Dupont, MVM, Drăgean, CA & Coche, EE 2011, 'Right ventricle function assessment by MDCT', *American Journal of Roentgenology,* vol. 196, pp. 77-86.

Einstein, AJ, Henzlova, MJ & Rajagopalan, S 2007, 'Estimating risk of cancer associated with radiation exposure from 64-slice computed tomography coronary angiography', *The Journal of the American Medical Association*, vol. 298, no. 3, pp. 317-323.

Filliben, JJ & Heckert, A 2003, *NIST/SEMATECH e-Handbook of Statistical Methods*, viewed 20 February 2012, http://www.itl.nist.gov/div898/handbook/eda/section3/eda3673.htm#ONE-05-1-10.

Frist, WH, Lorenz, CH, Walker, ES, Loyd, JE, Stewart, JR, Graham, TP, Pearlstein, DP, Key, SP & Merrill, WH 1995, 'MRI complements standard assessment of right ventricular function after lung transplantation', *Annals of Thoracic Surgery*, vol. 60, pp. 268-271.

General Electric Company 2001a, '2D FIESTA pulse sequences', in *Signa® LX Release 9.0: learning and reference guide*, Author, USA.

General Electric Company 2001b, 'Gating and triggering', in *Signa® MR/i™ with Signa Select™ (ASP2): learning and reference guide,* vol. 3, *Optimizing images with imaging options,* Author, USA.

Geva, T, Powell, AJ, Crawford, EC, Chung, T & Colan, SD 1998, 'Evaluation of regional differences in right ventricular systolic function by acoustic quantification echocardiography and cine magnetic resonance imaging', *Circulation*, vol. 98, no. 4, pp. 339-345.

Gray, H 1918, *Anatomy of the human body*, viewed 6 April 2011, http://www.bartleby.com/107/138.html#i490.

Grobner, T 2006, 'Gadolinium – a specific trigger for the development of nephrogenic fibrosing dermopathy and nephrogenic systemic fibrosis?', *Nephrology Dialysis Transplantation*, vol. 21, no. 4, pp. 1104-1108.

Grothues, F, Moon, JC, Bellenger, NG, Smith, GS, Klein, HU & Pennell, DJ 2004, 'Interstudy reproducibility of right ventricular volumes, function, and mass with cardiovascular magnetic resonance', *American Heart Journal*, vol. 147, no. 2, pp. 218-223.

Haddad, F, Hunt, SA, Rosenthal, DN & Murphy, DJ 2008, 'Right ventricular function in cardiovascular disease, part 1', *Circulation*, vol. 117, pp. 1436-1448.

Haddad, F, Couture, P, Tousignant, C & Denault, AY 2009, 'The right ventricle in cardiac surgery, a perioperative perspective: I. Anatomy, physiology, and assessment', *Anesthesia & Analgesia*, vol. 108, no. 2, pp. 407-421.

Herbst, CP, Diedericks, J, Uys, NJ, Brummer, J & Lötter, MG 1991, 'Use of a personal computer for fast acquisition of cardiovascular data over an extended period', *Computers in Biology and* Medicine, vol. 21, no. 6, pp. 407-415.

Ho, SY & Nihoyannopoulos, P 2006, 'Anatomy, echocardiography, and normal right ventricular dimensions', *Heart*, vol. 92, suppl. 1, pp. i2-i13.

Holinski, S, Knebel, F, Heinze, G, Konertz, W, Baumann, G & Borges, AC 2011, 'Noninvasive monitoring of cardiac function in a chronic ischemic heart failure model in the rat: Assessment with tissue Doppler and non-Doppler 2D strain echocardiography', *Cardiovascular Ultrasound*, vol. 9, no. 15, doi: 10.1186/1476-7120-9-15.

Hudsmith, LE, Petersen, SE, Francis, JM, Robson, MD & Neubauer, S 2005, 'Normal human left and right ventricular and left atrial dimensions using steady state free precession magnetic resonance imaging', *Journal of Cardiovascular Magnetic Resonance*, vol. 7, pp. 775-782.

Jiang, L, Siu, SC, Handschumacher, MD, Luis Guererro, J, Vazquez de Prada, JA, King, ME, Picard, MH, Weyman, AE & Levine, RA 1994, 'Three-dimensional echocardiography. In vivo validation for right ventricular volume and function', *Circulation*, vol. 89, no. 5, pp. 2342-2350.

Kerl, JM, Ravenel, JG, Nguyen, SA, Suranyi, P, Thilo, C, Costello, P, Bautz, W & Schoepf, UJ 2008, 'Right heart: Split-bolus injection of diluted contrast medium for visualization at coronary CT angiography', *Radiology*, vol. 247, no. 2, pp. 356-364.

Kjaergaard, J, Petersen, CL, Kjaer, A, Schaadt, BK, Oh, JK & Hassager, C 2006, 'Evaluation of right ventricular volume and function by 2D and 3D echocardiography compared to MRI', *European Journal of Echocardiography*, vol. 7, no. 2, pp. 430-438.

Kramer, CM, Barkhausen, J, Flamm, SD, Kim, RJ & Nagel, E 2008, 'Standardized cardiovascular magnetic resonance imaging (CMR) protocols, society for cardiovascular magnetic resonance: board of trustees task force on standardized protocols', *Journal of Cardiovascular Magnetic Resonance*, vol. 10, no. 35, doi: 10.1186/1532-429X-10-35.

Lalande, A, Legrand, L, Walker, PM, Guy, F, Cottin, Y, Roy, S & Brunotte, F 1999, 'Automatic detection of left ventricular contours from cardiac cine magnetic resonance imaging using fuzzy logic', *Invest Radiol.*, vol. 34, no. 3, pp. 211-217.

Larose, E, Ganz, P, Reynolds, HG, Dorbala, S, Di Carli, MF, Brown, KA & Kwong, RY 2007, 'Right ventricular dysfunction assessed by cardiovascular magnetic resonance imaging predicts poor prognosis late after myocardial infarction', *Journal of the American College of Cardiology*, vol. 49, no. 8, pp. 855-862.

Lorenz, CH, Walker, ES, Morgan, VL, Klein, SS & Graham, TP Jr. 1999, 'Normal human right and left ventricular mass, systolic function, and gender differences by cine magnetic resonance imaging', *Journal of Cardiovascular Magnetic Resonance*, vol. 1, no. 1, pp. 7-21.

Mahesh, M & Cody, DD 2007, 'Physics of cardiac imaging with multiple-row detector CT', *RadioGraphics*, vol. 27, no. 1, pp. 1475-1509.

Marabotti, C, Bedini, R & L'Abbate, A 2008, 'Right ventricular determination: not a matter for echocardiography', *Journal of Applied Physiology*, vol. 104, p. 1547.

Marcu, CB, Beek, AM & Van Rossum, AC 2006, 'Cardiovascular Magnetic Resonance Imaging for the assessment of right heart involvement in cardiac and pulmonary disease', *Heart, Lung and Circulation*, vol. 15, no. 6, pp. 362-370.

Markiewicz, W, Sechtem, U & Higgins, CB 1987, 'Evaluation of the right ventricle by magnetic resonance imaging', *Am Heart J*, vol. 113, no. 1, pp. 8-15.

Medical and clinical engineering n.d., *Cardiology*, viewed 10 April 2012, http://www.ebme.co.uk/arts/general/cardiology.htm.

Meeker, WQ & Escobar, LA 1998, *Statistical Methods for Reliability Data,* Wiley, Hoboken, New Jersey.

Meluzin, J, Špinarová, L, Hude, P, Krejčí, J, Dušek, L, Vítovec, J & Panovsky, R 2005, 'Combined right ventricular systolic and diastolic dysfunction represents a strong determinant of poor prognosis in patients with symptomatic heart failure', *International Journal of Cardiology*, vol. 105, no. 2, pp. 164-173.

Meyer, BJ, van Papendorp, DH, Meij, HS & Viljoen, M 2002, *Human Physiology*, Juta, Lansdowne, South Africa.

Miller, S, Simonetti, OP, Carr, J, Kramer, U & Finn, JP 2002, 'MR imaging of the heart with cine true fast imaging with steady-state precession: influence of spatial and temporal resolutions on left ventricular functional parameters', *Radiology*, vol. 223, no. 1, pp. 263-269.

Mitoff, PR, Beauchesne, L, Dick, AJ, Chow, BJ, Beanlands, RS, Haddad, H & Mielniczuk, LM 2012, 'Imaging the failing right ventricle', *Current Opinion in Cardiology*, vol. 27, no. 2, pp. 148-153.

Mooij, CF, de Wit, CJ, Graham, DA, Powell, AJ & Geva, T 2008, 'Reproducibility of MRI measurements of right ventricular size and function in patients with normal and dilated ventricles', *Journal of Magnetic Resonance Imaging*, vol. 28, no. 1, pp. 67-73.

Moore, KL & Dalley, AF 1999, *Clinically oriented anatomy*, Lippincott Williams & Wilkins, Canada.

Mosteller RD. 1987, 'Simplified calculation of body-surface area', *The New England Journal of Medicine*, vol. 317, no. 17, pp. 1098.

Murphy, DT, Shine, SC, Cradock, A, Galvin, JM, Keelan, ET & Murray, JG 2010, 'Cardiac MRI in arrhythmogenic right ventricular cardiomyopathy', *American Journal of Roentgenology*, vol. 194, pp. W299-W306.

Petitjean, C & Dacher, JN 2011, 'A review of segmentation methods in short axis cardiac MR images', *Medical Image Analysis*, vol. 15, no. 2, pp. 169-184.

Pfisterer, ME, Battler, A & Zaret, BL 1985, 'Range of normal values for left and right ventricular ejection fraction at rest and during exercise assessed by radionuclide angiography', *European Heart Journal*, vol. 6, pp. 647-655.

Pitcher, A, Ashby, D, Elliott, P & Petersen, SE 2011, 'Cardiovascular MRI in clinical trials: expanded applications through novel surrogate endpoints', *Heart*, vol. 97, no. 16, pp. 1286-1292.

Plumhans, C, Mühlenbruch, G, Rapaee, A, Sim, KH, Seyfarth, T, Günther, RW & Mahnken, AH, 'Assessment of global right ventricular function on 64-MDCT compared with MRI', *American Journal of Roentgenology*, vol. 190, pp. 1358-1361.

Prakken, NH, Velthuis, BK, Vonken, EJ, Mali, WP & Cramer, MJ 2008, 'Cardiac MRI: Standardized right and left ventricular quantification by briefly coaching inexperienced personnel', *The Open Magnetic Resonance Journal*, vol. 1, pp. 104-111.

Quain, J 1836, *Elements of Anatomy*, vol. 3, Sharpey, W & Ellis GV (ed), Walton and Maberly, London.

Robertson, HE & Duff, PH 1922, 'A proposed method for estimating the capacity of the left ventricle of the heart', *The Journal of Medical Research*, vol. XLIII, no. 3, pp. 253-266.

Rogers, J 1999, 'Cardiovascular Physiology', *Update in Anaesthesia*, vol. 1, no. 10, pp. 2-8.

Roos-Hesselink, JW, Meijboom, FJ, Spitaels, SEC, van Domburg, R, van Rijen, EHM, Utens, EMWJ, McGhie, J, Bos, E, Bogers, AJJC & Simoons, ML 2004, 'Decline in ventricular function and clinical condition after mustard repair for transposition of the great arteries (a prospective study of 22-29 years)', *European Heart Journal*, vol. 25, pp. 1264-1270.

Sandler, H & Dodge, HT 1968, 'The use of single plane angiocardiograms for the calculation of left ventricular volume in man', *American Heart Journal*, vol. 75, no. 3, pp. 325-334.

Saremi, F, Grizzard, JD & Kim RJ 2008, 'Optimizing cardiac MR imaging: Practical remedies for artifacts', *RadioGraphics*, vol. 28, no. 4, pp. 1161-1187.

Selton-Suty, C & Juillière, Y 2009, 'Non-invasive investigations of the right heart: How and why?', *Archives of Cardiovascular Disease*, vol. 102, pp. 219-232.

Shors, SM, Fung, CW, François, CJ, Finn, JP & Fieno, DS 2004, 'Accurate quantification of right ventricular mass at MR imaging by using cine true fast imaging with steady-state precession: study in dogs', *Radiology*, vo. 230, no. 2, pp. 383-388.

Tandri, H, Daya, SK, Nasir, K, Bomma, C, Lima, JAC, Calkins, H & Bluemke, DA 2006, 'Normal reference values for the adult right ventricle by magnetic resonance imaging', *The American Journal of Cardiology*, vol. 98, pp. 1660-1664.

Taylor, AM, Jhooti, P, Wiesmann, F, Keegan, J, Firmin, DN & Pennell, DJ 1997, 'MR navigator-echo monitoring of temporal changes in diaphragm position: implications for MR coronary angiography', *Journal of Magnetic Resonance Imaging*, vol. 7, no. 4, pp. 629-636.

Testani, JM, Khera, AV, St. John Sutton, MG, Keane, MG, Wiegers, SE, Shannon, RP & Kirkpatrick, JN 2010, 'Effect of right ventricular function and venous congestion on cardio-renal interactions during the treatment of decompensated heart failure', *American Journal of Cardiology*, vol. 105, no. 4, pp. 511-516.

Uribe, S, Tangchaoren, T, Parish, V, Wol, I, Razavi, R, Greil, G & Schaeffter, T 2008, 'Volumetric cardiac quantification by using 3D dual-phase whole-heart MR imaging', *Radiology*, vol. 248, no. 2, pp. 606-614.

Van Wolferen, SA, Marcus, JT, Boonstra, A, Marques, KMJ, Bronzwaer, JGF, Spreeuwenberg, MD, Postmus, PE & Vonk-Noordegraaf, A 2007, 'Prognostic value of right ventricular mass, volume, and function in idiopathic pulmonary arterial hypertension', *European Heart Journal*, vol. 28, no. 10, pp. 1250-1257.

Weissler, AM, Harris, WS & Schoenfeld, CD 1969, 'Bedside technics [sic] for the evaluation of ventricular function in man', *The American Journal of Cardiology*, vol. 23, no. 4, pp. 577-583.

Williams, L & Frenneaux, M 2008, 'Assessment of right ventricular function', *Heart*, vol. 94, no. 4, pp. 404-405.

SUMMARY

Until recently, the right ventricle (RV) has been somewhat neglected in cardiac health. More recently, RV dysfunction has been recognized as a prognostic factor in many cardiovascular diseases. However, the RV has been difficult to evaluate using traditional imaging methods because of its geometric structure and location within the chest cavity. Cardiac Magnetic Resonance Imaging (MRI) provides a non-invasive means of assessing changes in RV function. The aim of this study was the assessment of a manual quantification method for normal right and left functional parameters using standard cardiac MRI at Universitas Hospital, Bloemfontein.

Twenty eight healthy normal volunteers with no known cardiac abnormalities were entered into the study, of which 20 were included in the analysis: 10 males and 10 females in the age range 22 to 53. Informed consent was obtained from all the volunteers. The evaluation was based on multi-slice imaging in three imaging planes (2-Chamber View, 4-Chamber View and Short Axis View) of both ventricles using standard cardiac MRI. Manual contours representing end-diastole (EDV) and end-systole (ESV) were sampled on the cardiac MR images for the left and right ventricles, and the corresponding volumes calculated. Stroke volumes (SV) and ejection fractions (EF) were derived from the measured data. Three observers repeated the sampling process. Inter-observer reliability, inter-method reliability and the validity of the data was investigated. The values were also compared to available published data. The data were tested for possible correlations between the cardiac parameters (EDV, ESV, SV and EF) and demographic factors (gender, age, BMI, BSA). If subdivision was possible and correlations do exist, normal values were to be given either per subgroup, or adjusted for BMI, BSA, and/or age.

No statistically significant difference was found between the average EFs of the different observers, although there were significant differences in the respective volumes. No imaging views could be rejected on the grounds of statistically significant deviations. With the reliability of the data proven, the average values from the three observers and three imaging views were used to analyze the validity of the data, to develop and stabilise the method.

The results followed the prediction from the anatomy that the right ventricle should have a larger volume than the left, the stroke volumes should be equal, and the resulting RV EF should be lower than the LV EF. The overall average difference in SV between the LV and RV was less than 1 teaspoon of blood. With all the artefacts and imaging difficulties taken into account, as well as the thickness of the imaging slices and the resulting loss in accuracy, these values are acceptable, and thus the data were valid.

There was no correlation found between EF and BMI, BSA or age. The average ejection fractions and their standard deviations for the normal group of female volunteers were 64.6% [3.9%] and 58.9% [5.3%] for the left and right ventricle respectively. The average ejection fractions and their standard deviations for the normal group of male

volunteers were 64.3% [5.5%] and 58.5% [4.8%] for the left and right ventricle respectively. The ejection fraction values overall were comparable to those of published studies on MR cardiac data, thus supporting the reliability and validity of this study's measured data.

The few correlations with demographics found were insignificant, and the values derived in the study cannot be adjusted according to these results, or given as specific ranges of normal values. Therefore, the ranges derived in this study were offered as average cardiac functional parameters for the normal volunteer group studied. With the resources available, this study, as a first investigation for Universitas Hospital, delivered acceptably reliable and valid results.

OPSOMMING

Tot onlangs is the regterventrikel (RV) van die hart effens afgeskeep in hartgesondheid, maar regterhartwanfunksie word onlangs al hoe meer gesien as 'n belangrike prognostiese faktor in baie kardiovaskulêre siektes. Vanweë die geometriese struktuur en die ligging van die regterventrikel in die borskas, is dit egter moeilik om die regterventrikel te evalueer met behulp van tradisionele beeldingsmetodes. Daarteenoor verskaf rolprentformaat Magnetiese Resonansbeelding (MR) 'n nie-ingrypende manier om veranderinge in RV funksie vas te stel. Die doel van hierdie studie was dus die ondersoek en waardebepaling van 'n metode waar kwantifisering vir normale regter- en linkerventrikelfunksie met die hand gedoen word, in Universitashospitaal, Bloemfontein.

Agt-en-twintig gesonde normale vrywilligers met geen bekende hartafwykings is toegelaat in die studie, waarvan twintig in die analise ingesluit is: tien mans en tien vrouens in die ouderdomsgroep 22 tot 53. Alle vrywilligers het oorwoë toestemming toegestaan. Die evaluering is gebaseer op veelvuldige-snit beelding in drie beeldingsvlakke (2-kamer aansig, 4-kamer aansig en kort-as aansig) van beide ventrikels, met die gebruik van standaard MR hartbeelding. Kontoerlyne wat eind-diastool (EDV) en eind-sistool (ESV) voorstel is met die hand geteken vir die linker- en regterventrikel op die MR beelde. Die ooreenstemmende volumes is daarmee bereken. Slagvolumes (SV) en uitwerpfraksies (UF) is afgelei uit die gemete data. Drie waarnemers het die proefneming herhaal. Tussen-waarnemer betroubaarheid, tussen-metode betroubaarheid en die geldigheid van die data is ondersoek. Die waardes is ook vergelyk met beskikbare gepubliseerde data. Die data is getoets vir moontlike korrelasies tussen die hartparameters en demografiese faktore (geslag, ouderdom, liggaamsmassa-indeks, liggaams-oppervlak). As onderverdeling in die data moontlik was en korrelasies wel bestaan, sou die normale waardes óf gegee word per groep, óf aangepas word vir die invloed van demografiese faktore.

Geen statisties betekenisvolle verskil is gevind tussen the gemiddelde UF's van die verskillende waarnemers nie, alhoewel daar betekenisvolle verskille in die onderskeie volumes was. Geen beeldingsaansig kon uitgeskakel word op grond van statisties betekenisvolle afwykings nie. Met die betroubaarheid van die data bevestig, is die gemiddelde waardes van die drie waarnemers en die drie beeldingsaansigte gebruik om die geldigheid van die data te toets en om die metode te ontwikkel en te stabiliseer.

Die resultate het ook die verwagting uit die anatomie gevolg, deur te wys dat die regterventrikel groter is as die linkerventrikel, die slagvolumes gelyk, en die gevolglike RV UF laer as die LV UF. Die algehele gemiddelde verskil in slagvolume tussen die LV en RV was minder as 'n teelepeltjie bloed. Met al die artefakte en struikelblokke in die beelding in ag geneem, sowel as die dikte van die beeldingsnitte en die gepaardgaande verlies aan akkuraatheid, was hierdie waardes aanvaarbaar, en die data dus geldig.

Daar is geen korrelasie gevind tussen UF en enige van die demografiese faktore nie. Die gemiddelde UF's en hul standaardafwykings vir die normale groep vroulike vrywiligers was 64.6% [3.9%] en 58.9% [5.3%] vir die linker- en regterventrikels onderskeidelik. Die gemiddelde UF's en hul standaardafwykings vir die normale groep manlike vrywiligers was 64.3% [5.5%] en 58.5% [4.8%] vir die linker- en regterventrikels onderskeidelik. Die uitwerpfraksies was oor die algemeen vergelykbaar met dié van gepubliseerde studies oor MR hartdata, wat weereens die geldigheid van hierdie studie se gemete data ondersteun.

Die paar korrelasies met demografiese faktore was onbeduidend, en die waardes afgelei in die studie kon nie aangepas word hiervolgens nie, of gegee word as 'n spesifieke reeks normale waardes nie. Daarom is die reeks waardes afgelei in hierdie studie aangebied as die gemiddelde funksionele parameters van die hart vir die normale vrywilligergroep wat bestudeer is. Met die beskikbare hulpbronne, het hierdie metode as 'n eerste ondersoek vir Universitashospitaal aanvaarbare betroubare en geldige resultate gelewer.

KEY TERMS

Right ventricular function

Cardiac Magnetic Resonance imaging

Manual quantification

Stroke volume

Ejection fraction

Inter-observer reliability

Inter-method reliability

Gated MRI

Gender-specific ventricular size and function

Prognostic importance of right ventricle